Abstract

Remote sensing of natural waters has many practical applications, but its use requires overcoming many delicate problems. The intention with this work is to design and construction of radiometer to study the effect of pollution on the optical and electrical properties of water. The key parameters common to the visible and infrared regions are; reflectance, absorptance and transmittance. These parameters are functions of the wavelength, angle the incidence and polarization. In microwave, the voltage reflectivity is related to the electric properties of the water, dielectric constant and its conductivity. The dependence on the angle of incidence and polarization plays an important role in the remote sensing.

Three channels radiometer (visible, IR, MW) was designed and implemented in this thesis. This radiometer was used to study the water quality. The measurements were taken for different polluted water samples in electromagnetic spectrum above, to indicate the effect of pollution on the optical and electrical properties of water. The results from the measurement samples are in good agreement with theoretical results with percentage error of 10%, due to system calibration, approximation in the theoretical mathematical model and background noise from the other sources of electromagnetic radiation.

الخلاصة

هنالك عدة تطبيقات عملية للتحسس النائي للمياه الطبيعية ولكن تحتاج الى التغلب على عدة مشاكل معقدة. يتضمن البحث توضيح كيفية تاثير نوعية المياه على الخواص البصرية والكهربائية وامكانية استخدامها في التحسس النائي. ان العامل المشترك بين الطيف المرئي والحراري هو الانعكاسية ، والامتصاصية والشفافية وكون هذه العوامل دالة لزاوية السقوط والاستقطاب. اما فيما يخص المايكرويف والموجات الدقيقة فان فولتية الانعكاسية تعتمد على الخواص الكهربائية للماء ، والمتضمن ثابت العزل الكهربائي والتوصيلية الكهربائية وكذلك اعتماد فولتية الانعكاسية زاوية السقوط والاستقطاب لكونها عامل مهم في التحسس النائي.

في هذا البحث تم تصميم وبناء منظومة مقياس ريدومترية متكونة من ثلاث قنوات (الاشعة المرئية ، الأشعة تحت الحمراءالقريبة ، حزمة X-). تم استخدام الجهاز في قياس خواص الماء وتم اخذ القياسات باستخدام نماذج ملوثة مثل الملح والزيت ودراسة تاثير التلوث على الخواص البصرية والكهربائية مع النتائج النظرية وتبين ان نسبة الخطأ كانت (10%) وان السبب في ذلك يعود الى معايرة الجهاز والتقريب في المعادلات الرياضية النظرية ، أضافة الى الضوضاء الناتجة عن المصادر الخارجية الأخرى .

Table (C.1): The review of the some properties for selected photodetectors [9]

Photodetectors parameter	Photodetectors						
	Vacum diod	Si	Ge	pbS	Jnsb S77Kc	(Hg.cd) S77Kc	Pytoelectric
Detector type	PV	PV	PV	PC	PV.PC	PV.PC	PC
Detector active area limit A_d mm^2	1000	100	5	1000	10	10	100
Resposivity peak wavelength λ_p μm	0.2-0.4	0.85	1.55	2.2	5.0	10-11	-
Resposivity cutt-off wavelength λ_p μm	Up to1	1.1	1.7	3	5.6	13	Window
Dark resistivity Rd Ω	-	-	-	1M	15	30	10^{12}
Dark current td [PA]	< 10	$< 10^4$	$< 10^6$	-	1.10^7	1.10^7	-
Current Resposivity R_A [A/W]	> 0.1	0.6	1	-	2	2.5	-
Voltage Resposivity Rv [V/W]	-	-	-	10^5	10^4	10^4	1
Peak detectors D^*_λ [cm $\sqrt{H} = W$]	$> 10^{16}$	$>10^{12}$	$>10^{11}$	$>10^{10}$	$>10^{10}$	10^{10}	10^8
Time constant τ_r [ms]	$<10^{-6}$	$<10^{-5}$	0.1-0.5	10^{-3}	10^{-3}	10^{-3}	10
Operating temperature limit T_e [^oC]	100	125	100	100	80	80	60
Response temperature stability [%/^oC]	< 0.1	0.1	0.3	3	-	-	1
Linearity S% over decade C	2	1	1	1	1	1	5
Response linearity limit	1 μA	1 mA	1 mA	1 mW	1 mW	1 mW	1 μW
Basic voltage	50	0-100	0-40	< 100	<20	< 10	10/FET
Price	Low	Low	high	medium	high	high	Low

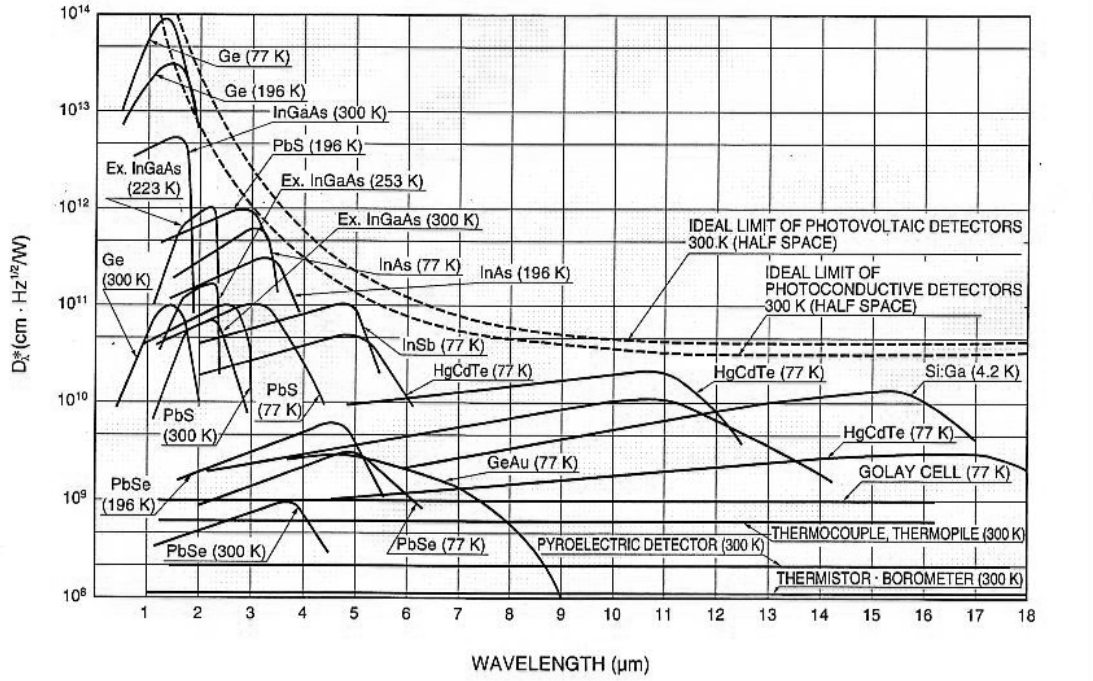

Fig.(C.2): Spectral response characteristics of various infrared detectors [9]

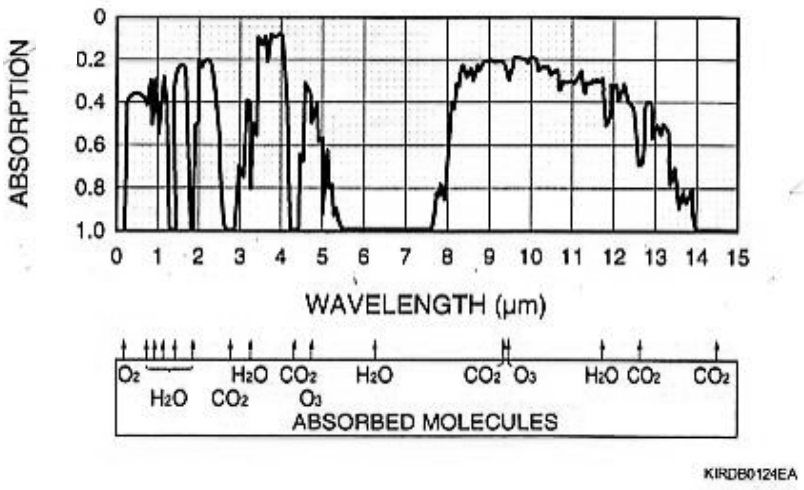

Fig. (B.1): Atmospheric absorption on area surface [9]

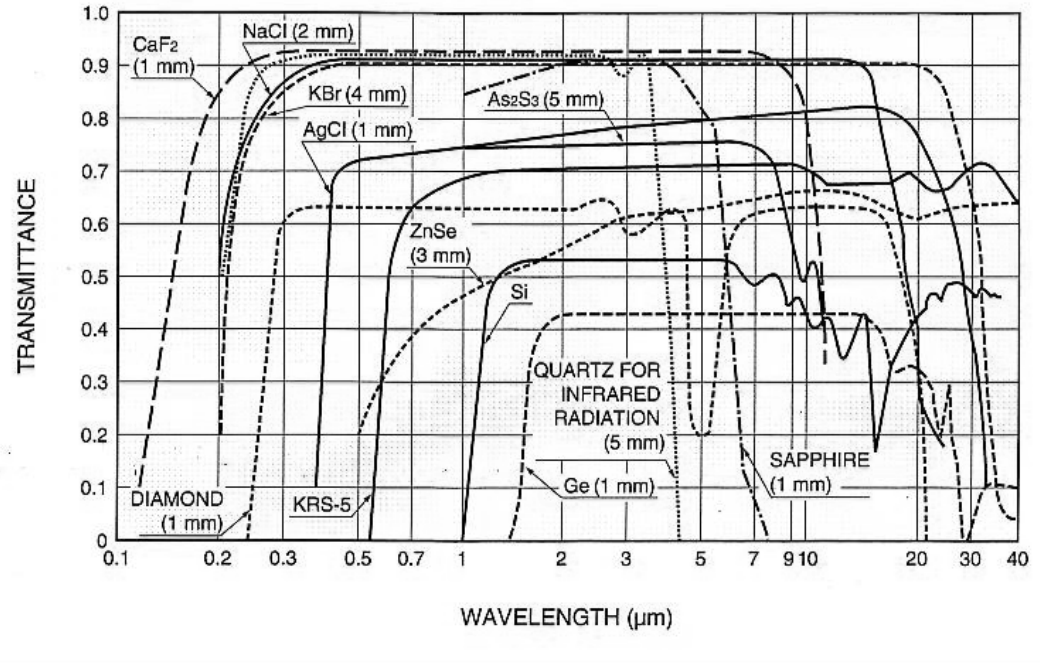

Fig. (B.2): Transmittance of various optical material [9]

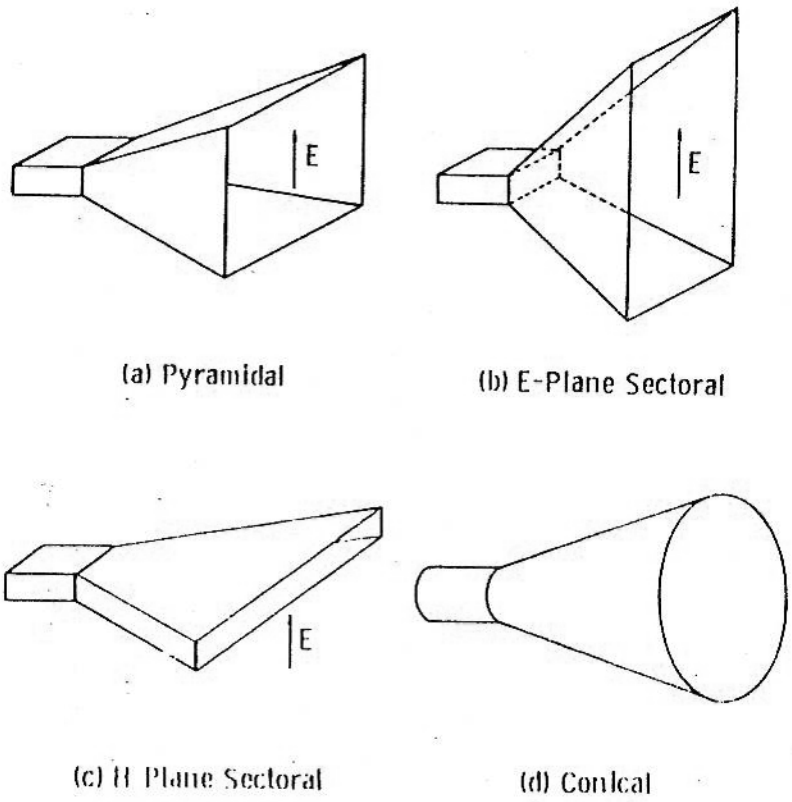

Appendix D. Commonly used horn types

Table (A.1) : Summary of Radiometric Concept [2]

Name	Symbol	Unite	Concept
Radiant energy	Q_e	Joules, J	Capacity of radiation within a specified spectral band to do work.
Radiant flux	ϕ_e	Watts, W	Time rate of flow of energy on to, off or through a surface
Radiant flux density at surface			
Irradiance	E_e	Watt per square meter, Wm^{-2}	Radiant flux incident upon a surface per unit area that surface.
Radiant exitance	M_e	Watt per square meter, Wm^{-2}	Radiant flux leaving a surface per unit area that surface.
Radiant intensity	I_e	Watt per steradian meter, Wsr^{-1}	Radiant flux leaving a small source solid angle in a specified direction.
Radiance	L_e	Watt per steradian square meter, Wsr^{-2}	Radiant intensity per unit of projected source area in specified direction.
Hemispherical reflectance	ρ_e	Dimensionless	$\phi_{e\ \text{reflected}} / \phi_{e\ \text{incident}}$ for any surface
Hemispherical transmission	τ_e	Dimensionless	$\phi_{e\ \text{transmitted}} / \phi_{e\ \text{incident}}$ for any surface
Hemispherical absorptance	α_e	Dimensionless	$\phi_{e\ \text{absorbed}} / \phi_{e\ \text{incident}}$ for any surface

Certification

We certify that we have read this thesis entitled **(*Construction of Radiometer system*)** and examined the student (Mohammed M.Salih) in its content and that in our opinion ;it meet the standard of a thesis for the degree of doctor philosophy in Optoelectronics Engineering

.

Signature:
Name: Dr.Mohammad Radi Mohammad
Title: professor (chairman)
Date: / /2008

Signature:
Name: Dr.Mohammed Hussain Ali
Title: Assist. Professor (member)
Date: / /2008

Signature:
Name Dr.Salah Abdul Hameed
Title: Assist. Professor (member)
Date: / /2008

Signature:
Name Dr.Mohammed Saleh Ahmed
Title: Assist. Professor (member)
Date: / /2008

Signature:
Name Dr. Khaled Abrahim Hasson
Title: Assist. Professor (member)
Date: / /2008

Signature:
Name Dr.Hussain Jumaa Abass
Title: Assist. Professor (supervisor)
Date: / /2008

Signature:
Name Dr.Abedul Razzaq .T.Ziboon
Title: Assist. Professor (supervisor)
Date: / /2008

Approved by University of Technology- Laser and Optoelectronics Engineering Department.

Signature:
Name: Dr.Mohammed Hussain Ali
Title: Assist. Professor (member)
Head of Department
Date: / /2008

Linguistic Certification

I certify that this thesis entitled **" Design and construction of visible , near infrared and microwave detectors for pollution studies"** was prepared under my linguistic supervision. Its language was amended to meet the style of the English language.

Signature:

Name: Dr.Mohammed S.Ahmed

Date: / / 2008

Chapter One

Introduction

1.1 Electromagnetic Spectrum

The electromagnetic radiation found in the electromagnetic spectrum is a limitless source of energy capable of conveying and propagating information. Remote sensing deals largely with the manner by which this energy can be utilized by mankind.

Narrow and broad bands of this electromagnetic radiation are selected by remote sensors for the observation and study of the Earth and its atmosphere. These same sensors are found on satellites launched to observe the surface and atmosphere of various planets in the solar system. Figure 1.1 shows the extent of the EM spectrum, the various named bands (ultraviolet, visible, infrared, radar, etc.), the transmittances of the Earth's atmosphere to this EMR, and the effects caused by its interaction or presence.[1]

The electromagnetic radiation collected by the remote sensor is characterized by the spectrum of the generating source, the atmosphere through which it propagates, and the reflecting surface from which it is largely received. Changes in the source electromagnetic radiation due to the reflecting surfaces and the atmosphere are sources of data which, after processing, can provide information about each. Thus, knowledge of the properties of this EMR as a function of wavelength and other pertinent variables is vital to the analysis of remote-sensor data.

Table 1.1 is a preview of but a few of the many remote sensors which utilize the EM spectrum. Included are comments on what is measured and data presentation.[1,2]

1.2 Water Quality

Pure water, by chemical standards, is almost nonexistent in natural environments. Because of biological activity and natural processes of erosion, drainage, and atmospheric fallout, all water occurring on or beneath the Earth's surface contains various types and amounts of impurities. When it becomes unfit for domestic or industrial use, we refer to it as "polluted." The definition of water pollution is not clear cut, however, and ultimately must rest on the type of use to which the water is to be put. Nevertheless, recognized water pollutants consist of:

1. Organic wastes contributed by domestic sewage and industrial wastes of plant and animal origin which remove oxygen from the water through decomposition;
2. Infectious agents contributed by domestic sewage and by certain kinds of industrial wastes which may transmit disease;
3. Plant nutrients which promote nuisance growths of aquatic plant life such as algae and water weeds;
4. Synthetic-organic chemicals such as detergents and pesticides resulting from new chemical technology which are toxic to aquatic life and potentially to humans;
5. Inorganic chemical and mineral substances resulting from mining, manufacturing processes, oil plant operations, and agriculture practices which interfere with natural stream purification, destroy fish and aquatic life, cause excessive hardness of water supplies, produce corrosive effects, and in general add to the cost of water treatment;
6. Sediments which fill streams, channels, harbors, and reservoirs, cause erosion of hydroelectric power and pumping equipment, affect the fish and shellfish population by blanketing fish nests,

spawn, and food supplies, and increase the cost of water treatment;

7. Radioactive pollution resulting from the mining and processing of radioactive ores, from the use of refined radioactive materials, and from fall-out following nuclear testing;
8. Temperature increases which result from the use of water for cooling purposes by steam electric power plants and industries, and from impoundment of water in reservoirs, and which have harmful effects on fish and aquatic life, and reduce the capacity of the receiving water to assimulate wastes.

Only in rare cases is it possible to make a positive identification of a pollutant by remote sensing. Even then, for enforcement actions it is mandatory to visit the site to collect specimens of the materials both within and outside of the plume of polluted discharge to provide legal verification that the substance observed did, in fact, come from the discharge in question and its identity has been confirmed by expert analysis.[3]

It is, however, possible by remote sensing to detect the point at which a discharge reaches the body of water, where that discharge goes, and the general characteristics of its dispersion pattern. All of these data are vital to the officials responsible for setting standards of water quality and enforcing regulations on discharges of pollutants.

Another factor of equal importance is making an evaluation of the effect of a discharge on the aquatic and shoreline system. This factor is more difficult to assess and requires establishing ground-control stations whose locations can be selected by interpreting remote sensing imagery to determine where the inhabitants can be observed for their health, vigor, and concentration of population. Microorganisms are usually counted and identified by laboratory analysis of carefully collected water samples.

Sample collecting points can be marked and located by reference to known ground features or by anchoring plastic floats at sample points.

Similarly, larger organisms are inventoried by either collecting specimens by a suitable netting technique or by observing the numbers and types of individuals passing a given point over specified times. Some organisms, such as schools of fish, whales, seals, and otters and large flocks of birds, can be seen in or on water on aerial photography taken under controlled conditions.

Documentation and positive identification of samples of water and associated organisms are required to supplement remote-sensing data for water-polluting studies. Many man-caused and natural phenomena interact to create complex water-quality problems, and the resource scientist must be prepared to establish the true identify and source of conditions and material observed on remote-sensor imagery.

1.3 I.R and Optical Remote Sensing

Optical and electronics combiners have designed to permit the various tonal characteristics present in a series of black - and -white photographs (or in other kinds of remote-sensing imagery) covering a given area to be color coded and combined into a single composite stage [1]. To the extent that these multiple images provide a unique "tone signature" for each type of feature, it is possible to identify that type of feature more consistently, and certainly more easily, by observing the unique characteristics of the composite color image than by attempting to discern special combinations of tone values on the individual sets of black-and-white images form which the color composite had been made.

Means have been devised for automatically converting these signatures into accurate identifications of objects and conditions. This capability is achieved primarily through a process known as "automatic

data processing" and is based on electronic computer techniques. To implement such techniques, each tone or brightness value that is exhibited on a photograph or other kind of imaginary is assigned a digit. Use is made of a "calibration area" in which the locations are known of several examples of each type of feature that is to be identified. From a study of the images of these examples one can ascertain the multiband series of digits associated with each type of feature. Once the multiband pattern of tone or brightness values has thus been derived for any given type of feature one can readily develop a computer program means of which, in principle, all other examples of this same type of feature can be identified. Because for the series of digits representing the tone signature for a given type of feature comprise a " pattern" of numbers, the identification process has come to be known as " pattern recognition." The computer print-out from such a system provides a map sheet on which the printout symbol appearing at any given point indicates the type of feature located at the corresponding point on the ground.

The significant development in photography have occurred since the 1950’s in four important areas, viz., sensors, platforms, the combing and enhancing of multiple images, and automatic data processing.

1.4 Microwaves Remote Sensing

The microwaves for remote sensing have been in application only since the early 1960’s, where as aerial photography has been used for over one forty years. The most important reasons for using microwaves are their capability to penetrate clouds and to some extent rain and their independence of the sun as a source of illumination. Another reason for the use of microwaves is that they are able to penetrate more deeply into vegetation than optical waves can. Athired reason for the use of microwaves is simply that the information available in the visible and

infrared regions complement each other. For example, the color observed in the visible and near-infrared region is determine primarily by molecular resonances in the surface layer of the vegetation or soil, where as the color in the microwave region is a result of geometric and bulk-detective properties of the surface or volume studied.

The nomenclature, symbolism and units used to express radiometric quantities, which often are different from those used in optical and infrared radiometry, are chosen from the stand point of microwaves are engineering. Appendix A provides a list of these quantities along with their optical counterpart.[2]

1.5 Radiometers

All matter radiates electromagnetic energy. The radiation is a consequence of the interaction between the atoms and molecules in the material. A material may also absorb and/or reflect energy incident upon it. When in thermodynamic equilibrium with its environment, a material absorbs and radiates energy at the same rate. A blackbody is defined as an ideal material that absorbs all of the incident radiation, reflecting none. Since energy absorbed by a material would increase its temperature if no energy were emitted a prefect absorber also is a prefect emitter. The blackbody radiation spectrum is given by Plank's radiation low, which was formulated by Max Plank in 1901 on the basis of the quantum theory of matter. This spectrum is used as a reference against which the radiation spectra of real bodies at the same physical temperature are compared.

The spectral, polarization and angular-variations of the radiation emitted, absorbed, and scattered by a medium are governed by the geometrical configuration of the surface and interior of the medium, and by the spatial distributions of its dielectric and temperature.[3]

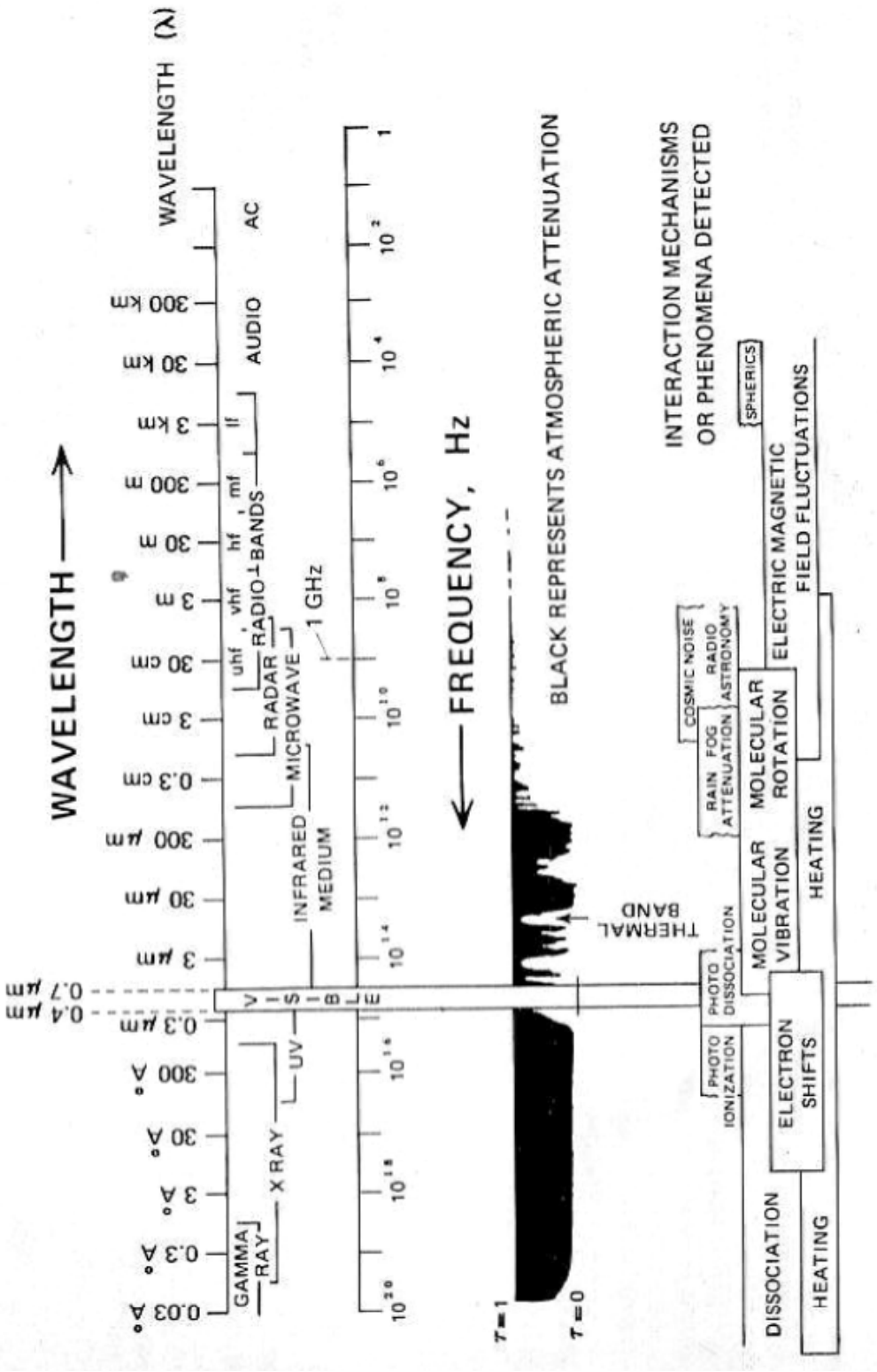

Figure (1.1): The electromagnetic Spectrum [1]

Table 1.1: Remote-Sensor Types and Application [1]

Remote sensor		Comments
Scintillation counters		
Gamma-ray spectrometer, Geiger counters	<0.003-10nm (<0.03-100A)	Measurement of emitted natural radiation by gamma ray detectors: Nal, film, etc.
Scanners with photomultipliers		
Image orthicons and cameras with filtered infrared film > 2900A	10 - 400 nm	Records incident natural radiation. Imaged ultraviolet spectroscopy available.
Cameras		
Using conventional B&W and color film	400 - 700 nm (0.4 -0.7 μm)	B &W film for high spatial detail. Improved spatial detail through contrast.
Using infrared film (B&W and IR color)	600 - 900 nm (0.6 -0.9 μm)	Greater reflectance gradients useful for vegetation surveys.
Multispectral units	300-900 nm (0.3 -0,9 μm)	Individual narrow band scenes available with multi-camera vege- steins
Lidar		
Laser radar	400- 1100 nm (0.4 -1.1 μm)	Monochromatic active system for measuring backscattered LMR from atmosphere, par-ticularly particulates.
Radiometers (infrared)	Thermal IR band (2.5 - 14 μm)	Generally measures total radiation in a wide band in the infrared region. Imagery ob-tained by scanning techniques.
Photometers	400-700 nm (0.4 -0.7 μm)	Measures luminous flux in various bands of the optical region for distribution, color, etc.
Spectrometers	In any spectral region	Narrow-band data available sequentially EMR amplitude VS frequency.
Solid-state detectors Single detectors Linear arrays Matrices	1 μm - 1 mm	Single detecting element used in scanners, radiometers. One- and two-dimensional arrays for sequential data gathering.
Radars	1mm-0.8m	Narrow-band active systems. Both analog data and imagery available.
Radiometers microwave	1mm-0.8m	Passive systems. Both analog and imagery available.

The information to be used for remote sensing is derived from quantitative measurements of the properties of EMR arriving at a sensor, the principal function of which is to make these measurements.

It is helpful to use a common nomenclature and symbolism for expressing these quantitative measurements unambiguously.[4]

1.6 Literature Review

Radiometers for remote sensing of water quality parameters need to be characterized the pollution water optical and electrical properties of water. Different studies using remote sensing in combination with theoretical and experiment work for study the water pollution are covered in the following sections:

Optical remote sensing of oceanic was developed as a science in the seventies and eighties by works like Gordon (Gordon, Brown et al., 1975 [5]; Gordon, Brown et al., 1988) [6]. Morel (Morel and Prieur 1977), [7] Sathyenranath (Sathyenranath, Lazzara et al., 1987) [8] and their associates. A driving forces was the development of satellite technology, which in 1978 led to the launch of the Nimbus 7 satellite carrying the costal zone color scanner (CZCS).

This was the first optical satellite instrument design especially for remote sensing of oceans and its main focus was spatial distribution of technology II (ocean color). Today, the sea WiFS (sea-viewing Wide Field-of-View Sensor) on the Seastar satellite has replaced CZCS as the dominant source of remote sensing data of the oceans. Remote sensing of lakes has developed in parallel to that of the oceans but has had a somewhat more difficult start as no specially-designed satellite sensors were available which in turn lead to slower integration of remote sensing with studies aquatic optics. (Dekker, 1993) [9] also partly related this somewhat slower development to the fact freshwater science is less

organized than oceanography. Despite this, early studies were performed using the MSS (Milti-spectral Scanner) and the TMC (Thematic Mapper) sensors onboard the landsat satellites a lthough they were primarily designed for terrestrial applications. Already in 1979 (Bukata, Harris et al., 1979) [10, assessed chlorophy II concentration in Lake Ontario, Canada from Landsat data. Almost two decades later, Dekker and Coworker (Dekker, Mathus et al. 1999) [11] concluded after using optical modeling together with satellite data that the Landsat systems not could be used to discriminate between chlorophyII concentration and suspended matter with general algorithms. In the mid nineties, the focus on satellites was widened as airborne multispectral sensors, more suitable for remote sensing of freshwater become commercial available.

However today, there is an apparent lack of in-water optical data from freshwaters, and we rely mainly on data from the oceans. One reason for this is that the concentrations and we rely mainly on data from the oceans. One reason for this is that the concentrations and the relationships between the optically active substances in freshwater can in some cases demand a slightly different approach to the measurements of optical properties (Davies-Colley and Vant 1987 , Tassan and Ferrari 1995; Strombeack 2001)[12,13,14]

The most abundant quantity radar back-scatter data are those for water surfaces. For remote sensing purposes, the most significant are the measurements by the-frequency airborne system of the Naval Laboratory and the fan-beam airborne of NASA[2].

One of the first experiments to yield information concerning the angular variance of radar backscatter indicated significant differences with wind velocity [15,16]. Several attempts have been made to develop a mathematical model would embody simultaneously the physical characteristics of a water surface and the radar backscatter behavior. The

polarization and depolarization dependence on the backscatter from water surfaces is likewise default to quantify. Whatever horizontally or vertically polarized incident energy will yield greater backscatter is dependent upon the surface roughness in a manner which the polarization has not yet been defined [7].

1.7 The aim of the study

The main purpose of this study is to design and implement I.R, visible and x-band microwave radiometers . Then these types of radiometers will be used to study the water pollution.

1.8 Thesis layout

The study is presented in eight chapters

Chapter one: Gives general introduction of electromagnetic spectrum, water pollution I.R and optical, microwave remote sensing radiometers, the literature review and the aim of study.

Chapter Two: Presents the I.R and visible Remote sensing theory blackbody radiation and standard units used in radiometers system for these range of bands. Also studying the electromagnetic interaction with matter and the parameters effect the radiometer in these band.

Chapter three: In this chapter microwaves remote sensing theory is studied. The reflection of radar for different shape of material reviewed with the mathematical model.

Chapter Four: In this chapter, the principle and mathematical theory of microwave is studied.

Chapter Five: In this chapter, the source of polluted water, the computable radiometric methods used in studying water pollution are reviewed, with the mathematical model.

Chapter Six: In this chapter, the design procedure of I.R, visible, and microwave radiometers is presented together with the implementation of this design in laboratory.

Chapter Seven: This chapter contains, the measurement and results for different types of design radiometers system, also include the calculation methods of different parameters for water pollution.

Chapter Eight: Presents and demonstrates the conclusions and recommendations.

Chapter Two

I.R and Visible Remote Sensing Theory

2.1 Introduction

Any complicated wave form can be considered as being composed of sinusoidal component waves or spectral components, each of which transports some share of the radiant flux of the complicated wave form. In remote sensing it is usual to consider restricted spectral bands of such spectral components rather than all components together. Sometimes the wavelength or frequency interval under consideration is clear from context. Multispectral sensing, wherein a large number of different spectral bands are considered at one time, is growing in popularity. In such cases, it is important to designate the spectral band of components to which each radiometric symbol applies. If it is desired to denote radiant flux for all components with wavelengths between 0.4 μm and 0.7 μm, as compared to the radiant flux for all components between 0.7 μm and 1.0 μm, then the symbols ϕ(0.4 to 0.7 μm) and ϕ(0.7 to 1.0 μm) may be used. From this, it is quite clear that the radiant flux for all components in the wavelength interval of 0.4 to 1.0 μm is simply.[6]

$$\phi(0.4 \text{ to } 1.0\ \mu\text{m}) = \phi(0.4 \text{ to } 0.7\ \mu\text{m}) + \phi(0.7 \text{ to } 1.0\ \mu\text{m}) \qquad \ldots(2.1)$$

An alternative is to designate the bands by band number-such as band 1, band 2, etc., and then the radiant flux for all the spectral components of band 1 is symbolized as ϕ(l).

2.2 Spectral Radiant Flux, ϕ_λ or ϕ_ν

One of the important properties of a complicated wave form of EMR is the share of the radiant flux contributed by each sinusoidal or spectral component. The manner in which this flux is distributed among the components of different wavelengths or frequencies is called the spectral

distribution. The spectral distribution of radiant flux is found by measuring the radiant flux in a narrow wavelength or frequency interval about each wavelength or frequency value through use of spectrographic equipment. For example, at wavelength, λ, with wavelength interval, $\phi[\lambda-(\Delta\lambda/2)to\lambda+(\Delta\lambda/2)]$ is measured. It should be apparent that, as the interval become smaller, the number of spectral components which are measured also become fewer. The value of $\phi[\lambda-(\Delta\lambda/2)to\lambda+(\Delta\lambda/2)]$ will become smaller and dependent upon the interval size $\Delta\lambda$. However, by dividing this narrow-band radiant flux by the wavelength interval, the ratio will approach a finite limit as wavelength interval is made smaller and smaller. This ratio is called the spectral radiant flux, and is designated by the symbol ϕ_λ for wavelength intervals, or ϕ_v, for frequency intervals. (Unit symbols for ϕ_λ are W/wavelength unite and for ϕ_v,W/frequency unit.) The spectral radiant flux value for all wavelengths specify the spectral distribution of the radiant flux.[6,7]

The spectral radiant flux values at all wavelengths provide all that is needed to calculate the radiant flux in any spectral band. The radiant flux in each narrow band is merely the value of the spectral radiant flux at the band center times the narrow band wavelength interval. The sum of the appropriate adjacent narrow band contribution yields the radiant flux of the wide band.[1]

Using the symbol of calculus,

$$\phi(\lambda_1 \text{ to } \lambda_2)=\int_{\lambda_1}^{\lambda_2}\phi_\lambda(\lambda)d\lambda \qquad \ldots(2.2)$$

2.3 Other Spectral Quantities

Just as it may be desirable to designate radiant flux with reference to a restricted band of spectral components, so this may be done for the other radiometric quantities, *Q*, *E*, *M*, *I*, and *L*. Additionally, the above applies

also for the spectral distribution of each of these quantities. When the spectral distribution is to be specified, the modifying word, spectral, is used with appropriate quantity. Thus,

Q_λ : spectral radiant energy,

ϕ_λ : spectral radiant flux,

E_λ : spectral irradiance,

M_λ : spectral exitance,

I_λ : spectral radiant intensity,

L_λ : spectral radiance.

In each case the subscript, λ, is used to indicate wavelength interval and the subscript, v, is used to indicated frequency interval. The units of the spectral entities incorporate the appropriate wavelength or frequency units in addition to the units previously given.

Spectral quantities are most often expressed as functions of wavelength per unit of wavelength interval indicated by, for example, $\phi_\lambda(\lambda)$]. For some special reason it may on it may be desired to express the same quantity as a function frequency per unit frequency interval. The relation between $\phi_\lambda(\lambda)$ and $\phi_v(v)$ is easily found from the fundamental relationship between frequency and wavelength, and between frequency interval and wavelength interval, thus,

$$\lambda v = c \text{ and } |\Delta\lambda| = (c/v^2)|\Delta v| \qquad \ldots(2.3)$$

and

$$\phi_\lambda(\lambda) = \phi_v(v)\frac{V^2}{c} \qquad \ldots(2.4)$$

Or conversely,

$$\phi_v(v) = \phi_\lambda(\lambda)\frac{\lambda^2}{c} \qquad \ldots(2.5)$$

Where c: velocity of light

In using these relations, care must be given to assure that the units of frequency, wavelength, and velocity of light are compatible.

2.4 Luminous Quantities

Human vision constitutes the most commonly used remote-sensing system, the human eye being the sensor. The eye responds to spectral components in the 0.4 to 0.7 μm range by photochemical changes in the retina.

Within the spectral range 0.4 to 0.7 μm, the photochemical response of the eye is not uniformly efficient in converting radiant flux to a visual response. The relative effectiveness of the daylight-adapted eye in diverting radiant flux of different wavelengths to visual response is called the spectral luminous efficiency and uses the symbol V(λ). Spectral luminous efficiency, a dimensionless quantity having a maximum of unity it about 0.55 μm, and decreasing to small fractions at 0.4 μm and at 0.7 μm. The visual espouse capability that can be expected from spectral flux, ϕ_λ, can be computed by using this efficiency factor in the relation:[1]

$$\phi_{\mathrm{v}} = \left(680 \ell m W^{-1}\right) \int_0^\infty \phi_{e\lambda}(\lambda) V(\lambda) d\lambda \qquad \ldots(2.6)$$

Where:

$\ell m W^{-1}$: lumens/watt , and

subscripts v and *e* are inserted to identify visual or luminous flux , ϕ_{v}, from radiant flux , ϕ_e

Luminous flux is a measure of the capability of the radiant flux to produce a visual response. The factor, 680 *lumens*/*watt*, converts the radiant unit of flux, the watt, to the luminous unit of flux, the lumen (unit symbol, ℓm). The lumen is a visual efficiency-weighted flow of radiant flux. While radiant flux is the flow of the capability of radiation to do work

or heat an object, luminous flux, as stated, is the flow of the capability to produce a visual response in humans.

2.5 Relationship between Luminous Radiant Quantities

When luminous quantities are used to describe the response of a sensor which is not the human eye, the luminous quantity is used only as a means of specifying the magnitude of a corresponding radiant quantity from a standard lamp. To illustrate, assume that a standard point source lamp has a spectral radiant intensity of $I_{e\lambda}(\lambda)$. The spectral irradiance, $E_{e\lambda}(\lambda)$, on a panel at range, R, with its normal directed at the lamp, is $I_{e\lambda} / R^2$. The illuminance on the panel, E_v, is then [1]

$$E_v = \left(680 \ell m W^{-1}\right) \int_0^\infty E_{e\lambda}(\lambda) V(\lambda) d\lambda \qquad \ldots(2.7)$$

Or

$$E_v = \frac{\left(680 \ell m W^{-1}\right)}{R^2} \int_0^\infty I_{e\lambda}(\lambda) V(\lambda) d\lambda \qquad \ldots(2.8)$$

The irradiance from the same source at the same range some spectral band of interest between wavelength λ_1 and λ_2 is

$$E_e\ (\lambda_1 \text{ to } \lambda_2) = \int_{\lambda 1}^{\lambda_2} E_{e\lambda}(\lambda)\, d\lambda \qquad \ldots(2.9)$$

Or

$$E_e\ (\lambda_1 \text{ to } \lambda_2) = \frac{1}{R^2} \int_{\lambda 1}^{\lambda_2} I_{e\lambda}(\lambda)\, d\lambda \qquad \ldots(2.10)$$

Therefore the ratio of the luminous to the radiant quantify is

$$\frac{E_{\mathrm{v}}}{E_e}(\lambda_1 \text{ to } \lambda_2) = \frac{\left(680\ell mW^{-1}\right)\int_{\lambda 1}^{\lambda_2} I_{e\lambda}(\lambda)V(\lambda)\,d\lambda}{\int_{\lambda 1}^{\lambda_2} I_{e\lambda}(\lambda)\,d\lambda} \qquad \ldots(2.11)$$

As long as the same standard source lamp and wavelengths λ_1 and λ_2, are used, still the ratio has a fixed value. The illuminace E_v is proportional to $E_e(\lambda_1 \text{ to } \lambda_2)$ and, can be used as a substitute measure for it. The standard lamp for photographic film tests has the spectral radiant intensity of a 6,000°K blackbody in the visible and near infrared spectral ranges. However, standard tungsten lamps operating at temperatures between 3200 K and 2850 K are sometime; used in tests of photoemissive tubes. Unless the spectral radiant intensity of the standard lamp and wavelenght interval of sensor operation are specified, the relation between the luminous quantity and the radiometric quantity, which it is supposed to measure, is unknown.[1]

2.6 Hemispherical Reflectance , Transmittance , and Absorptance

There are three important ratios of radiometric quantities which should be mentioned here. These are the hemispherical reflectance, transmittance, and absorptance for the entire spectrum of radiation.

The hemispherical reflectance (symbol ρ), is defined by the dimensionless ratio of the reflected exitance of a plane of material to the irradiance on that plane: [1,2]

$$\rho = M_{reflected} / E \qquad \ldots(2.12)$$

The hemispherical transmittance (symbol τ), is defined by the dimensionless ratio of the transmitted exitance leaving the opposite side of a plane, to the irradiance:

$$\tau = M_{transmitted} / E \quad \ldots(2.13)$$

The hemispherical absorptance (symbol α) is defined by the dimensionless relation:

$$\alpha = 1 - \tau - \rho \quad \ldots(2.14)$$

These definitions imply that radiant energy must be conserved. Incident flux is either returned back by reflection, transmitted through, or is transformed into some other form of energy inside a panel. The corresponding spectral hemispherical quantities may be defined with use of the spectral exitance and spectral irradiance, so that spectral hemispherical reflectance, $\rho(\lambda)$, is given by

$$\rho(\lambda) = M_{\lambda reflected} / E_{\lambda} \quad \ldots(2.15)$$

Spectral hemispherical transmittance, $\tau(\lambda)$, is given by:

$$\tau(\lambda) = M_{\lambda transmitted} / E_{\lambda} \quad \ldots(2.16)$$

and the spectral hemispherical absorptance, $\alpha(\lambda)$, is given by

$$\alpha(\lambda) = 1 - \rho(\lambda) - \tau(\lambda) \quad \ldots(2.17)$$

In this latter case, one must assume that the internal conversion by fluorescence of radiation of short wavelength to long wavelength does not occur.[1,2]

The spectral reflectance, transmittance, and absorptance are also dimensionless quantities. The implied wavelength dependence is indicated by the usual function symbol (λ), rather than by subscript, since the use of

the subscript λ has been reserved to indicate a differential quantity with a change in units. The radiometric concepts are summarized in Appendix A

2.7 Responsivity, R

the output of a radiation detector is an observable physical change, response, or signal indicative of the character of the incident flux on the sensor. The ideal radiometer for incoherent radiation would be one that produces a signal in proportion to the radiant flux arriving at the sensor from a well defined direction within a known solid angle or cone angle including that direction, and which contains spectral components only in some spectral band wavelengths, λ_1 and λ_2. The proportionally constant, R, relating signal out of the radiometer to incident flux having these qualities, called the radiometer responsivity, also symbolized as R. Thus [8,9]

$$S = R\phi(\lambda_1 \text{ to } \lambda_2) \qquad \ldots(2.18)$$

Where:

S : value of the signal. (volt)

Responsively can be determined by a calibration experiment where a source supplies a known incident flux, $\phi(\lambda_1 \text{ to } \lambda_2)$, and the radiation detector responds with the corresponding signal for that flux. The value of R is determined so that one may infer from the signal the value of incident flux for unknown sources.

Actually, radiometers are not equally responsive to radiant flux at all wavelengths within their operating range. Their responsively to radiant flux depends upon the wavelength of the incident flux. The calibration of a radiometer can be done for flux at every wavelength by laboratory test. The set of responsively values for each wavelength is called the spectral responsively , and is symbol R (λ). A small amount of radiant flux in a

narrow spectral band, $\Delta\lambda$, centered at wavelength, λ_1, when applied to a radiometer produces a small signal, Δs, so that

$$\Delta S_1 = R(\lambda_1)\,\phi_\lambda(\lambda_1)\Delta\lambda \qquad \ldots(2.19)$$

By changing the center wavelength to λ_2, a small signal, ΔS_2, is obtained:

$$\Delta S_2 = R(\lambda_2)\,\phi_\lambda(\lambda_2)\Delta\lambda \qquad \ldots(2.20)$$

An important assumption is made concerning the simultaneous response to flux in two different spectral regions by actual radiometers. That is, the signal resulting from simultaneous exposure to flux in different spectral bands is the sum of the signals which would result from exposure to each separately.

Therefore, it is assumed that when the flux from the two spectral bands centered at λ_1, and λ_2 are both incident upon the radiometer, the resulting signal, $\Delta S_{combined}$ is

$$\Delta S_{combined} = \Delta S_1 + \Delta S_2, \text{ or} \qquad \ldots(2.21)$$

$$\Delta S_{combined} = [R(\lambda_1)\,\phi_\lambda(\lambda_1) + R(\lambda_2)\,\phi_\lambda(\lambda_2)]\,\Delta\lambda \qquad \ldots(2.22)$$

The signal for incident broad-band spectral flux is then , in integral,

$$S = \int_0^\infty R(\lambda)\,\phi_\lambda(\lambda)\,d\lambda \qquad \ldots(2.23)$$

It is important to note that the signal, S, is not uniquely indicative of the value of the incident flux, ϕ(λ_1 to λ_2), which is given by; [8,9]

$$\phi = \int_{\lambda 1}^{\lambda_2} \phi_\lambda(\lambda)\,d\lambda \qquad \ldots(2.24)$$

unless R(λ) does not change with wavelength in the range λ_1 to λ_2, and is otherwise zero. Yet, it is the value of signal, S, which the remote sensor supplies rather than the value of ϕ.

2.8 Normalization

Therefore, real radiometers, the spectral responsivities of which are not constant over the spectral range in which they respond, have an inherent inaccuracy. It is important to devise a measurement procedure which minimizes inaccuracy. The plan is to find a means of calculating an average or effective spectra! band of operation. Such a calculation is said to normalize the spectra1 responsively.

The most frequently used normalization is called normalization to the peak. The spectral responsively of a real radiometer generally has a maximum (.or peak) [value for flux at one wavelength which reduced values for flux at other wavelengths. Let the maximum responsively be symbolized as R_{peak}. Now one might infer the value of incident flux from the signal valise by the approximate relation

$$S \cong R_{peak}\ \phi(\lambda_1\ to\ \lambda_2), \qquad \ldots(2.25)$$

Where

λ_1 and λ_2 are the effective spectral limits of response of the radiometer to be determined by normalization.

The effective spectral bandwidth, $\lambda_2 - \lambda_1$, of a real radiometer is found by the relation, [8,9]

$$R_{peak}\ (\lambda_2 - \lambda_1) = \int_{\lambda 1}^{\lambda_2} R(\lambda)\, \Delta\lambda, \qquad \ldots(2.26)$$

2.9 Blackbodies

An ideal thermal emitter, called a blackbody, is one which transforms heat energy into radiant energy with the maximum rate permitted by thermodynamic laws. This is a useful concept since it establishes the maximum conversion rate possible when emission is due to heat energy conversion. Planck derived a formula for the spectral exitance which a blackbody should have, based upon theoretical thermodynamic

reasoning. Any real material at the same temperature cannot emit thermally at a rate in excess of that of a blackbody Figure (2.1). The reverse process of absorption must likewise be maximum so that a blackbody must absorb and convert all incident radiant energy into heat energy regardless of the spectral band of radiant energy. Planck's formula for blackbody spectral exitance M_λ is given as, [1]

$$M_\lambda = c_1 \lambda^{-5} [\exp(c_2 / \lambda T) - 1]^{-1}, \quad \ldots(2.27)$$

Where:

$c_1 = 3.74 \times 10^{-16}\ Wm^2$

$c_2 = 1.44 \times 10^{-2}\ m\ ^0K$

$\lambda =$ wavelength in meters.

$T =$ absolute temperature in Kelvin.

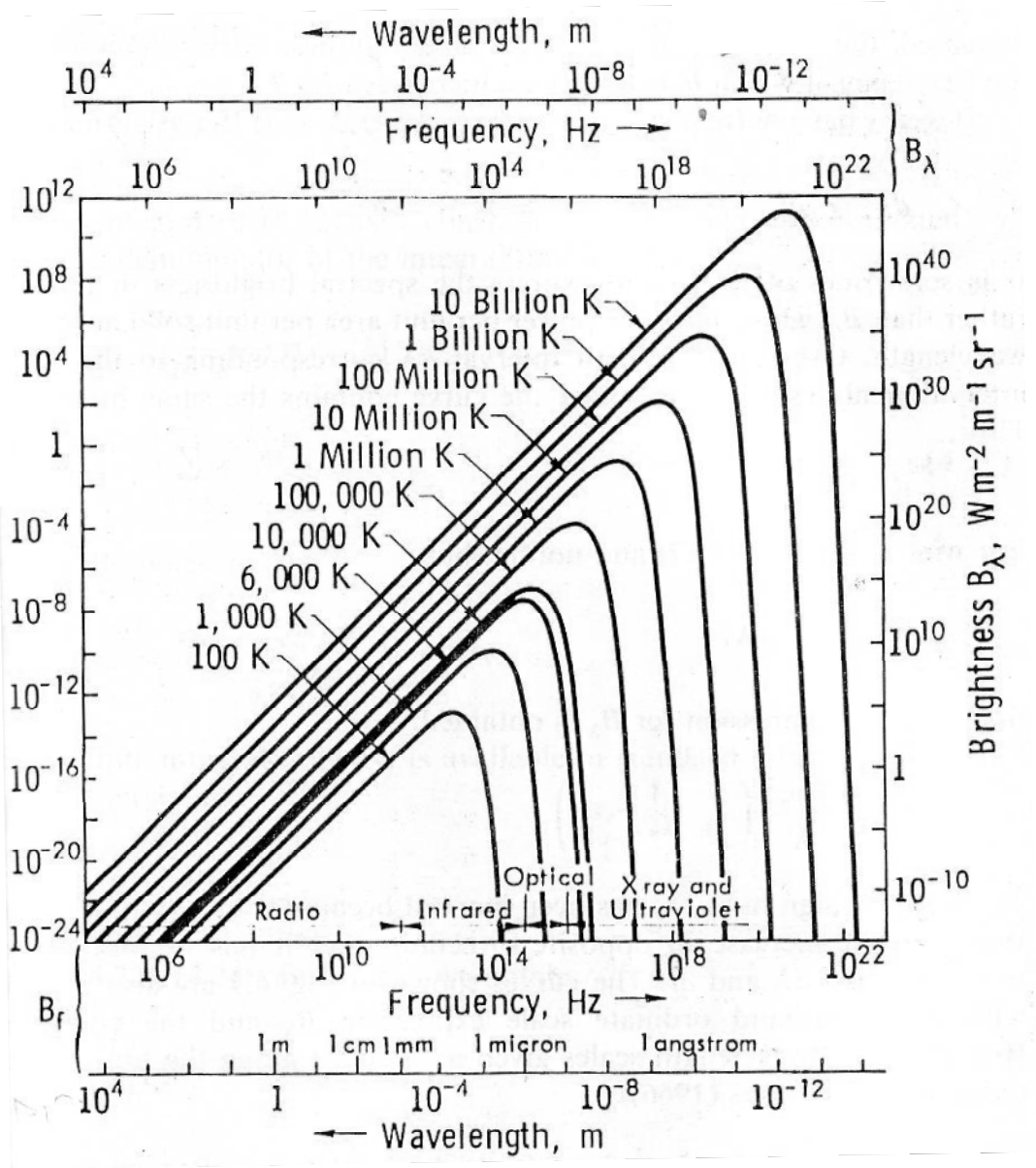

Figure. (2.1) : Planck radiation-low curves [1]

The spectral exitance of a blackbody at a given temperature is not the same at all wavelengths. For very long and very short wavelengths, the spectral exitance is low as shown in Figure 2.1. For some wavelength in between, the spectral exitance readies a maximum value depending upon the temperature of the blackbody. That wavelength, λ_m, for which the spectral exitance has its maximum value, is given by the Wien displacement law

$$\lambda_m = c / T \qquad \ldots(2.28)$$

Where

$c = 2.898 \times 10^{-3}\ m\ ^{0}K$

The exitance of a blackbody for the spectral band of wavelengths is given by the Stehan-Boltzmann Law,

$$M_{(blockbody \text{ at T})} = \sigma T^4 \qquad \ldots(2.29)$$

Where:

$\sigma = 5.669 \times 10^{-8}\ \text{W}\ m^{-2}\ ^{0}K$

2.10 Spectral Emissivity, $\varepsilon(\lambda)$

Any body of material at a specific temperature emits radiation in accordance with its own characteristics. It is convenient and customary to express the capability to it radiation due to thermal-energy conversion as the ratio of the spectral exitance of a material to the spectral exitanee of a blackbody at the same temperature. This ratio is called the spectral emissivity of the martial, and is given by the .symbol, $\varepsilon(\lambda)$. Thus [1]

$$\varepsilon(\lambda) = \frac{M_{\lambda(material,^{o}K)}}{M_{\lambda(blockbody,^{o}K)}}, \qquad \ldots(2.30)$$

the spcctra1 emissivity is nearly independent of temperature for most common materials and for temperatures of a terrestrial environment. Significant changes in spectral emissivity can be expected whenever the material undergoes a change of state such as melting, vaporization, oxidation, or any other change which alters the fundamental arrangement of the atomic and molecular components.

For those conditions where the spectral emissivity does not change significantly with temperature, the spectral extence of any material at any temperature can stated if the spectral emissivity is known for the materials. These calculations are simply done by use of the defining relations above

and the blackbody spectral exitancc formula, or a suitable blackbody spectral exitance table of values.

Kirchioff's Law states that, under conditions of thermal equilibrium, the spectral emissivity of a material must be equal to the spectral absorptions of that material. Experience has shown that Kirchioff's Law holds with good accuracy, even in conditions where thermal equilibrium is not present, provided that temperature differences are not extreme. One can expect Kirchioff's Law to apply to most terrestrial conditions. Therefore, it is common practice to determine (lie spectral emissivity of a substance by measuring the spectral absorptance of that substance.

The thermal emission spectrum contains the same spectral details as does the spectral absorptance. Thus, the thermal emission spectra of solids and liquids have fewer spectral details by which they can be identified. Many common materials are spectrally similar in the 8 to 14 μm infra-red range, with a spectral emissivity between 0.85 and 0.95. In the spectral range from 3 to 6 μm, the spectral emissivity of those materials tends to differ considerably. When a temperature measurement is made of a terrestrial material by remote means, it is wise to use the 8 to 14 μm band, where it may be assumed that the emissivity of the various terrestrial materials are similar; and an estimated emissivily of 0.90 is probably not far from the truth. [1]

2.11 Blackbody Standards

It is frequently necessary to utilize a source of radiation, the spectral radiance of which is known, in order to calibrate a remote sensing apparatus. For microwave systems, these sources are signal generators with known frequency and power output. For the infrared and visible spectral ranges, blackbody cavities at a known temperature are used in conjunction with Planck's formula. Any closed cavity with opaque walls coated with an absorbing material produces blackbody radiation within the

cavity, provided only that the walls are all at the same temperature. A small hole in one wall will allow a small part of the radiation to escape, the spectral radiant exitance of that hole being given by Plank's formula if the hole is very small. Even a nonce can construct reliable blackbody standards out of old tin cans with constant temperature water jackets if the blackbody temperature is near the ambient temperature.

If considerable flux is to be generated in the visible spectral range, the blackbody temperature should be above 1,000°K. A blackbody cavity operating at these temperatures poses numerous practical problems with which the novice should not tangle. Commercial black-body sources are available which may be checked against the accurate high-temperature blackbody source of the National Bureau of Standards.

A true blackbody surface is necessarily a Lambertian radiator, so that the relation between spectral radiance and spectral exitance is simply. [1,2]

$$L_{\lambda(blockbody)} = M_{\lambda(blockbody)} / \pi , \qquad \ldots(2.30)$$

Practical blackbody standards are not necessarily Lambertian radiators unless the cavity hole perimeter lies in a plane and the depth of the hole in the cavity wall is small as compared with the width of the hole.

2.12 Apparent, Brightness, and Color Temperatures

Remotely sensed temperature readings form one of the important remote-sensing tasks. The radiant flux arriving at a sensor from a remote object is measured.

The apparent temperature of a surface is the temperature of a blackbody surface which, when placed in front of the receiver aperture, would produce the same received flux within the spectral band of the receiver. Thus, the apparent temperature of a surface is determined not only by the actual temperature of the surface material but also by the emissivity of the material, the atmospheric effects between surface and sensor, and the spectral band used by the receiver.

The brightness temperature of a surface is the same as the apparent temperature. The former term is frequently used in literature relating to microwaves, while apparent temperature is more often used in literature relating to infrared applications.

Color, temperature may have a number of meanings depending upon context. If the ratio of emitted spectral radiance of a surface is measured at two different wavelengths, the color temperature is the temperature of a blackbody surface which will produce that same spectral radiance ratio at these two wavelengths. For visual contexts the color temperature of a source is the temperature of a blackbody which will produce the same visual color as that source.

Most materials in a natural environment do not produce blackbody radiation because of the variations of the spectral emissivity with wavelength and, in addition, most objects do not have one temperature only; the temperature varies over the surface and below the surface. Radiant flux may originate within the material if it is partially transparent to the emitted radiation. When such temperature ; emissivity variations are not large, the emitted flux spectrally similar to blackbody radiation in cert restricted spectral bands. Under such conditions the three concepts of temperature -apparent, brightness and color are useful.[1,2]

2.13 Classifications of Parameters

2.13.1 Source Parameters

The parameters relating to the ground are, in part both structural and textural. Information about the gross and fine details of the ground surface is important in the analysis of remote-sensor data. Even more important is information about the electrical parameters of the surface, how they vary with location and time, and their relationship with ground or soil properties. The key parameters common to the visible and infrared regions are: reflectance ρ, absorptance α, enmittance ε, and transmittance τ.

These parameters are functions of the wavelength, angle of incidence, and polarization.

2.13.2 Power and Voltage Parameters

The common terminology in the longer wavelength radar range is a voltage designation, or the Fresnel reflection coefficient R, which is called reflectivity, and is generally accepted to relate to an interaction at a single boundary. The relation between the voltage and power parameters is given: the absolute magnitude of the voltage reflection coefficient squared, $|R|^2$, is equal to the reflectance, ρ . The voltage reflectivity *R* is found to be related to the dielectric properties of the substance, its dielectric constant, and its conductivity. The dependence on the angle of incidence and polarization plays an important role in remote sensing .

Polarization, p, and wavelength, λ, are two other parameters included in models. They are controllable to a certain degree and become useful tools of remote sensing.

2.13.3 Atmospheric Parameters

The atmosphere is also described by those parameters identified above, except that textural properties are no longer appropriate for defining conditions; rather, terms such as stratification, layering, and turbulence are noted.

2.13.4 Platform and Sensor Parameter

Another set of parameters associated with the platform and remote sensor, and important in modeling and in the consequent interpretation of results, is geometric; these parameters establish the spatial relations of the remote sensor and the ground or region being surveyed. Generally, spherical coordinates are used to show Sun, satellite, or aircraft position and the direction of the EMR.

2.14 Interaction Mechanism

Interaction of electromagnetic radiation (EMR) with surfaces causes the incident EMR to be reflected either specularly or diffusely; transmitted or diffracted into the surface; absorbed by the surface and subsurface and all, or partially, reradiated or scattered. Reflection, transmission, absorption, and emission are often treated as surface phenomena; however, a complete analysis must include penetration into the medium below the surface. [8]

Physically, the incident electromagnetic radiation induces an oscillatory motion of free and bound charges in the surface, which in turn radiant a secondary field back into the first medium of forward into tire second medium.

Electromagnetic radiation interactions take place with substances of various geometries and extents such as land areas, buildings, and bodies of water; these interactions can be quite simple or exceedingly complex.

The incident electromagnetic radiation, upon interaction with a surface or object, can experience a number of changes; primarily of magnitude, direction, polarization, wavelength, and phase.

The same changes take place in the atmosphere; however the interactions are considered on a volume basis rather than as a surface phenomenon.

Electromagnetic radiation interactions are detected by remote sensors, which may be relatively simple or highly complex, and which are designed to selectively respond to radiation from different parts of the electromagnetic spectrum. The art or ability to extract useful information from remote sensor data plays a major role in establishing remote sensing as a useful tool for mankind. For example, a color photograph of a land area taken from a space platform supplies the analyst with both spatial and spectral information. The spatial detail-size, geometry, orientation provides

the analyst with information to recognize boundaries, vegetated areas, etc. Spectral information -color or color variations-can provide, with additional aids, the identification of soil and vegetation types. The reliability of identifications is a function of the degree of correlation possible between the photograph, the spatial and spectral data, and a valid information base. The information base may be derived from a library or data center containing pilots or computed results obtained from the EMR interaction. [31].

2.15 Optical Properties of Pure Water

Sunlight entering a water body (solar radiation and diffuse sky radiation) is subjected to depletion as a result of (1) absorption and scattering by the pure water, and (2) scattering, diffraction and reflection by suspended particles in the water. The color of water is believed to result from that part of solar radiation that penetrates into the water and which as so-called underlight reaches the surface again after selective scattering and reflection on suspended particles. The penetration of radiation into pure water is described by means of an extinction coefficient, k, which takes into account the effects of both scattering and absorption. [23,24,25]

A parallel (unscattered) beam of radiation of wavelength λ passing through a distance, *dx*, in water is reduced in intensity by an amount *dI*, which is proportional to the intensity and to the distance, *dx*, or

$$dI = -kIdx \qquad \ldots(2.31)$$

Where k has dimensions of L^{-1} (*L* is length) and is dependent on wavelength λ.

If the intensity of the radiation at $x = 0$ is I_o, then for some distance *x*

$$I = I_o e^{-kx} \qquad \ldots(2.32)$$

The introduction of suspended organic and inorganic materials introduces further scattering, absorption, and reflection by these particles. Scattering by small (in comparison to the wavelength of light) particles is

wavelength selective and Rayleigh's law applies. The small wavelengths are scattered most, and the basic blue color of the water remains relatively unchanged. As particle size increases, scattering becomes independent of wavelength so that a color shift of the water towards the green begins to occur. With increasing turbidity, water color shifts even more towards yellowish green until the color of the water approaches or becomes that of the natural color of the particles creating the turbidity.[26,27,28,29]

Discoloration of water can also occur as a result of the presence of life forms, such as algae. In these instances, the color of the predominant life form will basically determine the water color. Finally, in shallow waters, the natural color of the bottom can be seen and water color will be altered toward bottom color.

2.16 Infrared Radiant Flux Reflected or Emitted from Water Surfaces

A simplified optical-ray diagram is shown in Figure 5-3 for an experimental application of an airborne multispectral scanner or spectrometer for sensing radiant flux reflected and/or emitted from a water surface. An active radiant source may be needed for such applications. The active source should be the Sun, a wavelength-tunable laser, an array of different lasers, high intensity lamps, flash lamps, or a microwave unit, whichever would be most satisfactory for a particular application. As shown, the source emits radiant flux that is incident on a smooth water surface at angle θ and is then partially reflected at angle θ to the scanner or spectrometer.

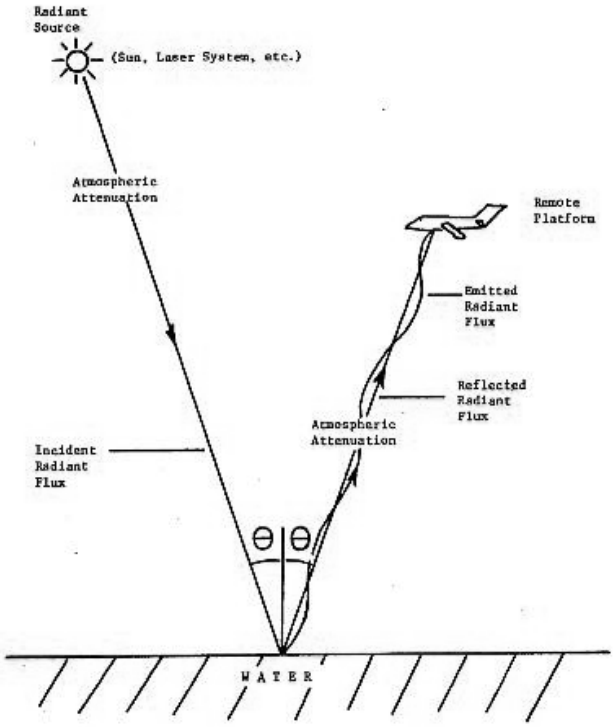

Fig. 2.2. A simplified optical ray diagram for a typical reflectance-emittance type remote-sensing experiment using an airborne multispectral scanner or spectrometer. [30]

The Cox and Munk (1956) [1] model for the slopes of sea surfaces applies for investigations that include rough water surfaces. In longer wavelength regions of the infrared, $\lambda \geq 8\ \mu$m, radiant flux emitted from the water surface irradiates the detector system of the scanner or spectrometer. The signals produced and recorded from each individual channel of the scanner, or from the spectrometer at a particular wavelength setting, is represented by extending the equations of Kriegler et al, (1969) or Crane (1971) [1] to include (1) both components of polarization for radiant flux reflected from the water surface and (2) radiant flux emitted by the water surface. We have [30]

$$S(\delta\lambda) = \frac{mA\Omega\cos\theta}{\pi}\int_{\lambda_o}^{\lambda_o+\delta\lambda}\{\tau(\lambda,\theta)E(\lambda)_h[R(\lambda,\theta,T)_h K_h(\lambda) + \left(\frac{1+P}{1-P}\right)R(\lambda,\theta,T)_v k_v(\lambda)]\}dx + \frac{mA\Omega\cos\theta}{\pi}\int_{\lambda_o+}^{\lambda_o+\delta\lambda}\{\tau(\lambda,\theta)\frac{p(\lambda,T)}{2}[\varepsilon(\lambda,\theta,T)_h k_h(\lambda) + \varepsilon(\lambda,\theta,T)_v k_v(\lambda)]\}dx + ma\int_{\lambda_o}^{\lambda_o+\delta\lambda}[E(\lambda,\theta)_h^s k_h(\lambda) + E(\lambda,\theta)_v^s k_v(\lambda)]dx + noise \quad ..(2.33)$$

Where:

m: proportionality constant representing sensitivity and gain of the associated amplifier system (volts/amp);

A: area of water surface viewed by the detector (m^2);

θ: angle of incidence and angle of reflection (rad);

$d\Omega$: solid angle subtended by detector (strad);

a : surface area of detector (m^2);

π :normalization factor obtained by integrating cos θ over a hemisphere

λ: wavelength (μm);

$\tau(\lambda,\theta)$: spectral atmospheric transmittance (unitless);

$E(\lambda)$: irradiance at water surface (watts/m^2);

v,h : denote linear polarization of radiant flux perpendicular (vertical) and parallel (horizontal) to the water surface respectively (unitless);

T: absolute temperature (°K);

$R(\lambda,\theta,T)$: specular spectral reflectance at angle θ for water surface at temperature, T (unitless);

$k(\lambda)$: product of reflectance and transmittance factors of optical system and spectral sensitivity of detector (amp/watt);

p : degree of polarization of incident radiant flux (unitless);

$p(\lambda,T)$: Planck, blackbody, spectral radiance (watts/m^2 . μm)

$\varepsilon(\lambda,\theta,T)$: monochromatic, specular emittance at angle θ, for a plane water surface at temperature, T, in the infrared $\varepsilon(\lambda,\theta,T)=1-R(\lambda,\theta,T)$ (unitless);

$E(\lambda,\theta)^s$: irradiance of the detector surface by scattered radiant flux (watts/m^2);

$\delta\lambda$: wavelength interval of single multi-spectral channel,

The first term in Eq. 5-8 represents the portion of the signal due to radiant flux emitted from the source and then reflected from the surface of the water. The second term represents the portion of the signal due to radiant flux emitted from the water surface. The third term represents an extraneous portion of the signal which is due to radiant flux scattered by the atmosphere to the detector of the scanner or spectrometer. The final term represents the inherent, electronic noise associated with optical instruments that sense radiant flux of relatively low wattage. If the radiant source is not present, then E(λ) = 0 and the first term vanishes from the equation; the resultant equation has application to investigations of nighttime use of scanners or spectrometers.

Chapter Three

Microwave Remote Sensing Theory

3.1 Introduction

Microwave sensors can measure through cloud cover and some rain, although the measurement is almost independent of the weather at the lower microwave frequencies. Thus, microwave sensors are unique in their capability to provide timely information under conditions when other sensors are rendered inoperable by the weather. [17,18,19]

Microwave responses are functions of the frequency (or wavelength), polarization, and look angle, as are responses in other parts of the spectrum. The micro-wavelength range is far from "micro," as compared with the visible and infrared ranges; it may be considered to extend approximately from 1-mm to 1-m wavelength. The wavelength ratio between the longest and shortest microwave is therefore greater than that between the longest useful infrared and the shortest visible wavelength. Polarization is often used as a discriminant in the microwave region because microwave antennas used for reception are most easily built with a single polarization direction, whereas most optical detectors are relatively independent of polarization, and special effort must be made to polarize the signal prior to detection. Incident angle variations in observed signals are common to all regions of the spectrum, but of course at each point in the spectrum these variations are different. The geometry of radar range measurement encourages the use of observational angles well away from the vertical, while the radiometer (much as with the optical and infrared sensors) tends to be used more often in a near-vertical mode.

Active microwave sensors provide their own illumination, while passive systems measure radiation originating somewhere other than in the radiometer. Normally the radar source is coincident with the receiving point, so the optical analog would be observation with backlighting from

the sun and no sky-lighting whatever. Most active microwave sensors both detect and measure range, but some measure only amplitude or speed, not range. Nevertheless, the term radar (meaning Radio Detecting And Ranging) is used commonly to describe even the nonranging active microwave systems, and it will be used that way here.

Resolution with microwave sensors normally is poorer than with sensors operating in the optical and infrared region. This happens because the diffraction limit for angular resolution is directly proportional to the wavelength, and the shortest micro-wavelength is used a factor of 1000 larger than the wavelength for thermal infrared sensing. Fine-angular-resolution microwave sensors therefore require very large apertures. Radars may achieve large apertures by coherent storage of the observed signal and subsequent synthetic aperture production, but passive microwave sensors are restricted to those apertures that can be physically constructed.

The observed phenomena different from those observed in the optical and infrared parts of the spectrum. Thus applications of radar depend both on the all-weather illumination-independent nature of their performance and on the fact that they "see" different things.

Range measurement and Doppler beam sharpening are possible with a radar because the designer can correlate the received signal with the illumination signal. Since the radiometer measures signals emitted by the target or by the atmosphere or extra-terrestrial sources, this correlation is essentially impossible for a passive system.

A radar scatterometer is a device that measures the scattering properties of the region observed. Any radar that makes an accurate measurement of the strength of the observed signal is therefore a scatterometer. However, most existing radars that produce images are uncalibrated; consequently, most radar scatterometers are not imaging systems. A calibrated imager, however, would also be a scatterometer.

The radar scatterometer has merit of its own in oceanographic applications where its poor resolution is not of great significance. Over land its primary purpose is collecting information which can then be used to design other radars. The altimeter is primarily of use for low altitude profiling, although some altimeter systems have been made that provide additional information, and an altimeter over the sea can be useful for very high accuracy profiling of mean sea level from satellites.

The term microwave radiometer is normally applied to passive microwave systems. The signal received by the radiometer is a complex combination of thermally emitted radiation from ground and atmosphere, together with scattered emission originating in the atmosphere and extra-terrestrially, both in the sun and outside the solar system. Strictly speaking, a scatterometer is also a radiometer, since it measures a signal radiated by the scatterometer itself and scattered from the target area, but the term radiometer is reserved here for passive devices.

Microwave radiometers have proven quite useful for meteorological measurements, and like radars, they are sensitive to soil moisture and snow properties. The radiometer is particularly valuable for meteorological purposes because of the sensitivity to atmospheric emission, and because the resolution is too poor except from quite low altitudes for most land applications. On the other hand, microwave radiometers carried in low-altitude aircraft can produce images with characteristics complementary to those of other imaging systems. Because of the inherently poorer resolution of the radiometer, its greatest application will lie in meteorological and oceanographic uses, rather than land observations.[16]

3.2 The Radar Equation

The performance of a radar is conveniently described by the radar equation, which relates the received power to the target parameters and the

parameters of the radar. With the path losses neglected, the received power may be written as one form of the radar equation, [7]

$$W_r = \frac{W_t G_t}{4\pi R^2} \sigma \frac{1}{4\pi R^2} A_r \qquad \ldots(3.1)$$

Where:

W_r : received power

W_t : transmitted power

G_t : gain of the transmitting antenna in the direction of the target

R: distance between radar and target

σ : radar cross section; effective backscatter area of the target, explicitly, the actual cross section of a sphere which, when placed in the same position as the target, would scatter back to the radar the same amount of energy as is returned by the target

A_r : effective receiving area of the receiving antenna aperture.

The above equation assumes that the same antenna is used for both transmitting and receiving; implying, of course, that the transmitter and the receiver are in the same location.

The transmitted EMR received at the target is given by $W_t G_t / 4\pi R^2$. This expression, multiplied by σ, indicates the total EMR scattered by the target, which can be shown by W_s. Thus, the amount of EMR received at the receiver is $W_s / 4\pi R^2$, and the received power should be the density of EMR multiplied by the effective size of the receiving antenna aperture, A_s.

Most sense applications involve extended targets that usually are much larger than a resolution cell of the radar. In this case, it is more convenient to define an average differential cross-section or radar cross-section per unit area, and to consider the average return power. The total average received power is then given by integrating the return from each differential area over the entire irradiated area. The average differential

cross-section is also known as the scattering coefficient, and is commonly denoted by σ_o . Thus, the average received power, when written in terms of the scattering coefficient, is

$$W_{ar} = \int_{A_o} \frac{W_t G_t}{4\pi R^2} \sigma_o \frac{A_r}{4\pi R^2} ds, \qquad \ldots(3.2)$$

S: Surface, the surface integral is taken over the irradiated area A_o

σ_o : scattering coefficient

The effective size of the antenna aperture is related to the antenna gain by

$$A_r = G_t \lambda^2 / 4\pi \qquad \ldots(3.3)$$

Hence, W_{ar} may be written more compactly as

$$W_{ar} = \frac{\lambda^2}{(4\pi)^2 R^2} \int_{A_o} \frac{W_t G_t^2}{R^2} \sigma_o ds \qquad \ldots(3.4)$$

When a radar is used to observe a volume distribution of materials rather than a surface distribution, the scattering cross-section per unit volume should be used in place of σ_o in Eq. 3-4. Of course, the integral should also be changed to a volume integral over the illuminated volume. Examples of volume scattering are found in radar observations of clouds, rain, and any non-homogeneous layer, such as snow-covered terrain.

The equation for the received power indicates that W_t, G, and λ are parameters of the radar system, and R is determined by the location of the radar with respect to the target. Design and operation of radars are such that these quantities normally either remain constant or are known during use of the radar. The factor that governs the average return power strength as a function of the way in which the incident EM interacts with the surface is, therefore, σ_o .

3.3 Interaction Parameters

The scattering coefficient, σ_o, in general, is a function of polarization, look angle, wavelength, and interaction properties of the target: geometric, dielectric, and conductive. When transmitted power, antenna gain, wavelength, and polarization are fixed by system design, the average return power strength varies only with σ_o.

The grey tone on a radar image is proportional to the average return power strength and hence, to σ_o. If the imaging radar system is amplitude calibrated and enough levels of calibration signals are placed on the same film which records the radar signal, a microdensitometer reading of the film may be related to the average received power and σ_o.

The variation of σ_o with the look angle may also be obtained if similar regions can be identified at different look angles and with different parts of the image. Conversely, if measured or computed scattering coefficients are available for certain targets, the variation of the grey tone on the images of these targets may also be inferred. In so doing, it is important to realize that the tonal variation on a radar image depends upon the relative rather than the absolute scattering strengths of individual targets.

3.4 Basic Principles of Radar Returns

Radar returns from a target depend upon both the strength of the transmitted energy and the reflecting capability of the target. Most radar targets reflect with different strengths, different directions, and their reflection characteristics may be conveniently described in terms of their reflection, or re-radiation, patterns (plots of signal strength versus angle). The backscatter pattern is of particular importance; it shows the return signal strength in the opposite direction of the incident radiation.

For an extended target (a corn field for instance) the instantaneous return fluctuates (fades) over a wide range as the radar beam moves over it.

This is due to changes in the relative phase of signals from different parts of elements forming the target. Despite the rapid signal fluctuation, the radar is supposed to be looking at the same target under similar conditions. Hence, it is meaningful only to speak of the average return rather than the instantaneous return for extended targets. Such an averaged backscattered power is related directly to the scattering coefficient. The purpose of the averaging is to smooth out the fluctuation (fading) of the return signal. If the amount of averaging is not enough to produce a smooth signal, "speckles" will show up on the images.

Many complicated radar targets can be approximated by a collection of facets, spheres, or cylinders. Corner reflectors may also be needed in modeling man-made ground targets, such as a side wall located on a flat piece of ground.

3.5 Polarization and Look Angle

Imaging radars usually transmit a horizontal electric-field vector, and receive either horizontal or vertical return signals, or both. The HH (transmit and receive horizontal electric-field vector) return is also known as the like-polarized return; the HV (receive vertical electric-field vector) return is known as the cross-polarized return. Radar images produced by the like-polarized return signal may be different from those produced by the cross-polarized return, because of the differences between the physical processes responsible for the two types of returns. Such differences have been shown to provide potentials for differentiation of geologic and geographic features [1].

The basic physical processes responsible for the like-polarized return are quasi-specular reflection and scattering. The quasi-specular reflection normally accounts for the high return near vertical incidence. As imaging radars transmit at moderate to large incident angles, the scattering process plays a dominant role in polarized returns, both surface and volume

scattering being commonly encountered in applications. Returns due to surface scattering are normally stronger near vertical incidence and decrease with increasing incident angle, with a slower rate of decrease for rougher surfaces. Returns due to volume scattering tend to be uniform for all incident angles away from grazing.

3.6 Depolarization Mechanisms

Four mechanisms known to be able to cause depolarization of EMR-that is, to produce cross-polarized radar returns-are: (1) quasi-specular reflection as a result of the difference between the Fresnel reflection coefficients for a homogeneous two-dimensionally smoothly undulating surface: (2) multiple scattering as a result of target surface roughness; (3) volume scattering due to nonhomogeneities, especially those embedded within a skin-depth of the target surface; and (4) anisotropic properties of the targets.

Of these four mechanisms, only the first three are commonly encountered in applications. The first mechanism, applicable only to smoothly undulating surfaces, predicts essentially no cross-polarized returns near the vertical, and increasingly larger returns at larger incident angles, except near the grazing point. However, the level of the returns remains low as compared with the levels predicted by the second and the third mechanisms, both of which are applicable to rough terrains with or without vegetation cover (regardless of type). These mechanisms predict fairly uniform returns over all incident angles, except near the grazing point, where the return decreases to zero. In general, the third mechanism produces higher level returns that the second.

A significant point about the cross-polarized scattering is that the level difference (or contrast in imagery) between two types of terrain remains fairly constant as the incident angle increases, until close to the

grazing wave to decrease to about 37% of its original value. This quantity, denoted by δ, is related to the wavelength in this manner.[1]

$$\delta = \left(\frac{\lambda}{\pi g n} \right)^{1/2} \quad \ldots(3.5)$$

Where:

δ: skin depth

g: conductivity

$n = (\mu / \varepsilon)^{1/2}$: reflective index.

in which

ε: permittivity of the terrain

μ: permeability of the terrain.

3.7 Microwave Radiometry

The technique of microwave radiometric sensing of terrestrial materials is a relatively old addition in the electromagnetic remote sensing group. Although numerous passive microwave observations have been conducted since Dicke first introduced the switched receiver concept (Dicke, 1946) [1] , the interest was concentrated on measuring thermal emission from extraterrestrial objects (radio astronomy) and from the earth's atmosphere. During the late 1950's, [1] Straiton's group at the University of Texas used a 4.3-mm radiometer system, which had been developed to measure the solar temperature and atmospheric attenuation, to measure the apparent temperatures of several terrestrial materials, such as water, wood, grass, asphalt, gravel, and asbestos. These experiments represent the first genuine effort (other than classified military investigations) in which the radiometer antenna was pointed down rather than up. They also perhaps represent the first step towards the recognition of what is today known as Passive Microwave Remote Sensing as a major tool in the study of physical phenomena, either terrestrial or extraterrestrial in nature.

Over the past fifteen years, the science of microwave radiometry has established itself as an integral part of satellite remote sensing. Man's first close reconnaissance of another planet-Venus-was made by the Mariner 2 spacecraft on December 14, 1962 (Barrett and Lilley, 1963) [1]. The spacecraft was instrumented with several sensors, including a two-channel microwave radiometer operating at wavelengths of 1.35 and 1.9 cm. Spacecraft radiometric investigation of the earth was initiated in 1968 by the Russian satellite. Cosmos 243, which was equipped with four radiometers at wavelengths of 0.8, 1.35, 3.5, and 8.5 cm. Several of the US and USSR spacecrafts which have been launched since 1968 have carried microwave radiometers on board. The most notable example is perhaps the 1.55-cm wavelength Electrically Scanning-Microwave-Radiometer (ESMR) mounted on Nimbus 5, which has provided synoptic images of microwave emission over the entire globe, including the Arctic. Examples of false-color mosaics prepared from ESMR 1972 and 1973 data.

The passive microwave sensing process is illustrated in Figure 3-1. A radiometer receiver is connected to a pencil-beam antenna pointed at a scene of interest. The objective is to measure the thermal radiation emitted by the area covered by the footprint of the antenna effective main-beam; that is, it is desired to relate the radiometer output (represented by Vg) to the target emission *Tg*. The designation *Tg* is used in accordance with the correspondence between radiated power and equivalent blackbody (or brightness) temperature. As can be seen in Figure 3-1, other effects also have to be taken into account before the desired association can be established. Specification of these effects and the roles they play may be approached through the communication system analog shown in Figure 3-2. The system may be divided into four major blocks: Main-Beam Contributions: T_{ap} is the apparent temperature of the environment as seen through the antenna main beam solid angle, β.That is, it represents that

part of the energy incident on the antenna which is contained within the antenna main cone. In addition to direct emission (T_B) by the target area which is collected by the antenna main-beam, indirect contributions from other emission sources accompany T_B after reflection (or scattering) by the target area in the direction of the antenna. These two radiation fluxes, direct emission and indirect reflection, travel with losses through the atmosphere between the surface and the antenna. The atmosphere acts to attenuate their magnitudes through absorption and scattering, and to further deemphasize their significance, it adds another component, atmospheric self emission, Tup, to $T_{ap}{}^{s\ell}$. .Side-lobe Contributions: $T_{ap}{}^{s\ell}$ is the apparent temperature of the environment as seen by the antenna sidelobes in directions outside the main-beam solid angle. Among the various contributors, emission by the target background usually dominates. In some cases, however, other sources may become important, such as cosmic radiation at frequencies below 500 MHz, and direct atmospheric emission at frequencies above 500 MHz under high path loss conditions. The function of the antenna is to act as an interface between the incident radiation. $T_{ap}{}^{m}$ and $T_{ap}{}^{s\ell}$, and the input to the radiometer receiver. As the incident radiation is collected, it is weighted by the antenna radiation pattern according to direction. Since $T_{ap}{}^{s\ell}$ contains no information about the target under investigation, and hence represents interference, antenna design considerations play an important role in determining the overall radiometer system performance. The performance of the antenna in terms of rejecting $T_{ap}{}^{s\ell}$ is usually described by the antenna main-beam efficiency, α_m [17,18,19].

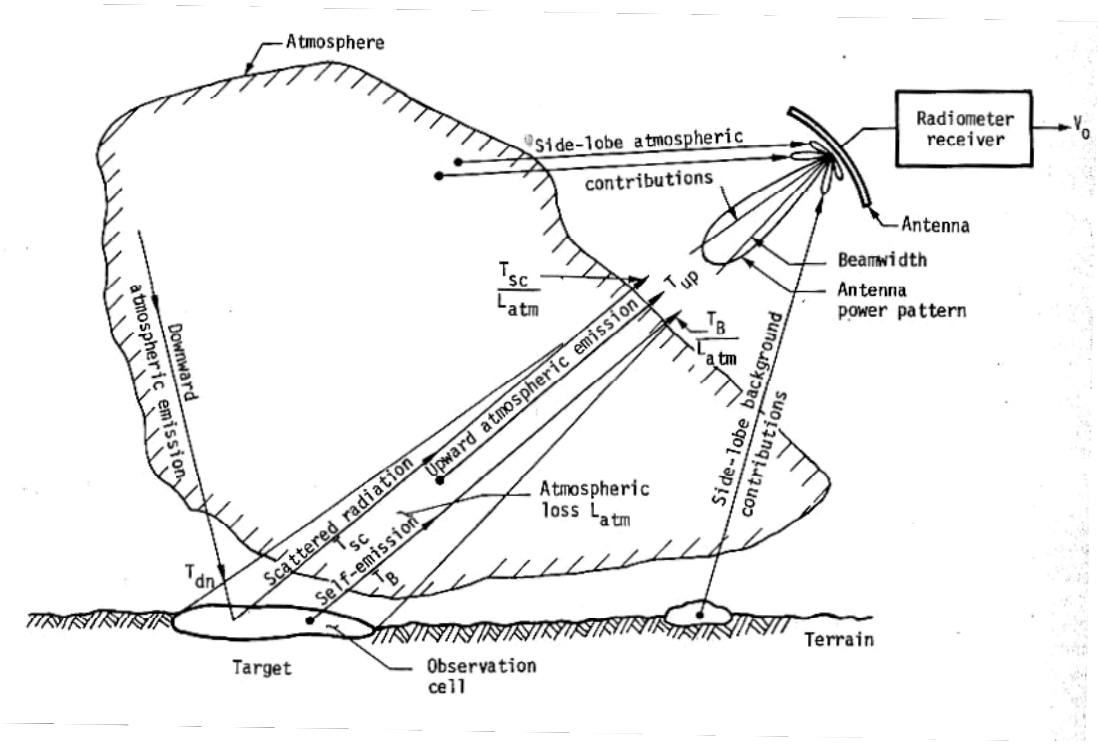

Fig. 3.1. Schematic representation of the various contributions to the energy received by the radiometer antenna. [1]

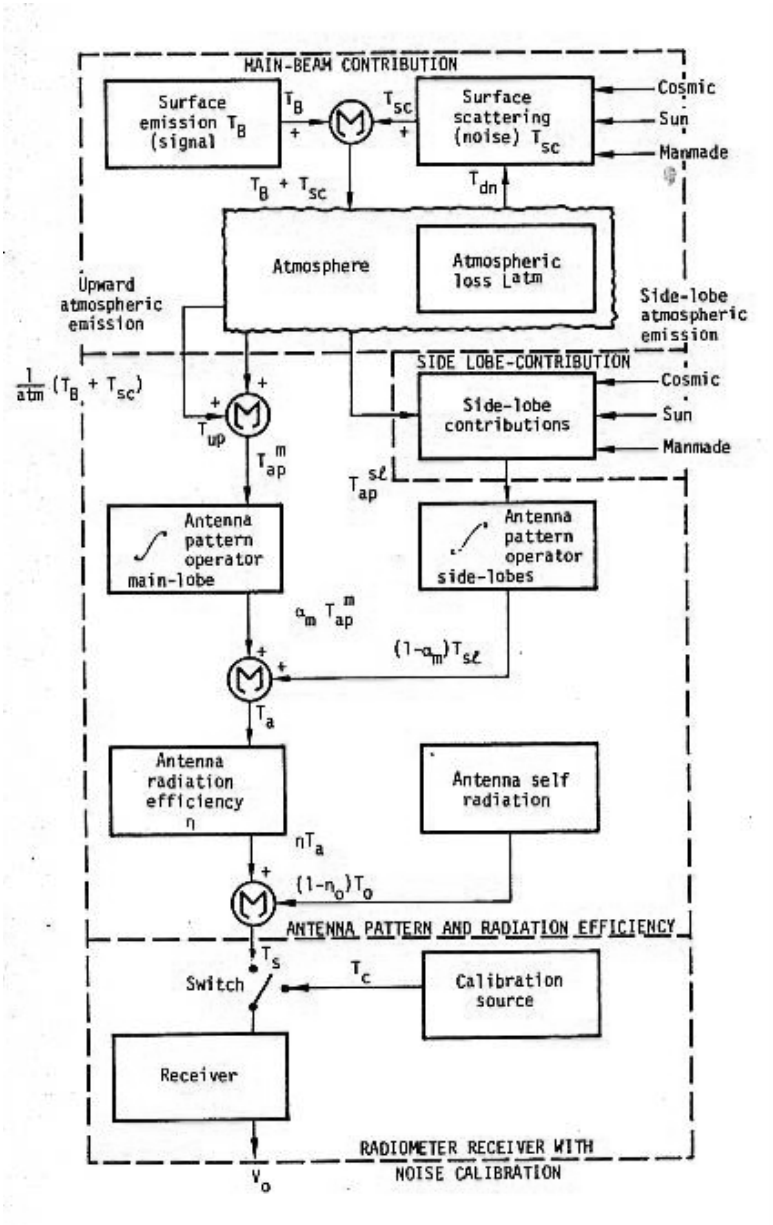

Fig. 3.2. Block diagram representation of the radio-metric process. [2]

The antenna radiation pattern is only part of the total antenna transfer function. Ohmic losses cause the antenna to introduce further losses. It will absorb part of the collected incident energy (designated antenna temperature T_a in Figure 3-2, and will add some of its own energy in the amount

$$Ta=(1-\eta)T_o. \quad \ldots(3.6)$$

Where:

T_o: is its physical temperature, and

η: is its radiation efficiency, or the antenna medium transmittance.

Although in principle the conversion between the antenna output T_s (receiver "signal" temperature) and T_a is straightforward if η and T_o are known, reduction in the magnitude of T_a causes an increase in the absolute uncertainty associated with the measurement of T_a by the radiometer receiver.

Receiver Transfer-Function: Radiometers employ highly sensitive receivers capable of detecting very weak signals, which are often one or more orders of magnitude smaller than the internally generated noise. By calibrating the receiver with a noise source of known output power (designated T_{cal} in Figure 3-2, the receiver output V_o can be related to its input, T_s.

3.8 Radiative Transfer

Radiometers are highly sensitive receivers capable of measuring EM radiation emitted by material objects. The radiation is attributed to the thermal motion of the electrons and protons within the material, covers a wide spectrum of frequencies and polarizations, and is temperature dependent. This section will provide an introductory treatment of these basic relationships in radiometry.

Consider a closed system consisting of a hollow container maintained at some fixed temperature T. Under these conditions, the inner walls will emit and absorb photons at the same rate. Now insert a flat horizontal plate within the container, as shown in Figure 3-3. Further, let the plate area (*A*) be very small with relation to the container dimensions so that the energy intercepted by the plate will disturb only minutely the state

of thermodynamic equilibrium. The infinitesimal power $d\Omega$ from a solid angle *dA* of the container walls incident on one side of an infinitesimal area *dA* is: [7,19]

$$dW(\theta,\phi) = B(\theta,\phi)\cos\theta\, d\Omega dA df \; . \qquad \ldots(3.7)$$

Where:

dW : infinitesimal power, watts

B: brightness of container at position (θ,ϕ), $Wm^{-2}Hz^{-1}Sr^{-1}$

$d\Omega = \sin\theta\, d\theta$: infinitesimal solid angle,

θ,ϕ: spherical coordinate angles defined in Figure 4-3, in radians

dA: infinitesimal area of plate surface,

df : infinitesimal element of bandwidth, Hz.

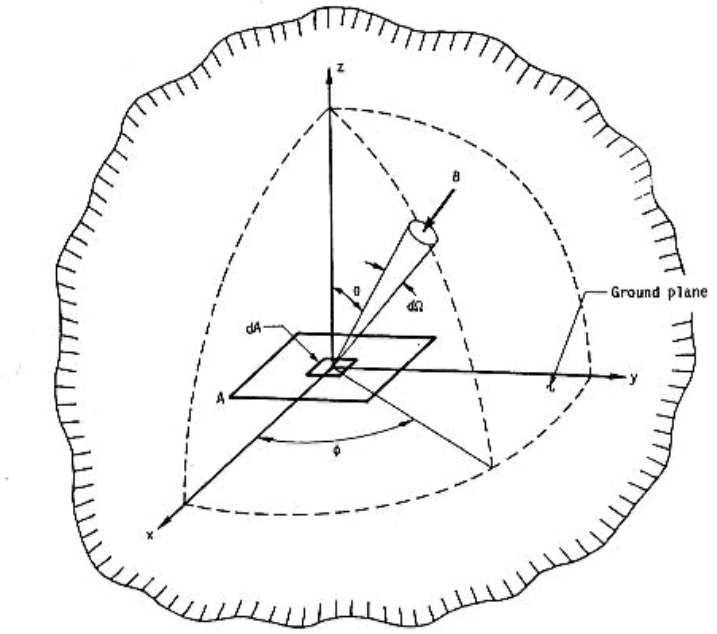

Fig, 3.3. Geometry of radiation incident on a flat plate enclosed in a constant temperature chamber. [19]

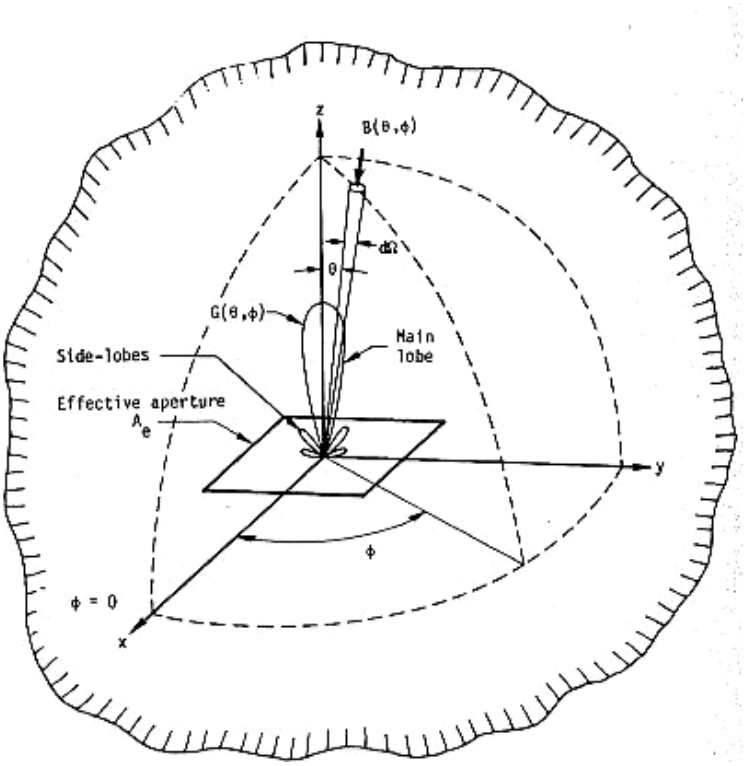

Fig. 3-4. Geometry of radiation incident on an antenna with effective aperture A_e and normalized power pattern $G(\theta,\phi)$,related to spherical coordinate system. [19]

The cos θ factor in Eq. 4-2 converts the area *dA* into an effective receiving cross section, *dA* cosθ, and thus acts as a weighting function or power pattern. If we now replace the horizontal plate with an antenna having an effective area Ae and a normalized pattern $G(\theta,\phi)$, as suggested in Figure 3-3, the total power received by the antenna over a bandwidth Δf (extending from a frequency *f* to a frequency *f*+ Δf) is then:

$$W = A_e \int_f^{f+\Delta f} \int_0^{4\pi} B(\theta,\phi)\, G(\theta,\phi)\, d\Omega df \ . \qquad \ldots(3.8)$$

Where:

The power pattern $G(\theta,\phi)$ is a dimensionless quantity with a maximum value of unity, and the integration is carried out over a solid angle of 4π.

If the antenna is linearly polarized and the incident radiation is unpolarized, then the antenna will only detect half of the total incident power, thus a factor of 1/2 should be introduced in Eq. 3-8 to become:

$$W = \frac{1}{2} A_e \int_{f}^{f+\Delta f} \int_{0}^{4\pi} B(\theta,\phi)\, G(\theta,\phi)\, d\Omega df \ . \qquad \ldots(3.9)$$

As will be seen in later sections, radiation emitted by terrestrial objects is often partially polarized. This property will be later accounted for through the definition of polarized emissivity.

3.9 Blackbody Radiation

As previously indicated, a blackbody is an idealized body capable of absorbing all the radiation falling upon it at all frequencies, reflecting none. Furthermore, in addition to being a perfect absorber, it has to be a perfect emitter since energy absorbed by a material would increase its temperature if no energy were emitted.

In 1901, Max Planck apparently solved the blackbody emission problem by showing that it is necessary to assume that the emitted radiation occurs only in discrete energy quanta. His assumption marks the origin of the Quantum Theory. His law of radiation states that the brightness of a blackbody radiator at a temperature T and frequency f is given by:[1]

$$B_{bb} = \frac{2hf^3}{c^2} \frac{1}{e^{fh/kT} - 1} \qquad \ldots(3.10)$$

Where:

h: Planck's constant $= 6.63 \times 10^{-34}$ joules sec

k: Boltzmann's constant $= 1.38 \times 10^{-23}$ joules $^{o}K^{-1}$

c: velocity of light $= 3 \times 10^{8} ms^{-1}$

T: temperature, °K.

It is to be noted that B_{bb} is only a function of frequency and temperature, and is independent of direction and position

At low frequencies, where

$$hf / kT \le 1,$$

a series expansion of

$$e^{hf / kT} - 1,$$

can be shown to reduce to the simple expression

$$hf / kT$$

so that Eq. 3-5 reduces to

$$B_{bb} = \frac{2 f^2 kT}{c^2} = \frac{2kT}{\lambda^2} \qquad \ldots(3.11)$$

Where:

$\lambda = c / f$, the wavelength is in m.

Eq. 3-6 is known as the Rayleigh-Jeans radiation formula after Jeans, who had derived it prior to Planck's Law according to classical theory, rather than in accordance with the quantum mechanical approach employed by Planck. The fractional deviation of the Rayleigh-Jeans expression Eq. 3-11 from Planck's Eq. 3-10 is less than 1 per cent when

$$\lambda T > 0.77 \text{ m } ^{o}\text{K}$$

or equivalently

$$f / T < 3.9 \times 10^{8} \text{ Hz } ^{o}\text{K}^{-1}$$

As an illustration, in a material at a room temperature of 300° K, the above inequalities will hold if

$$\lambda > 2.57 mm (117 GHz)$$

This covers the entire radio region and the usable part of the microwave spectrum. Even at a frequency as high as 300 GHz, the error will not exceed 3 percent.

3.10 Power-Temperature Correspondence

Now return to an examination of the power received by a lossless microwave antenna placed inside a blackbody, as illustrated in Figure 3-5. The antenna radiation resistance, *R*, is assumed to be matched to the terminals shown. With the absorbing-emitting material effectively enclosing the antenna, the antenna radiation resistance will assume the enclosure temperature, *T*. Introducing the Rayleigh-Jeans formula, Eq. 3-11, into Eq. 3-9, yields

$$W_{bb} = \frac{1}{2} A_e \int_{f}^{f+\Delta f} \int_{o}^{4\pi} \frac{2kT}{\lambda^2} G(\theta,\phi) d\Omega \, df \qquad \ldots(3.12)$$

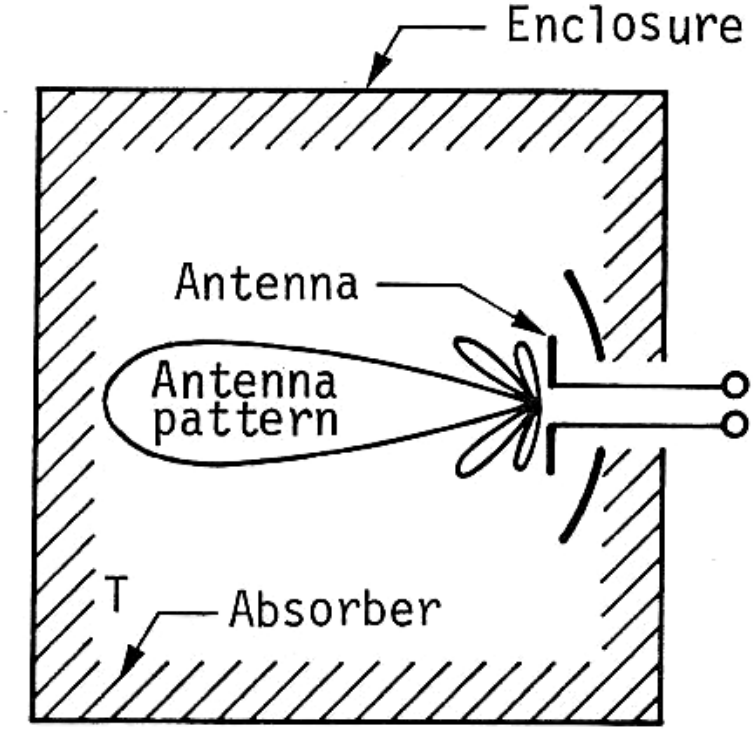

Fig. 3. 5. Antenna in absorbing (blackbody) enclosure at constant temperature T. [1]

If the detected power at the antenna terminals is limited to a narrow bandwidth

$$\Delta f \leq f^2$$

Which is customarily the case, then Eq. 4-7 can be reduced to:

$$W_{bb} = kT\Delta f \frac{A_e}{\lambda^2} \int_0^{4\pi} G(\theta,\phi) d\Omega \quad \ldots(3.13)$$

The integral in Eq. 3-13 is recognized as the antenna beam solid angle, and is also equivalent to:

λ^2 / A_e

Hence, Eq. 3.13 becomes:

$$W_{bb} = kT\Delta f \quad \ldots(3.14)$$

In terms of the power available at the antenna terminals. Figure 3-6 is an equivalent description for the antenna of Figure 3-5. In 1928 Nyquist showed that the noise power from a resistor R at temperature R_T is given by

$$W = kR_T\Delta f \quad \ldots(3.15)$$

which is identical to the result of Eq. 3-15, if the temperature of the antenna radiation resistor R_T = T. This identity, as simple as it may seem, is the key factor to the terminology used in describing the emission from material surfaces; the correspondence between power and temperature expressed in Eq. 3-15 has led to the interchangeable use of the two terms.

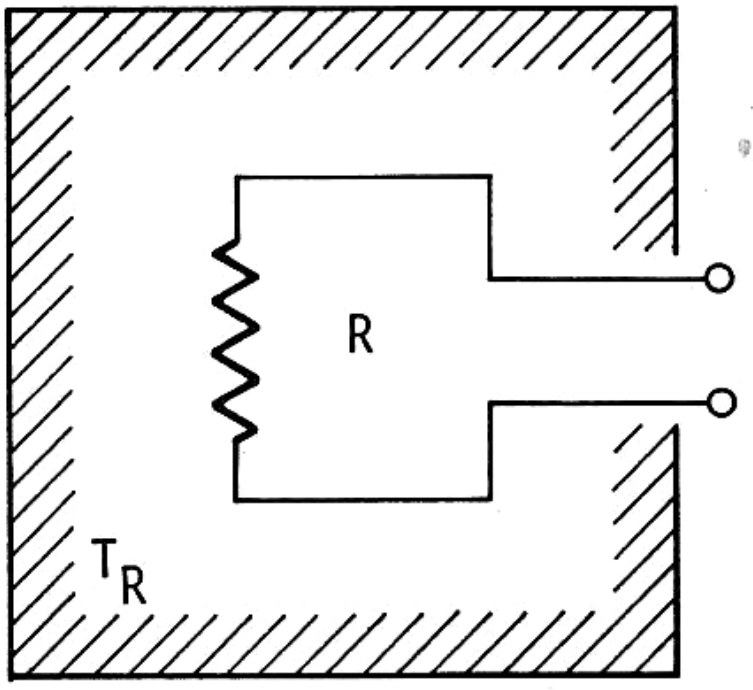

Fig. 3.6. Resistor maintained at constant temperature T_R [1]

3.11 Reflection Expression

The terms, reflectively and reflectance , which are found abundantly in literature on optics, infrared, microwaves, and EM theory in general, were purposely avoided in the introductory comments because they are defined differently and should not be used interchangeably. They do stem from the same basic concepts. Another reflection term, albedo, keeps appearing in remote-sensing literature; it too requires special definitions.

The analyses of these expressions for remote sensing are expedited by first presenting them in a popular form involving the angle of incidence only. The Fresnel reflection coefficients are ratios of the reflected electric field over the incident electric field, E_i/E_r , and are given by a pair of expressions R_i where $i = v$ or h, vertical or horizontal polarization. Significant changes in R_i result in corresponding amplitude changes in the detected signals, or density variations in an image. Thus, [1]

$$R_v \exp(j\phi_v) = \frac{E_r}{E_i} = \frac{n^2 \cos\theta_i - \sqrt{n^2 - \sin^2\theta_i}}{n^2 \cos\theta_i + \sqrt{n^2 - \sin^2\theta_i}} \qquad \ldots(3.16)$$

And,

$$R_h \exp(j\phi_h) = \frac{E_r}{E_i} = \frac{n^2 \cos\theta_i - \sqrt{n^2 - \sin^2\theta_i}}{n^2 \cos\theta_i + \sqrt{n^2 - \sin^2\theta_i}} \qquad \ldots(3.17)$$

Where:

$R_v \exp(j\phi_v)$: Reflection coefficient, or ratio, for vertical polarization where $\exp(j\phi_v)$ is a phase indication between E_r and E_i. (Symbols r and ρ also found in literature for reflection coefficients).

$R_h \exp(j\phi_h)$: reflection coefficient for horizontal polarization where $\exp(j\phi_h)$ is a phase indication between E_r and E_i.

E_i : incident electric held with v or h polarization.

E_r : reflected electric field with v or h polarization.

θ_i : angle of incidence of plane wave source.

n : index of refraction between two media (air and -ground) of intrinsic impedance Z_1 and Z_2.

Plots of the magnitude of $|R_i|$ and $|R_i|^2$ as a function of the angle of incidence, where the parameters are wavelength polarization and temperature, have been published for a wide variety of materials and soils. Values range from $0 \le |R_i| \le 1$. The magnitudes of R_i are implied and thus the magnitude symbols are seldom given of all the parameters making up R_v, and R_h the index of refraction of a medium is a major contributor in influencing values of the coefficients. The index of refraction is also related to Snell's law for the transmission of EMR between two media, where the law, includes the angles of incidence θ_i ,and transmission, Snell's law is quite general and gives η relative to free space for each medium, thus

$$\frac{\sin\theta_i}{\sin\theta_r} = \frac{|n_2|}{|n_1|} \qquad \ldots(3.18)$$

Where:

$$n = \sqrt{\frac{\mu(k - jg/\omega)}{\mu_o k_o}} \qquad \ldots(3.19)$$

When the media are air and ground, Eq. 3-19 substituted in Eq. 3-20 gives

$$\frac{\sin\theta_i}{\sin\theta_r} = \frac{n_2}{n_1} = \frac{\left|\sqrt{k_{r2} - jg_2/\omega k_o)}\right|}{\sqrt{k_{r1}}} \qquad \ldots(3.20)$$

Where:

k_{r1}, k_{r2} : dielectric constant of air and ground

g_2 : conductivity of ground

k_o : permittivity of free space

ω : angular frequency.

Note that the ground is taken to be nonmagnetic, thus μ_1 and μ_2 are assumed equal.

The ratio of impedances of air and ground for this special case can be shown to be, in a squared form,

$$\left(\frac{Z_1}{Z_2}\right)^2 = n^2 = \left(\frac{n_2}{n_1}\right)^2 = \frac{k_{r2} - jg_2/\omega k_o}{k_{r1}} = \frac{k_2}{k_1} \qquad \ldots(3.21)$$

Consequently, a simpler form of Eqs. 3-16 and 3-17 has evolved which requires mainly knowledge of k_2 of the reflecting medium since k_1 for air is taken as unity. Thus, Eq(3.16) becomes

$$R_v = \frac{-(k_2/k_1)\cos\theta_i + \sqrt{(k_2/k_1) - \sin^2\theta_i}}{(k_2/k_1)\cos\theta_i + \sqrt{(k_2/k_1) - \sin^2\theta_i}} \qquad \ldots(3.22)$$

And Eq.(3.18) can be simplified similarly.

For the case of normal incidence, R_v and R_h reduce to a single expression where polarization is not defined,

$$R = \frac{-\sqrt{k_2} + \sqrt{k_1}}{\sqrt{k_2} + \sqrt{k_1}} \qquad \ldots(3.23)$$

The expressions for the reflection coefficients appear quite formidable and justifiably so since they contain a number of terms that are sensitive to frequency, angle of incidence and the dielectric properties of the media. For example, the dielectric constant of water below (lie microwave frequencies is around k_r = 81; whereas in the visible spectrum, it is around k_r =1.77. The dielectric constant for water is clearly a function of frequency. This difference in dielectric constants was thought earlier to be a violation of Maxwell's theory.[1]

At this point, it is important to state the conditions under which the expressions for the reflection coefficients are applicable.

Fresnel's reflection coefficients are based upon Maxwell's equations and apply throughout the EM spectrum.

The expressions for R_i apply in general to the following: (1) A flat smooth boundary of practically infinite extent between two homogeneous and isotropic media. (smoothness is usually defined by Rayleigh's criterion, (2) A plane (not a spherical wave) incident at the boundary, (3) An incident EM wave that is monochromatic or of spectral quality. The reflection coefficient is usually taken to be a spectral value. Tins does not mean that the reflection coefficient cannot be averaged over a broad wavelength range λ_1 to λ_2, thus *R* would be designated as $R_{\Delta\lambda}$. For certain media, the reflection coefficients remain essentially constant over certain portions of the EM spectrum.) (4) A medium in which multiple reflections do not occur, such as to change the magnitude and phase of the surface-reflected electric field.

R_i is given by Eq. 3-16 and 3-17 for two dielectric media that can be either lossless (only real values) or lossy (having imaginary values). R_i is given explicitly as functions of the angle of incidence, wavelength, and Polarization. R_i is also a sensitive function of the complex dielectric constants of the two media k_1 and k_2 which are of the general form, [20]

$$k(\lambda,T) = k_r - jg/\omega k_o \qquad \ldots(3.24)$$

Where:

λ: wavelength (*m*)

T: temperature (^oK)

k_r: relative dielectric constant; representative values range from 1 to 10 for most land substances, pure water =81.

g: conductivity (ohms m^{-1}).

Besides being a function of wavelength, the value of k varies with temperature, compaction, and moisture content. The rate of change of k with these variables produces detectable changes in R_i in specific parts of the EM spectrum, as is clearly evident in reflected radiation from vegetation in tile near-infrared.

The second term of Eq. 3-24, $\sigma / \omega k_o$, is a loss or power dissipation term. This term, when modified slightly to $\sigma / \omega k$, where $k = k_r k_o$, is called the losstangent δ. In Eq. 4-19, if the frequency is low, the term $\sigma / \omega k$ predominant and the material behaves like a conductor; at microwave frequencies it acts like a quasi-conductor; and at *IR* and higher frequencies, it behaves like a dielectric.[20,21,22].

Where the reflecting medium is a surface of high conductivity (metal), the second term of Eq. 3-24 predominates and $\left|R_i(\theta)\right| = 1$ for all angles of incidence. Metal targets therefore stand out in a scene and are independent of polarization and the angle of incidence. At low frequencies, where $\sigma / \omega k$ is large, substances appear radiometrically like conductors.

3. 12 Microwave Radiometric Characteristics of Oil Slicks

An interesting and useful number of signatures occur for the detection of oil slicks when EM radiation interacts with the air-oil and oil-water boundaries. These are reviewed also in relationship to the theoretical data, models, and experimental data.

It has been indicated that long microwaves penetrate fresh-water ice, and that ice thickness can be determined with proper analytic methods. These laboratory measurements and developed theory were extended to include oil on sea water (Kennedy, 1967). The basic raw data are shown in Figure 3-7. [4]

An active microwave sensing system was used to prove the fact that two interface reflections interact to produce additive and subtractive EM interference values. When reflections from the air/oil interface are in time phase with the reflection from the oil/water interface, additive signals are received. When these reflections are 180° out of phase, then subtractive interference occurs, and the resulting signal magnitude is reduced. These

oscillations approach a sine wave configuration that can be associated with oil thickness on a quarter-wavelength basis.

If this is true for active microwave systems, then it should also be true for passive microwave systems, which have the advantage that the signal is entirely generated by the oil/water system. This established relationship of constructive and destructive emission levels should make it possible to determine oil thickness on water to a fraction of a wavelength, and to achieve even higher degrees of accuracy if refraction factors are considered.

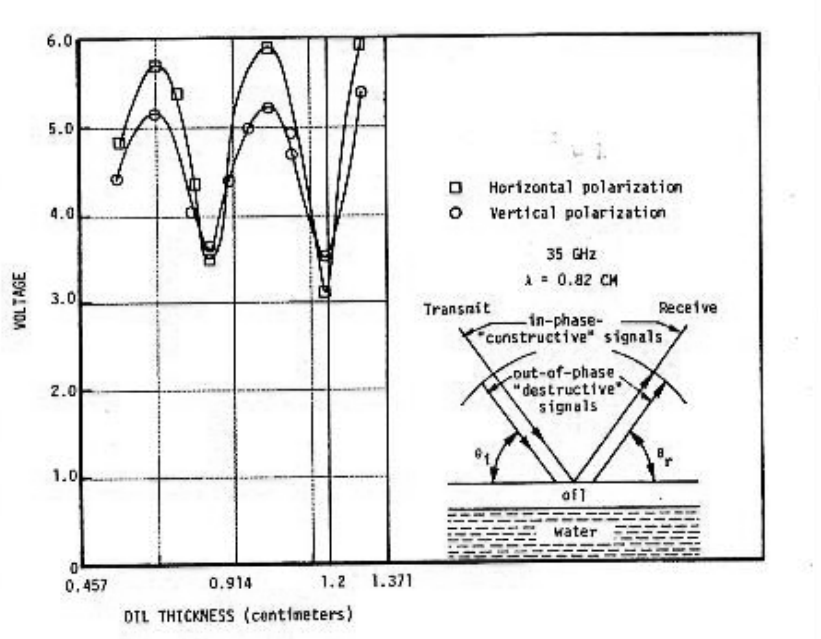

Fig. 3-7. Model of microwave interactions with oil on sea water.[4]

An important factor to note is the existence of points of ambiguity resulting from the oscillatory nature of the curve. That is, in two pattern wavelengths there are a number of oil thickness values that produce the same output values. This problem can be overcome by selecting instruments of proper operating wavelengths. If the instrument wavelength is too long, the difference in values between open water and oil-

contaminated water will be small, giving questionable accuracy. If the operating wavelength is too short, the ambiguity problem is present.

The objective is to operate within the straight line portion of the first constructive rise in emission. According to a Melpar Report (1969) [1], surface dispersion of oil is very rapid and fresh oil thickness on water does not usually exceed 2 mm. Therefore, if microwave radiometers with operating frequencies of the order of 20 mm are used, analysis of oil thickness should be confined to the first rise and straight-line portion of the constructive emission value. Also, the curve slope is steep enough that even small incremental values can produce useful data.

3.13 Water Electrical Properties

As a polar liquid, water exhibits a relaxation phenomenon in its electrical properties. The complex dielectric constant of pure water (no salt) was first formulated by Debye (1929). Lane and Saxton (1952) extended Debye's expressions to include the effect of ionic conductivity of salt solutions- Their expressions can be put in the form:[1]

$$k'_{rw} = \varepsilon_\infty + \frac{(\varepsilon_s - \varepsilon_\infty)}{1 + (f / f_o)^2}, \qquad \ldots(3.25)$$

And

$$k''_{rw} = (f / f_o)\frac{(k_s - k_\infty)}{1 + (f / f_o)^2} + \frac{g_i}{2\pi f k_o} \qquad \ldots(3.26)$$

k'_{rw} : real part of k_r for water

k''_{rw}: imaginary part of k_r for water

k_∞: relative permittivity at frequencies much higher than the relaxation frequency f_o

k_s : static relative permittivity,

g_i : ionic conductivity of the salt solution in mhos per meter.

At microwave and lower frequencies, k_∞, assumes a constant value of 5.5. In general, k_s f_o, and g_i, are functions of temperature and salinity, but not functions of frequency.

Water is a very important factor at microwave frequencies because its relaxation frequency lies in the microwave part of the spectrum. In terms of the water molecule relaxation time τ, f_o is given by:

$$f_o = 1/(2\pi\tau) \qquad \ldots(3.27)$$

Inspection of Eqs. 3-25 and 3-26 clearly indicate that k'_{rw} and k''_{rw} would vary with frequency the most near $f = f_o$. This is illustrated in Figures 3-5 a and b which show the real and imaginary parts, respectively, of the dielectric constant for pure water ($\sigma_i = 0$), fresh water (σ_i = 0.01 mhos m^{-1}), and sea water (salinity = 36°/oo).

The attenuation coefficient α (NP) m^{-1} defined in terms of the wavelength (m) and the relative dielectric constant k_r and permeability μ_r as follows:

$$\alpha = \frac{2\pi}{\lambda_o}\left\{\frac{\mu_r k'_r}{2}\left[\left(1+\left(\frac{k''_r}{\varepsilon'_r}\right)^2\right)^{1/2} - 1\right]\right\}^{1/2} \qquad \ldots(3.28)$$

Where λ_o is the free space wavelength.

The power absoption is given by:

$$K_a = 2\alpha \qquad \ldots(3.29)$$

The unite of K_a NPm^{-1}

The skin depth is

$$\delta = \frac{1}{\alpha} \qquad \ldots(3.30)$$

The complex index of refraction, *n*, must be known or assumed for computation of the single-drop interaction with the EM field. At

microwave frequencies, the most significant contribution to the possible polarization of water molecules, and hence the index of refraction of liquid water, is that due to dipole rotation. The contributions of ionic and electronic interactions occur in the infrared and optical regions of the spectrum, respectively. For this reason, the index of refraction is given accurately, for the microwave range, by the Debye formula (Debye, 1929)

$$n^2 = \frac{k_o - k_\infty}{1 + j(\lambda_o - \lambda)} + k_\infty \qquad \ldots(3.31)$$

Where:

k_o and k_∞ : static and optical dielectric constants

λ_o : Debye relaxation wavelength, resulting effects in the liquid

$j = \sqrt{-1}$

Chapter Four

Design and construction of the Radiometer Device

4.1 I.R and Visible Radiometer Design

4.1.1 Introduction

Radiation sensors are instruments that measure the intensity of radiation leaving a surface or object as functions of time, wavelength, space, geometry, including angular orientation of the target with respect to the observer and polarization of the radiation. No single instrument can do all of these things well, or even satisfactorily, for most applications, and as a result some parameters are stressed in each instrument at the expense of the others. In general, it is difficult to cover space, time, and wavelength adequately and simultaneously (geometry, is more a parameter of the scene than of the instrument); thus, sensors tend to group into imagers, which stress spatial resolution; and nonimagers, which stress time and wavelength resolution, and sometimes polarization.

Sensors may be classified as active or passive, image or nonimage forming, commercial or military. As ordinarily used, an active sensor provides its own source of illumination, whereas the passive sensor does not. A thermal infrared (TIR) imager (thermal mapper) would therefore be classified as a passive sensor, while a radar or a laser altimeter as an active sensor. Although cameras ordinarily are regarded as "passive," they do require source such as the Sun or other illumination.

4.1.2 Transmission Optical Filter

A. I.R Filter

Infrared radiation consists of EM waves in the wavelength region from 0.75 μm to 1100 μm. Due to the long wavelength the infrared radiation is less scattered and offers better transmission through various medium. A typical examples of infrared transmission media include a vacuum, the atmosphere and optical fibers. In the atmosphere as shown in Appendix B absorption by H_2O, CO_2 and other elements takes place at specific wavelengths. The bandwidth from 3 μm to 5 μm and from 8 μm to 12 μm, where the rate of absorption is lower, are sometimes called "atmospheric windows" and are often used for remote sensing applications.

To converge or Focus infrared radiation, optical lenses made of quartz, G_aF_2, Ge and Si, polyethylene Fresnel lenses, are used. Mirrors made of AL, Au or a similar material are used according to the wavelengths. Appendix B shows the transmittance for typical infrared optical materials. In some applications, band-pass Filters may be needed to utilize a specific wavelength, as well as choppers for passing and interrupting a beam of infrared radiation.[28]

When designing a band-pass filter, it is necessary to consider the center wavelength, half width (FWHM), and a 5% transmittance width. In addition, the side bands, meaning secondary transmission wavelength other than the target wavelength, must be considered , along with the transmittance at extraneous wavelengths, which is called blockingm see Fig.(4.1). Note that these characteristic vary with the temperature to be used and the angle of incident high.

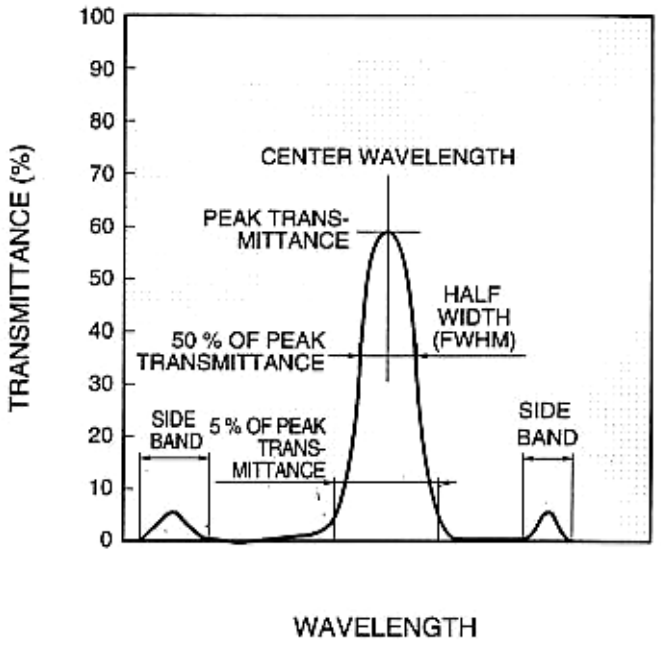

Fig. (4.1): Example of band-pass filter transmittance [1]

B. <u>Visible Filter</u>

Most spectral reflectance (P_λ) measurements are made in the photographic region of the EM spectral (0.67 - 1.0 μm), [Blue $\lambda = 0.43 - 0.48\ \mu m$, Green, $\lambda = 0.51 - 0.59 \mu m$, Red, $\lambda = 0.61 - 0.67 \mu m$ visible, $\lambda = 0.43 - 0.67 \mu m$] with the objective of determine the color of water. [26,27,28]

Data for multi-band photography consists of measurements of average, or integrated, spectral reflectance in a given wavelength band, such band reflectance may be derived from continuous spectral reflectance measurements, but may be more simply obtained by measuring energy directly in the band of interest. For example, water measurements in support of " standard multi-band photography-blue, green red and infrared bands would consist of only four measurements, the average reflectance of a target in each of four bands. The wavelength interval of these band would be defined by the transmission characteristics of the Wratten filter, 47B,57A and 89B, as shown in Fig (4.2).[1]

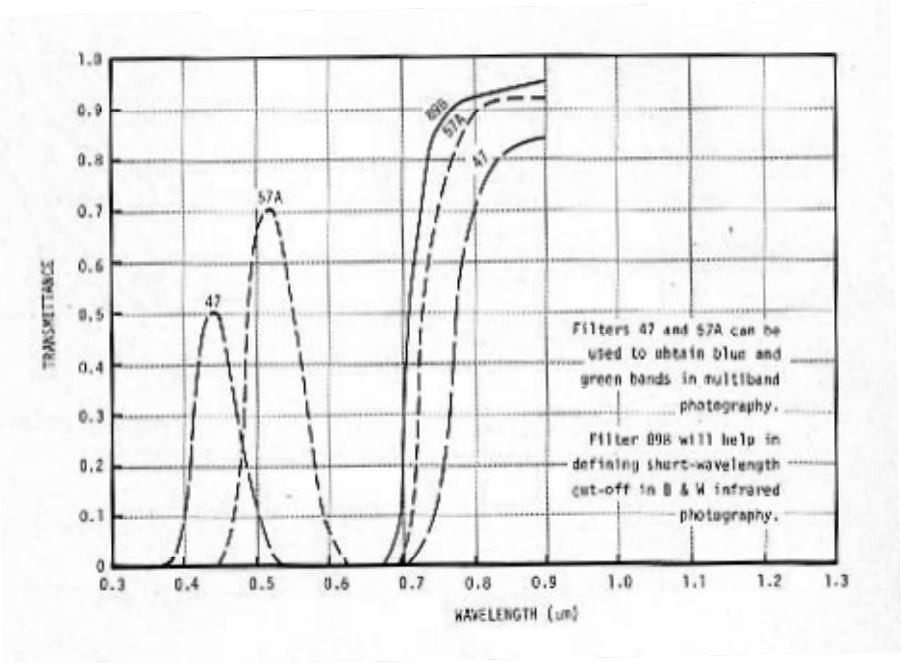

Fig. (4.2): Filter commonly used in multi-band photograph [1]

4.1.3 Detectors

Infrared detectors are classified into thermal and quantum types. Thermal detectors use the infrared energy as heat and their photosensitivity is independent of wavelength. Thermal detectors do not require cooling, but have disadvantages that response time is slow and detection capability is low. In contrast, quantum detectors offer higher detection performance and faster response speed, although their photosensitivity is dependent on wavelength.[6]

In general, quantum detectors must be cooled for accurate measurement expect for detectors used in the near infrared region. Types of infrared detectors are shown in Appendix C_1, and their typical spectral response characteristics are shown in Appendix C_2. Depending on the intensity of light signal and the type of information to be obtained photosensitivity and S/N required of infrared detectors differ, so the NEP and D^* are used as guides to select the optimum infrared detectors.[9]

In this design we selected a silicon photodetector with responsively of (R=0.6 A/W), the reason for this selection because the silicon photo detector cover the band of visible and IR radiation.

4.1.4 General Block Diagram

The proposed block diagram of the radiometer is shown figure (4.3,a,b).

It consists from the following units:

A. Modulated Power supply

According to the mathematical model of the system in chapter (5), the modulated power supply is needed to supply voltage to the detector at sampling frequency $f_s = \frac{1}{\tau_s}$. The pulse generator which is implement by a stable (555) timer (IC_1), two diodes (D_1& D_2) is illustrated by Fig.(4.4). the diodes are used here to generate a square wave with turn-on time equal to turn-OFF time (turn-on time = 0.7 RC) sampling time τ_s=1.4 RC.

$$f_s = \frac{1}{\tau_s} = 3.75KHz \text{ and } \tau_s = \frac{1}{f_s} = \frac{1}{3.75}0.267 \text{ m.sec}$$

B. High Gain Instrument Amplifier

Refer to the Fig.(4.5). The circuit topology is that of a high gain instrumentation amplifier. A differential voltage gain of 10000 for the input stage (IC_2 and IC_3) is definable through R_5, while the output stage (IC_4) also provides a differential voltage gain of 1000, IC_7 provides common mode rejection and offset compensation. Three trimmed resistors , R_5 , R_6 and R_{13} allow fine adjustment of the amplifiers gain CMRR and offset

respectively while R_7 provides scalling of photodetector is signal (C_2) is DC blocking capacitor to prevent DC component from pass to the next stage (lockin demodulator).

C. Lock-in-Demodulator

The lock-in-demodulator (also called phase sensitive rectifier) rectifiers the signal present of the 3.75 KHz oscillators signal which derive Q_1 and Q_3 providing the net effective equivalent of a narrow (1 Hz) band pass filter tuned to 3.75 KHz as shown in Fig.(4.5). The output of Lock-in-demodulator is sent through a low-pass filter.

D. Low Pass Filter

The low pass filter circuit consist of resistor R_{22} and capacitor C_3 connected as l-section circuits as shown in Fig.(4.5). The cutoff frequency of filter is set to 1.3 Hz the carrier component (3.75 KHz) and any other types of amplified noise is removed.

E. Main Disk Filter

The disk optical filter it contain four section visible filter, blue, red, green and white. This filter is rotate manually to select the suitable bans, used for measurement. This filter is made from plastic sheet with transmutation of about 0.9.

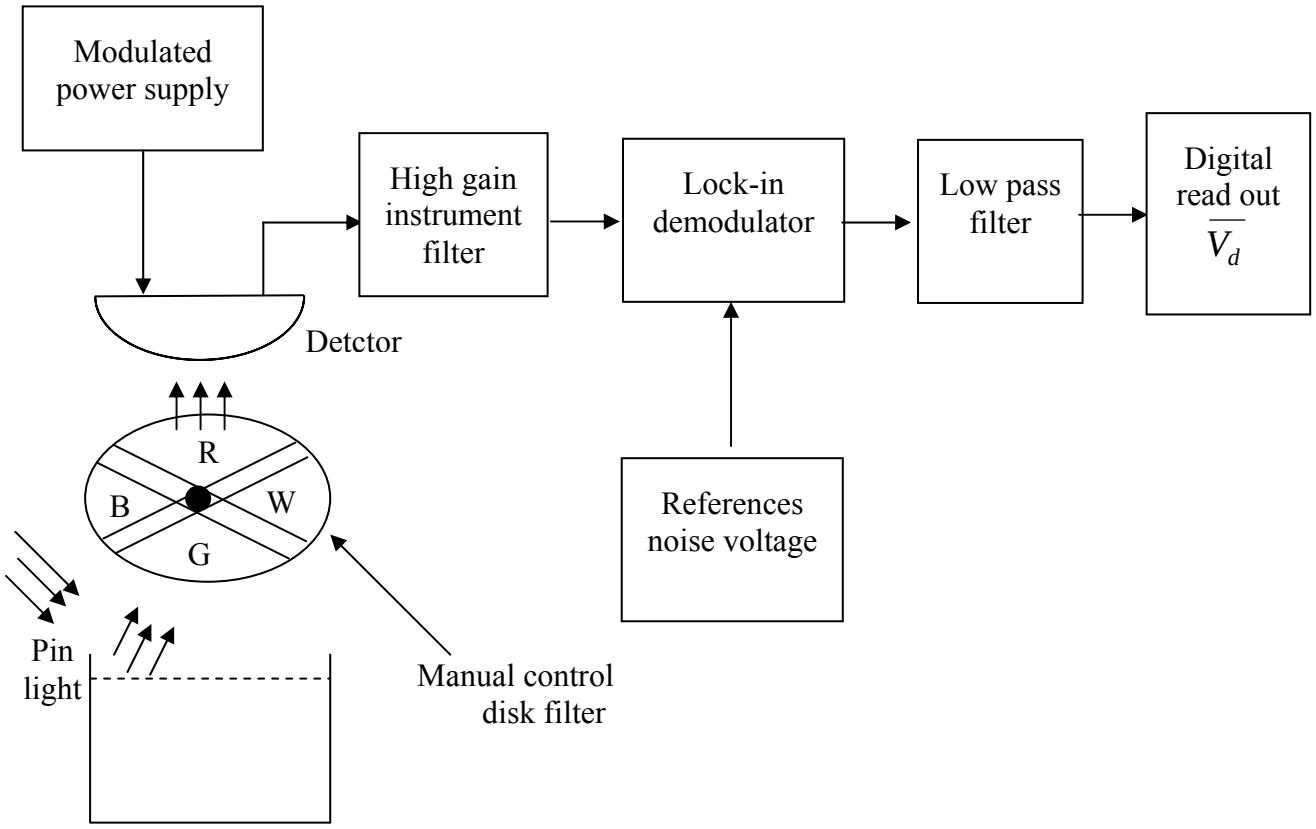

Fig.(4.3.a): Block Diagram of visible Radiometer

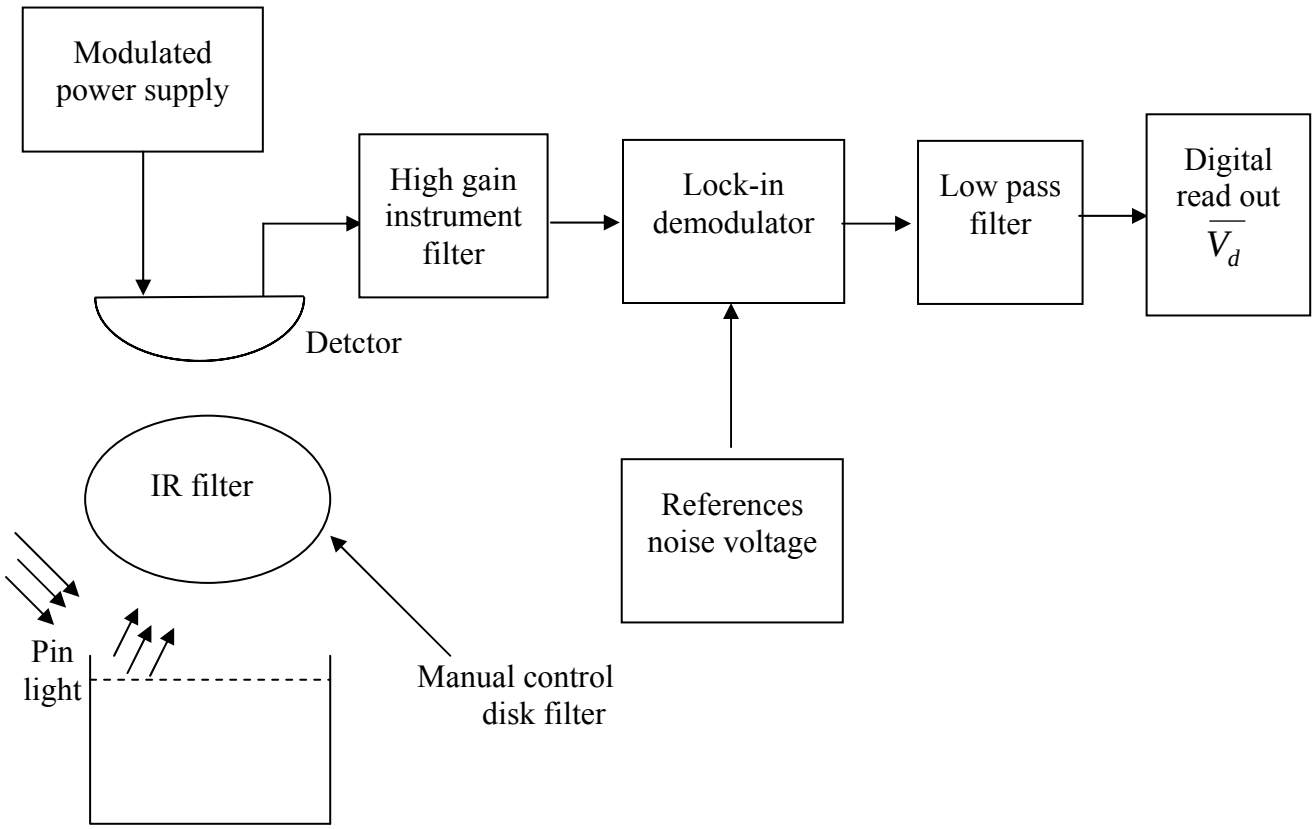

Fig.(4.3.b): Block Diagram of IR. Radiometer

4.1.5 Principle of Operation of optical radiometer System

The Fig.(4.4) shows the flow chart of the principle of operation can be divided to the following stages:

1. When the sun light incident on the body water part of light was absorber and other part was reflected from the surface of the water.
2. the reflected light was pass though optical disk filter to the photo detector.
3. the photo detector convert the optical signal to electrical signal. This detector was switch on-off by the modulated power supply to subtracted the external and internal noise.
4. the output of photo detector was amplified by the differential amplifier.
5. the lock-in amplifier is used to subtract the noise of electronic circuit.
6. the rectifier convert the a.c signal to the d.c signal.
7. the low pas filter is used to remove the all a.c component in the d.c signal.
8. the out put d.c signal is converted to digital A D. the digital signal then feed to the digital display. As shown in fig(4)

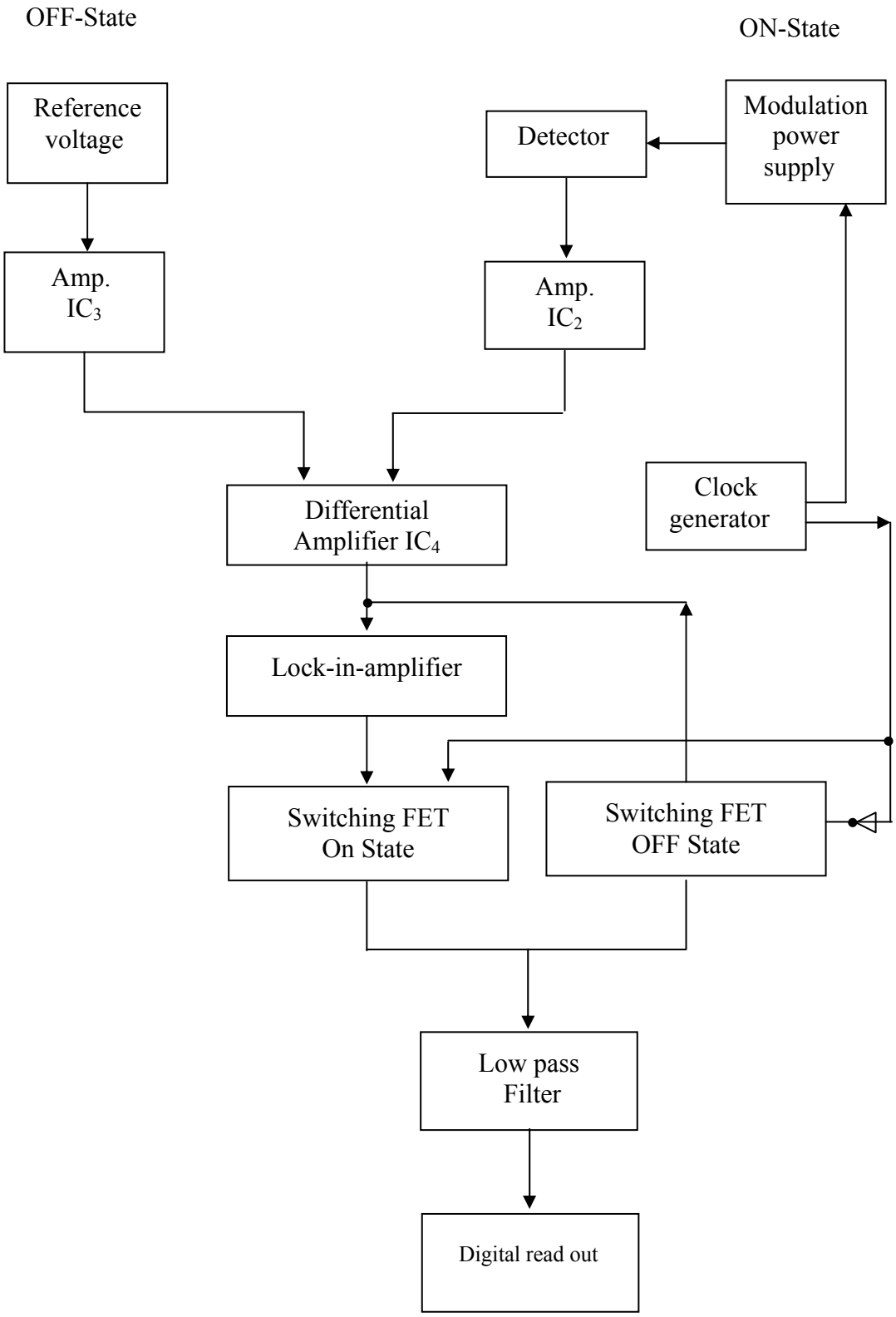

Fig.(4.4) The flow chart of the principle of operation of optical radiometer System

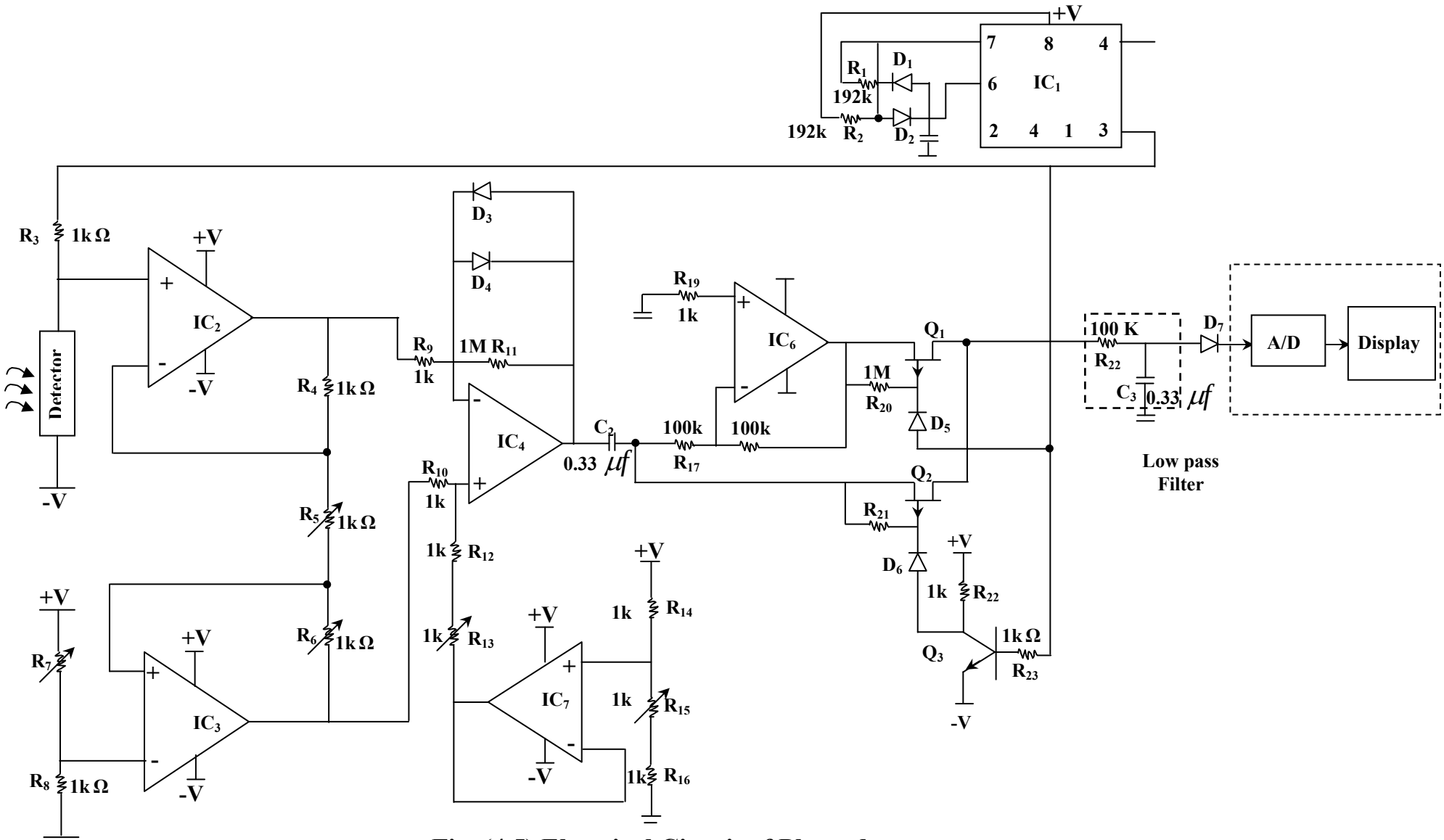

Fig. (4.5) Electrical Circuit of Photo detector

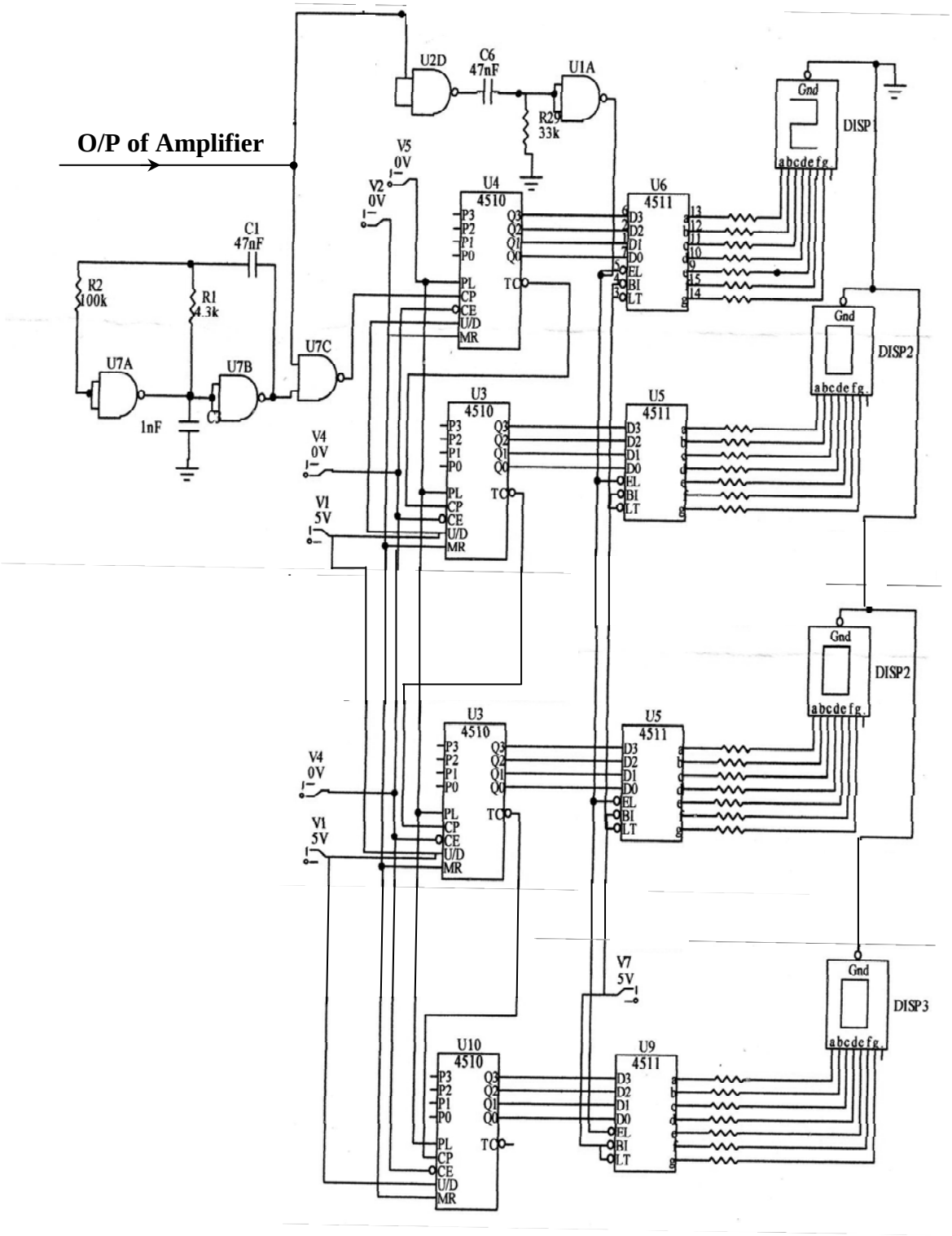

Fig.(4.6): Electronic Circuit of A/D and LCD Display

4.2 Microwave Radiometer Design

4.2.1 Introduction

A radar scatterometer is a device that measure the scattering properties of the region observed. Any radar that makes an accurate measurement of the strength of the observed single is therefore a scatterometer.

However, most existing radars that produce images are calibrated; consequently, most scaterometers are not imaging system. A calibrated imager, however, would also be a scatterometer.

The term microwave radiometer is normally applied to passive microwave systems. The signal received by the radiometer is a complex combination of thermally emitted radiation form ground and atmosphere, together with scattered emission originating in the atmosphere and extra-terrestrially, both in the sun and outside the solar system. Strictly speaking, a scatterometer is also a radiometer since it measures a signal radiated by the scatterometer itself and scattered from the target area, but the term radiometer is reserved here for passive devices.

4. 2.2 Basic Radar Block Diagram System

A radar system contains a transmitter which provides energy emitted from an antenna. Energy travels to the target and returns into a receiving an antenna; the output of the receiving antenna goes to a receiver which takes the returning signal. The signal from the receiver is related in some way to the transmitted signal and the result of this processing is displayed for the user. Figure (4.7) illustrates such a base system

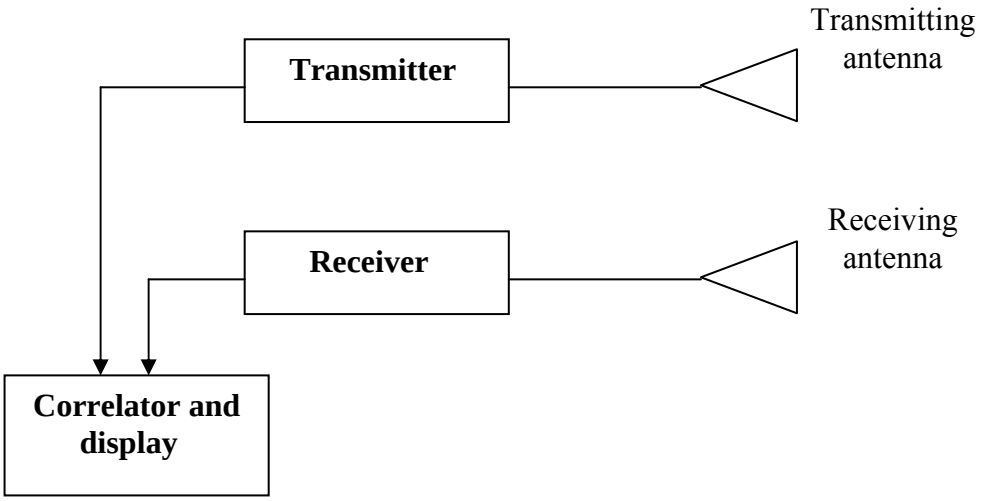

Fig. (4.7): Element of a Radar System [31]

4. 2.3 Radar Radiometer

In Fig.(4.8) the basic radar radiometer is indicated. For this radiometer, the receiver input is alternately switched between two integrates; one picks up the signal and receiver noise, and other picks up the noise source output and receiver noise. The subtractor at the output gives an estimate of the difference between the signal coming in the antenna and the level of noise . [31,33,34].

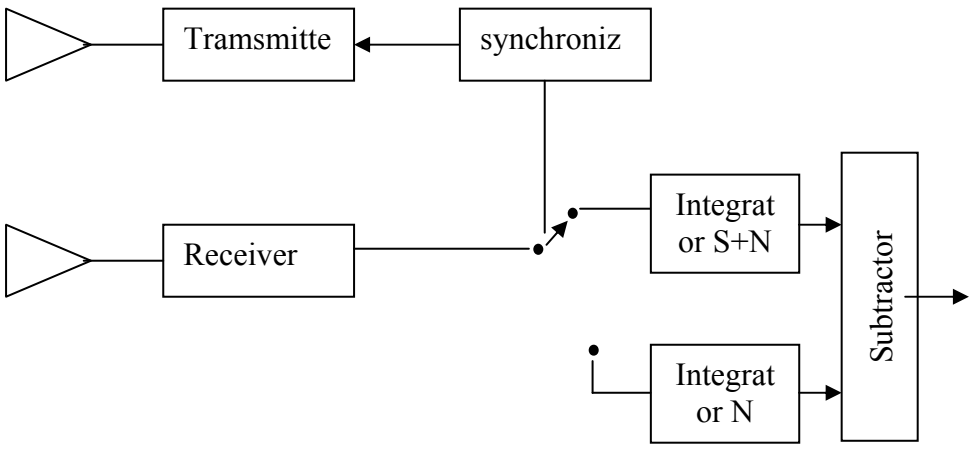

Fig. (4.8): Radar Radiometer

The radar radiometer consists the following element

A. Antenna

Electromagnetic horns are used widely in microwave communication and remote sensing systems. Small horns with modest gain are used commonly as primary antennas to illuminate ("feed") large apertures such as reflector-type antennas, while large horns with high gain are employed on their own in some applications.[19]

The horn antenna provides a gradual transition between a waveguide and free space. If the waveguide dimensions are such dial it can support only the dominant propagation mode, then by gradually flaring the terminal section of the waveguide, the excitation of higher-order modes may be avoided. Thus, a horn can provide simultaneously single-mode propagation (which is difficult to achieve with an oversize open-ended waveguide) as well as a large radiating aperture (compared to the single-mode waveguide). Furthermore, horns are broader-hand antennas than dipole and slot antennas.[19]

Horns are constructed in a variety of shapes, some of the more frequently used types are illustrated in Appendix D. The combination of size and shape of a horn dictates its directivity, impedance, shape of radiation pattern, and polarization properties.

Two rectangular horns antennas with size $(84\times80\times137mm)$ are used in the design of microwave radiometer.

B. Input Switch

The purpose of switch as shown if Fig.(4.8) is to receive periodically between the signal and noise at a high enough rate that the system-gain remains essentially constant over a period of one cycle. In other words, in order to successfully subtract out system-gain variations in the synchronous demodulation, the switching rate f_s should be higher than the highest significant frequency in the system-gain variation spectrum. Another

constraint on the lower limit of Fs is set by the effective bandwidth of the low-pass B_{LF}. To satisfy the sampling theorem, we must have $f_S > 2B_{LF}$. Integration time ($\tau = \frac{1}{2B_{LF}}$) used in grounded-based radiometer systems typically are around 1sec , which corresponds to $B_{LF} = 0.5\,\text{Hz}$, or $f_S > 1\,\text{Hz}$.

The upper limit of f_S usually is governed by the switch time τ_{sw}. To avoid the effects of switching time on the square –wave shape of the radiometer signal, it usually is recommended that;

$$\frac{2\tau_{sw}}{\tau_s} < 10^{-2} \qquad \ldots(4.2)$$

Electronically controlled microwave switches generally are one of two types ;(1) semiconductor diode switches and (2) ferrite circulators. The most commonly used diode switch in the PIN signal-pole double-throw (SPDT) switch, whose switching-time typically between to and 200 ns. Ferrite circulators are slower switching devices, with τ_{sw}-values in the 1-10 μs range, is equivalent to $f_S < 500\,\text{Hz}$. Most Dicke radiometers are operated at switching frequencies in the 10-100 Hz range.

C. Noise Sources and References Loads

Basically there are two types of noise sources available for calibration and balancing and as references sources;

1. **Passive Noise Source**:

Any device or component that delivers noise power at constant level without use of external power may be defined as a passive noise source. The simplest passive noise source is a matched load. When maintained at a constant physical temperature, it delivers an average noise power with an equivalent noise temperature equal to its physical temperature. Matched

load also are used for calibration, where by the antenna is replaced by a load, or the radiometer is switched to a load via calibration switch placed as close to the antenna as possible.

2. **Active Noise Source**:

Until the late 1960 s, the gas-discharge tube was the most commonly used noise generator at frequencies above 1 GHz. Today, solid-state sources, primarily avalanche diodes are available commercially up to 40 GHz.[34].

D. Receiver Front End

Most radiometers use super-heterodyne receivers with either an RF amplifier or a mixer-preamplifier at the front end. The choice is dictated by the noise figure or noise temperature of available devices, which in turn depends on the center frequency and bandwidth of the radiometer. Using hybrid microwave-integrated. Circuit (MIC) technology, radiometer receivers have been produced with double-sided noise temperatures as low as 230 at 35 GHz and 500 K at 94GHz (Cardiasmenos 1980). In the design of radiometer we select microwave amplifier type (PSI-1628) low noise amplifier provides 28dB again over an exceptionally wide bandwidth with noise figure about 2.5 [34]

4. 3 Principle of Operation of microwave Radiometer

Figure (4.9) shows the flowchart of measurement by using microwave radiometer, and the following stages explain the principles operations:

1. The transmitter and received point to each with distance of about 30 cm between them. The output voltage of the receiver was measured as shown in Fig.(4.9a).
2. the transmitter was pointed to the water body with the difference an gle and polarization as shown in Fig.(4.9b).

3. The back scattering from the water body was detected by the receiver .
4. The microwave signal was converted to the electrical signal.
5. Then the electrical signal was converted to the DC signal.
6. The DC signal to the digital signal by using A/D.
7. The read output of the display represent the value of reflected voltage which is proportional to the microwave reflected from the body water.

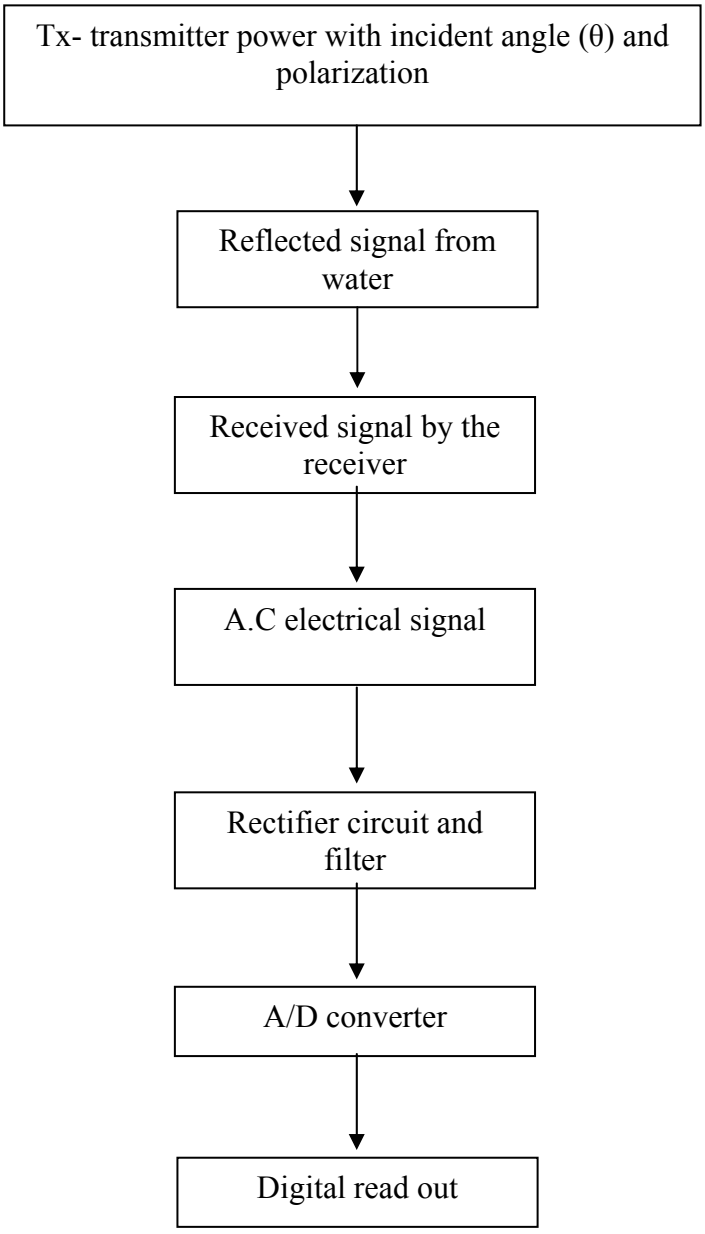

Fig. (4.9) :Flowchart of Microwave radiometer measurement

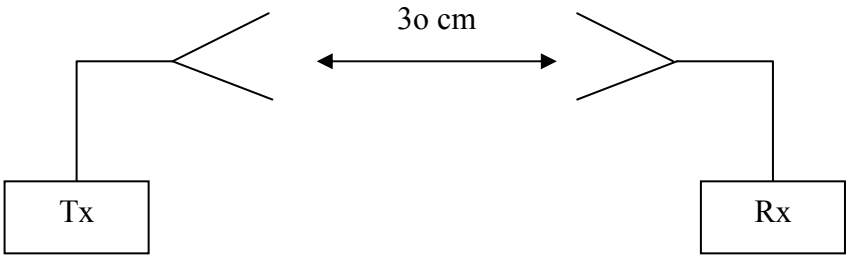

Fig. (4.10 a) calculate Transmitted power

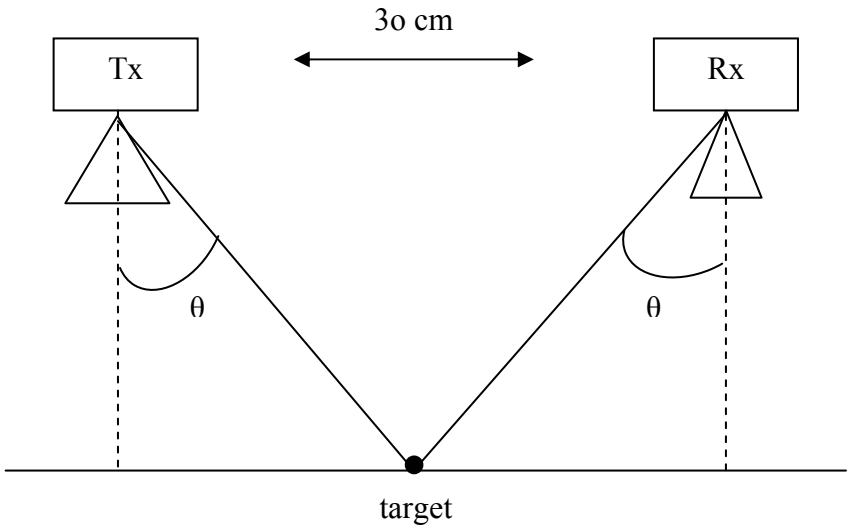

Fig. (4.10 b) calculate reflected power

4. 4 Mechanical Design

In this system all the electronic circuits, sensors, and display are contained inside a metallic box with the dimensions shows in Fig.(4.10). The box is moveable in the two directions, up-down direction, and rotational direction. For the up-down direction the distance between the sensors and water container can be adjusted to control the Field of View of the sensors. In the rotational direction the sensors can be directed to the sky to measure the radiance from the sky and to the water container to measure the radiance of the water under test.

Dimension of Box :

Box No. (1)
Volume of water = 6.25 liters

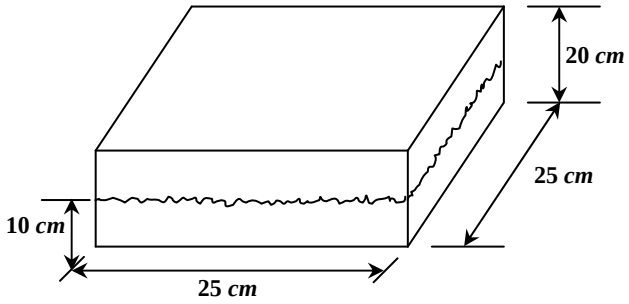

Box No. (2)
Volume of water = 16 liters

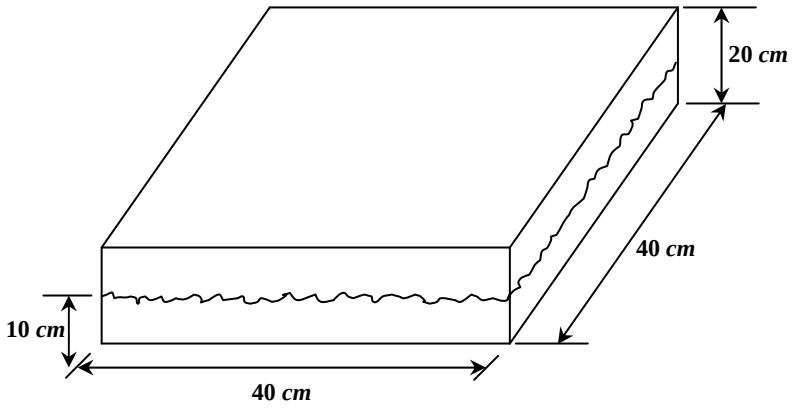

Fig.(4.8 a): water container m

Fig.(4.11): Mechanical part of the radiometer system

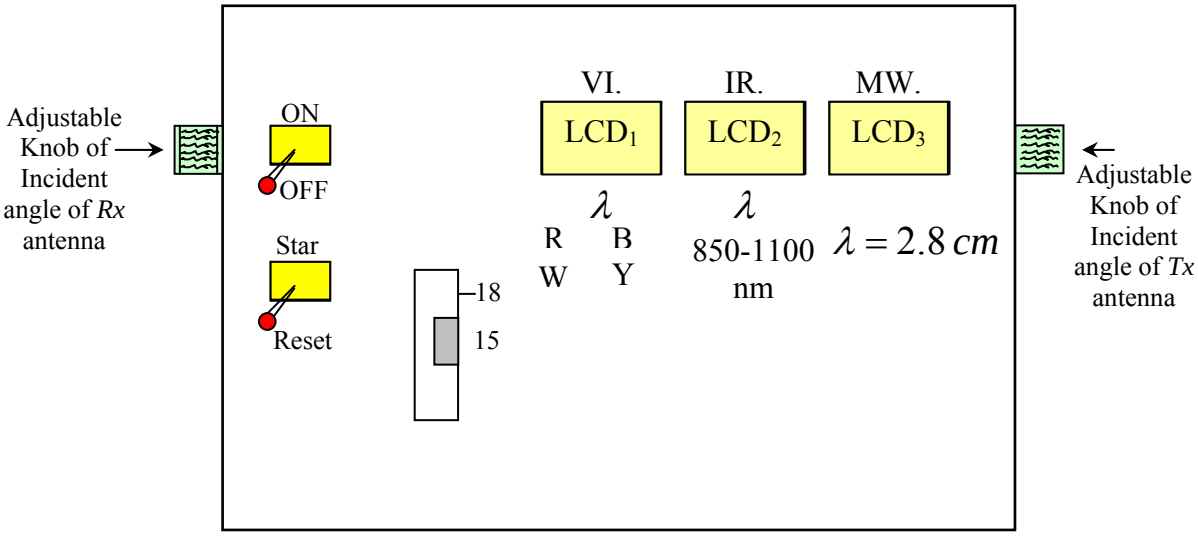

Fig.(4.11 b): front view of electronic

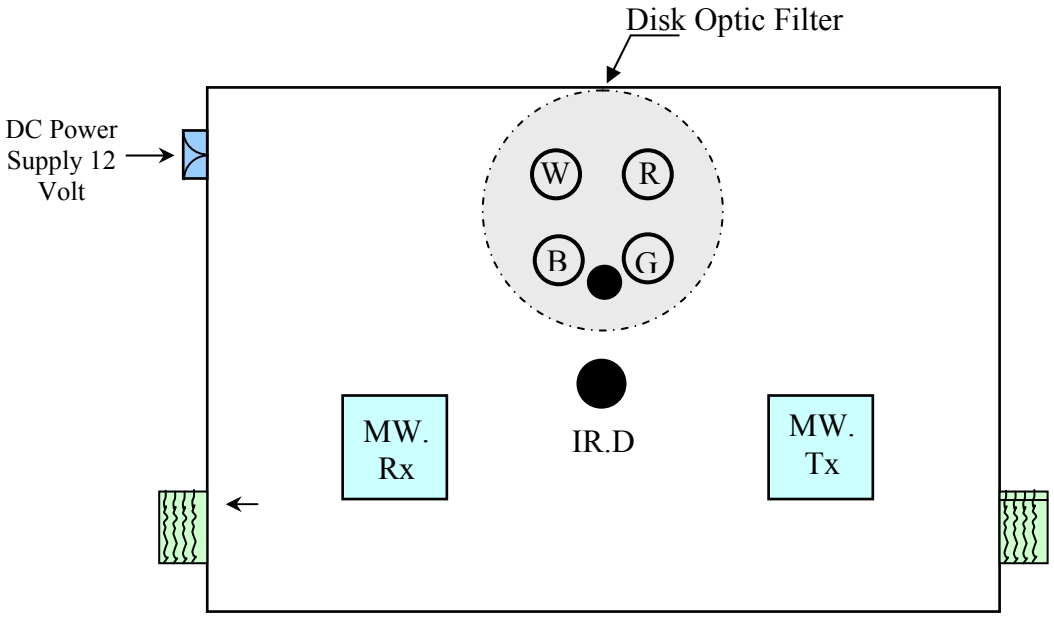

Down View

Fig.(4.11 c): Down view of electronic

Mechanical Design
Bench

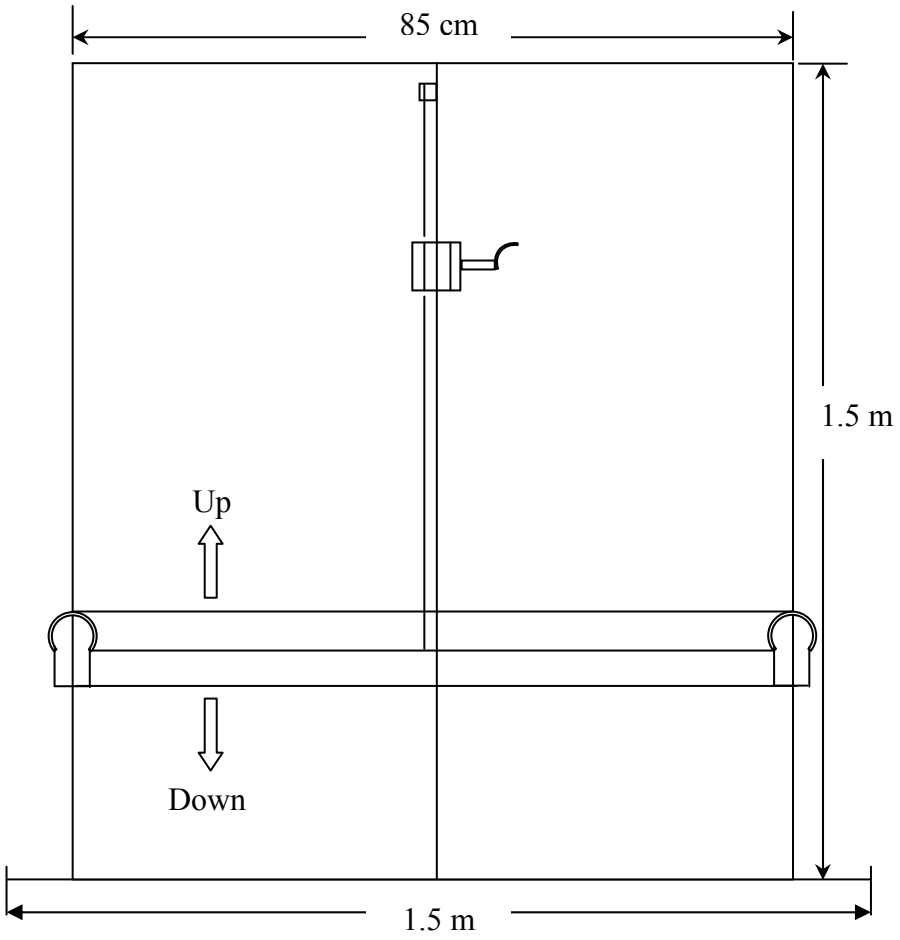

Fig.(4.11 d): Front of mechanical Bench

Mechanical Design Bench

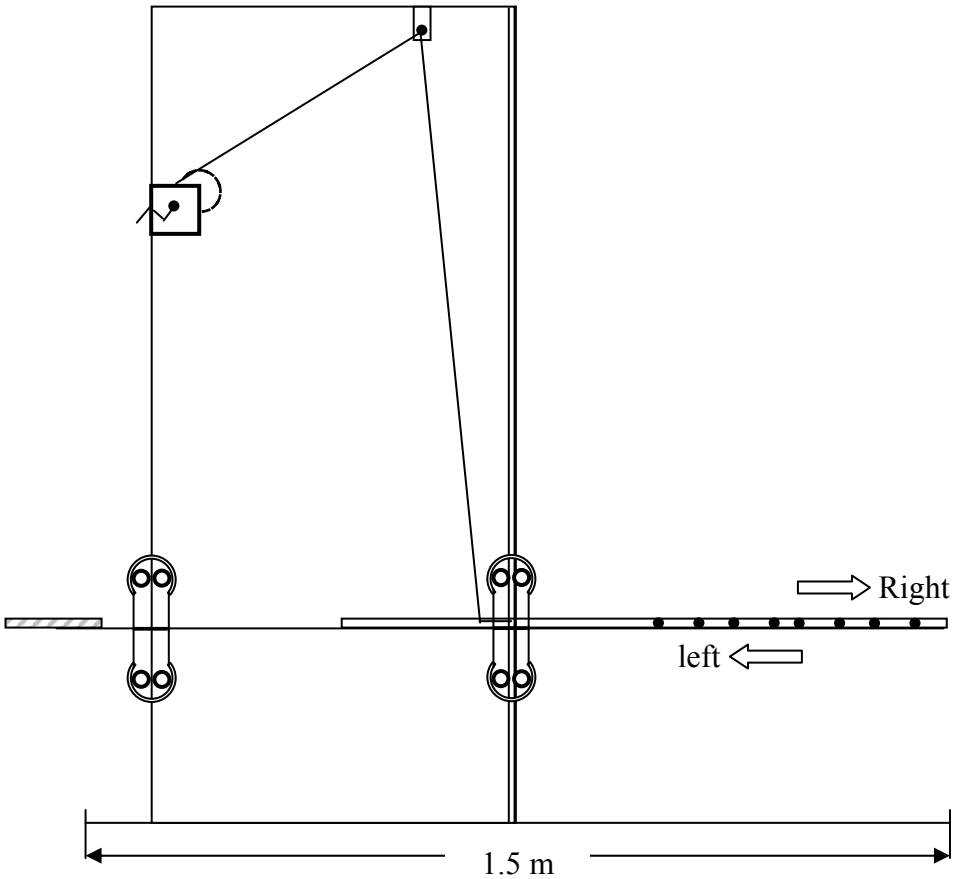

Fig.(4.11 E): Side view of Mechanical Bench

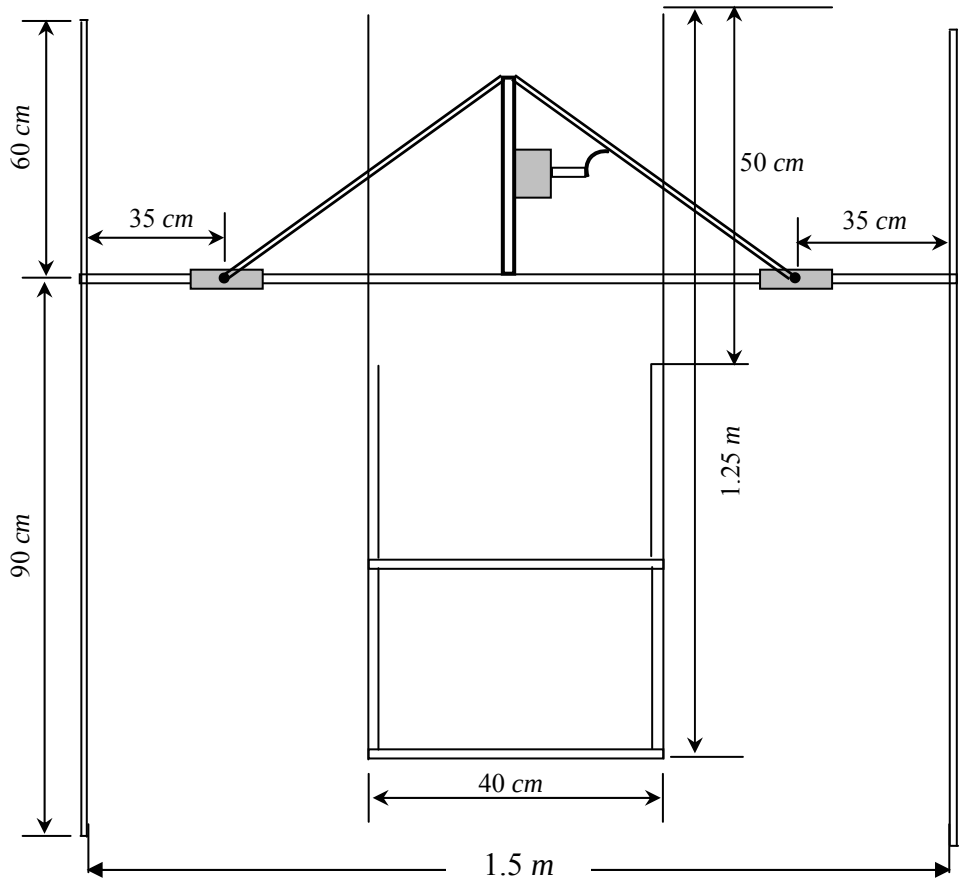

Fig. (4.11 F): Top view of mechanical Bench

Chapter Five

Mathematical Model

5.1 Geometry of Radiating Source and Optical Sensor

Quantitatitive assessment of shape and tone is possible only when the source is extended, i,e larger than the limiting resolution element of the sensor or field of view. Fig (5-1) shows the geometric relationship between such a source and optical sensor. The spectral radiant power P_λ, which enters the optical system and ultimately falls on the detector is [29]

$$P_\lambda = \frac{\tau(\lambda)\,\tau_o(\lambda)\,A_s A_c L_{e\lambda}}{R^2} \qquad \ldots(5.1)$$

Where:

A_s : area of the extended source with in sensor field of view.

A_c : effective area and collector optics.

$L_{e\lambda}$: spectral radiance of source.

R : distance to source.

$\tau(\lambda)$:transmissivity intervening atmosphere over the wavelength

$\tau_o(\lambda)$: transmissivity of optics over.

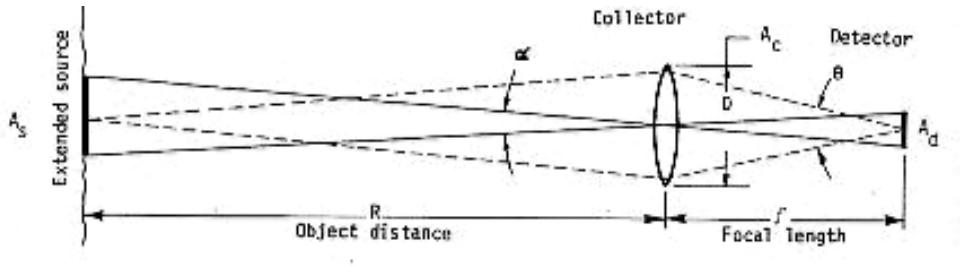

Fig. (5.1): Schematic geometry of radiating source and optical sensor [1]

This power incident on the detector produce an S/N given by;

$$S/N = \int_{\lambda_1}^{\lambda_2} \frac{P_\lambda d\lambda}{(NEP_\lambda)} \quad \ldots(5.2)$$

Where;

NEP_λ : spectral noise equivalent power of the detector.

The spectral NEP_λ is given by:

$$NEP_\lambda = (A_d \Delta v)^{1/2} / D_\lambda^* \quad \ldots(5.3)$$

Where

A_d : area of detector.

Δv : electronic bandwidth (inversely proportional to observation time).

D_λ^* : spectral detectivity.

Combining Eq(4.1), (4.2) and (4.3);

$$S/N = \int_{\lambda_1}^{\lambda_2} \frac{P_\lambda \, D_\lambda^* \, d\lambda}{(A_d \Delta v)^{1/2}} = \int_{\lambda_1}^{\lambda_2} \frac{\tau \tau_o A_s A_c L_{e\lambda} \, D_\lambda^* \, d\lambda}{R^2 (A_d \Delta v)^{1/2}} \quad \ldots(5.4)$$

From the Fig (5.1) the solid angle ; for square detector is given by:

$$\Omega = \alpha^2 = \frac{A_s}{R^2} = \frac{A_d}{f^2} \quad \ldots(5.5)$$

Where:

f : focal length of collector

Substitution of Eq(5.4) into Eq(5.5) yields

$$S/N = \int_{\lambda_1}^{\lambda_2} \frac{\tau \tau_o A_c L_{e\lambda} \, D_\lambda^* \, d\lambda}{f (\Delta v)^{1/2}} \quad \ldots(5.6)$$

The collector area can be expressed as; $A_c = \frac{\pi D^2}{4}$, and the aperture ration; $F = \frac{f}{D}$, substitution in Eq(5.6), we get

$$S/N = \int_{\lambda_1}^{\lambda_2} \frac{\tau\tau_o\alpha\,\pi D\,\mathrm{L}_{e\lambda}\,D_\lambda^*\,d\lambda}{4F(\Delta v)^{1/2}} \qquad \ldots(5.7)$$

Equations (5.6) and 5.7) were derived on the assumption that the detector served as field stop ;

$$\alpha = A_d^{1/2} / f \qquad \ldots(5.8)$$

The D_λ^* of a radiation limited thermal detector is proportional to the square root of its angular field of view , as defined by its cold shield , thus:

$$D_\lambda^*(\text{cold shield}) = D_\lambda^*(\text{unshielded})/\sin\frac{\theta}{2} \qquad \ldots(5.9)$$

Where

$\frac{\theta}{2}$: half angle of acceptance.

And

$$\sin\frac{\theta}{2} = \frac{D}{2f} = \frac{1}{2F} \qquad \ldots(5.10)$$

Substitution Eq.(5.10) and (5.9) in (5.7) , we get

$$S/N = \int_{\lambda_1}^{\lambda_2} \frac{\tau\tau_o\alpha\,\pi D\,\mathrm{L}_{e\lambda}\,D_\lambda^*\,d\lambda}{2(\Delta v)^{1/2}} \qquad \ldots(5.11)$$

In this situation, the resulting S/N is not a direct function of the aperture ratio of the optical system.

5. 2 Mathematical Model of Visible and Near IR Radiometer

when light penetrates a water body, it either be absorbed or scattered. Eventually, all light will be absorbed except for that it can leave the water body through the surface Fig,(5.2). the processes of absorption and scattering can be quantified and expressed as the fraction of light absorbed or scattered from a parallel light beam passing through a very short (actually infinitesimally small) layer of media [35].

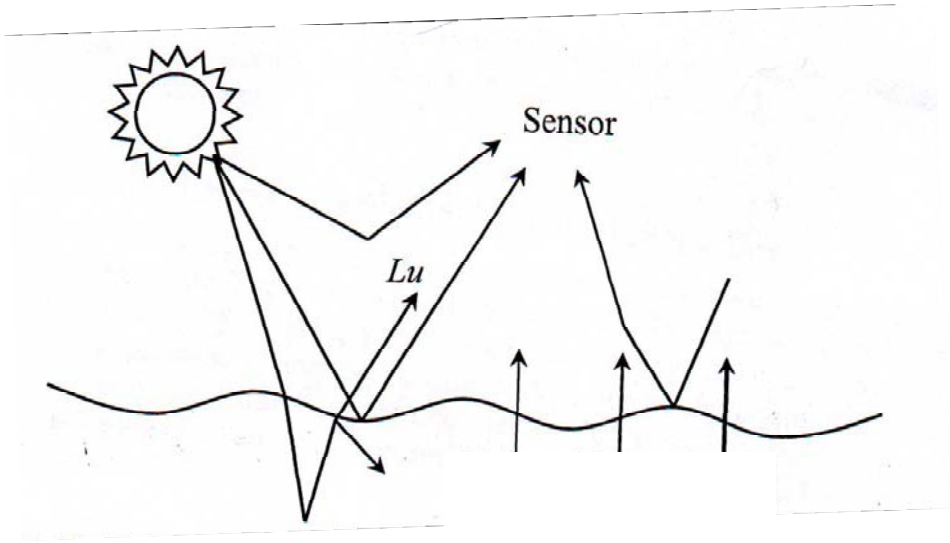

Fig. (5.2) Block Diagram Mathematical Model of Visible Radiometer

First we make use of the intermediate term absorptance, α

$$\alpha = \phi_a / \phi_o \qquad \ldots(5.12)$$

Where ϕ_o is the incident light flux in the parallel beam and ϕ_a is the light flux absorbed by the medium. Then we arrive at the absorption coefficient a by:

$$a = \Delta\alpha / \Delta r \qquad \ldots(5.13)$$

Where Δr is the thickness of the medium. The coefficient b is defined analogously to the absorption coefficient. Both are wavelength dependent (λ) and expressed in the unite of m^{-1}.a and b can added together from c;

$$c(\lambda) = a(\lambda) + b(\lambda) \quad \ldots(5.14)$$

Where c is the attenuation coefficient. These three optical properties are usually called inherent optical properties (from hereon called IOP;s) since they only are functions of the waterbody itself, and not of the incoming light. There is also a fourth IOP; the volume scattering function $\beta(\phi)$, which describes more in detail in which directions the light is scattered. The in situ volume scattering function is very hard to measure, and only a few measurements are today in use, of which a series of measurements reported by [25] stand out as the most reliable [21]. The volume scattering function is only briefly discussed in this work, although it is profound value in all aquatics optics. A fifth IOP;s that can be derived from the volume scattering function or from the scattering coefficient is the backscattering coefficient b_b i.e. the fraction of the incoming light that is scattered back towards the incident beam at angles less than 90^o . Based on the volume scattering depending on the type of water.[35].

A central term in aquatic optics and remote sensing is the reflectance of the water. In this case reflectance means the reflection caused by the waterbody itself and not reflectance caused by the surface (surface reflectance). The most common reflectance are defined as:

$$R(\lambda) = \frac{E_u(\lambda)}{E_d(\lambda)} \quad \ldots(5.15)$$

R is called the irradiance . and E is the irradiance through a horizontal plane weighted by the cosine of its incoming angle to the normal. The indices u and d means upwelling and down welling respectively. Radiance reflectance (R_r) is defined as:

$$R(\lambda) = \frac{L_u(\lambda)}{E_d(\lambda)} \quad \ldots(5.16)$$

Where L_u is the upwelling radiance and E_d is the down welling irradiance. Briefly explained, radiance is light measured in a narrow angle

using e.g. a lens. Irradiance on the contrary is light measured from all directions striking a horizontal plane from either an upward or downward direction. In remotes sensing, radiance reflectance is the desired parameter, since it is the reflectance that is measurable by a remote sensor. Radiance reflectance is an example apparent optical properties (AOP;s). These properties change not only with the constituents of the water but also with the nature of the incoming light.

The IOP;s and the AOP;s has been linked to each other through mathematical Monte Carlo simulations[35].

$$R = (0.975 - 0.629\,\mu_o)\frac{b_b}{a} \qquad \ldots(5.17)$$

Where μ_o is the cosine of the solar zenith angle just under the surface. This formula is based on the volume scattering function measured by [35] in the turbid ocean waters of San Diego Harbor; USA where b_b equals 1.9% of b and it is considered to be valid for many coastal and moderately turbid inland waters. Several similar expressions exist e.g [[6] but the main point here is that it is theoretically possible to determine the IOP;s a and b_b from a reflectance spectra of a water body.

The mathematical model of this system is given by;

$$\overline{V_{d1}} = G(P_\lambda + P_{n\lambda})R_\lambda \text{ for } 0 \le t < \frac{\tau_s}{2} \quad \text{(On-state)} \qquad \ldots(5.18)$$

$$\overline{V_{d2}} = GP_{n\lambda}R_\lambda \text{ for } \frac{\tau_s}{2} \le t < \tau_s \quad \text{(OFF-state)} \qquad \ldots(5.19)$$

Where

G : Gain of the circuit

P_λ : receiving power.

$P_{n\lambda}$: noise power.

R_λ : responsivity

$\tau_s = \frac{1}{f_s}$, sampling time.

The output are then summed and fed to low-pass filter (integrator), then the combination of Eq.(5.18) and (5.19) gives:

$$\overline{V_d} = \frac{1}{2}\left(\overline{V_{d1}} - \overline{V_{d2}}\right) = GP_\lambda R_\lambda \quad \ldots(5.20)$$

To calculate the reflectance of different types of polluted water the following expression is used

$$R_\lambda = \frac{\overline{V}_{band}}{\overline{V}_{sky}} \quad \ldots(5.21)$$

Where;

$\overline{V}_{band}$ band voltage (*mv*)

$\overline{V}_{sky}$ sky voltage (*mv*)

The relationship between emissivity and reflectance is given by;

$$\varepsilon_\lambda = 1 - R_\lambda \quad \ldots(5.22)$$

5. 3 Mathematical Model of Microwave Radiometer

5. 3.1 Equation For simplified Signal Conditions

A special case of great importance is a radar for which all parameters in Eq. (3.1) are essentially unchanged from one part of the resolution cell to the other. When this is true, the integral of Eq.(3.1) may be replaced simply by the product of the factors within it and the area A:[32]

$$W_r = \frac{W_t G^2 \lambda^2 \sigma^o A}{(4\pi)^3 R^4} \quad \ldots(5.23)$$

Many radar analyses assume this condition to prevail even though the approximations may be relatively imperfect. Figure (5.3) illustrates the geometry for a pulse radar for which this approximation may be applied.

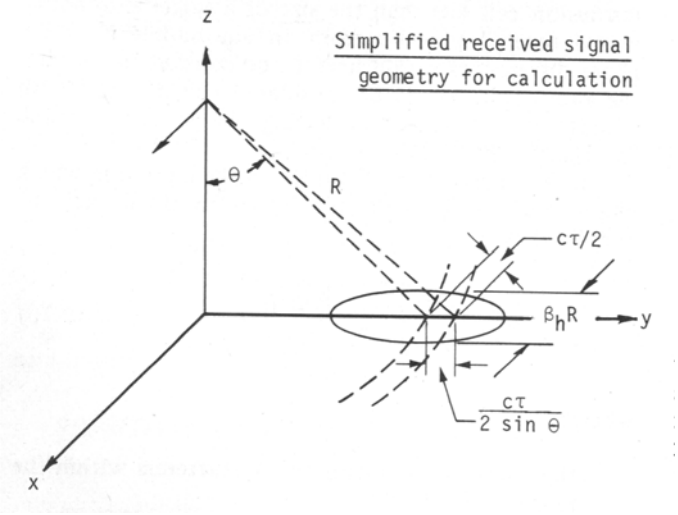

Fig.(5.3): Geometry for simplified received signal calculation [32]

The illuminated area *A* in this case is given by

$$A = (\beta_h R)\frac{c\tau}{2\sin\theta} \qquad \ldots(5.24)$$

Where:

β_h : is the effective beam width of the antenna, so that ,

$\beta_h R$: is the dimension of the area transverse to the radius vector.

The other factor gives the ground resolution cell size in the direction away from the radar for a pulse of duration τ

Where:

c is the velocity of light.

θ is the angle of incidence.

Substituting this expression into Eq.(5.24) gives a familiar from of the radar Equation:

$$W_r = \frac{W_t\, G^2\, \lambda^2\, \sigma^o\, \beta_h\, c\, \tau}{2(4\pi)^3 R^3 \sin\theta} \qquad \ldots(5.25)$$

This formula may be modified in numerous ways, since β_h and G are not independent, and it is often convenient to express distance in terms

of height rather than slant range. No attempt will be made to enumerate here the various forms of the equation.

5. 3.2 Surface Emission and Scattering

In Fig.(5.4) radiation of intensity (E_o Wm^{-2}) incident upon an element of surface area A at an angle of incidence θ_o and azimuth ϕ_o; the intensity of the scattered radiation in the direction (θ_s, ϕ_s) at a distance R from A being E_s (where the subscripts 0 and S designate incident and scattered radiation directions, respectively then the differential scattering coefficient $\gamma(\theta_o, \phi_o; \theta_s, \phi_s)$ is defined by:[32]

$$\gamma_{ij}(\theta_o, \phi_o; \theta_s, \phi_s) = \left(4\pi R^2 E_s\right)/\left(E_o A \cos\theta_o\right) \quad \ldots(5.25)$$

Where:

$i, j = h$ or h

v: vertical polarization.

h: horizontal polarization.

The first and second subscript of γ_{ij} indicate the polarization state of the incident and scattered radiation, respectively.

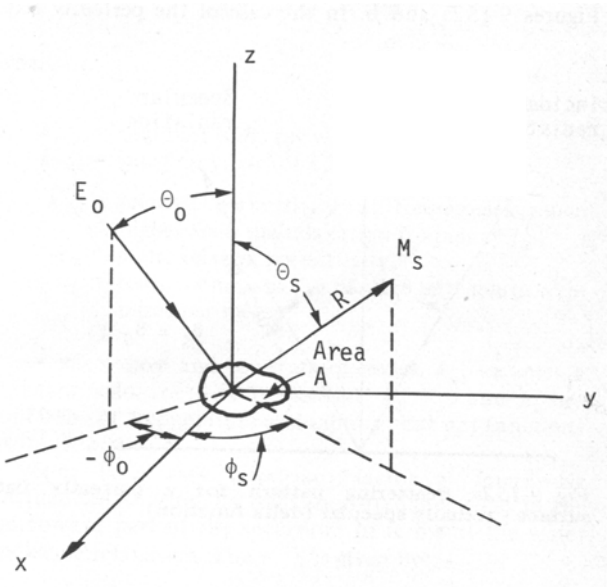

Fig.(5.4): Geometry of incident and scattered radiation [32]

Note that in the definition of γ_{ij} the $\cos\theta_o$ term was used to convert the area A into a project area, A $\cos\theta_o$, in the direction (θ_o,ϕ_o). A related quantity based on the actual area A (rather than the project area) is the bistatic scattering cross-section per unit area (also known as the bistatic scattering coefficient) σ_{ij}^o which is then given by:[34]

$$\sigma_{ij}^o,(o;s)=\gamma_{ij}(o;s)\cos\theta_o, \qquad \ldots(5.26)$$

Where (for brevity)

The direction (θ_o,ϕ_o) and (θ_s,ϕ_s) have been designated by the variables O and S respectively.

The physical meaning of σ^o (or σ) is clear ; for a given fixed direction of incident energy, σ^o represents the reradiation pattern as a function of s. in general σ^o consist of two components , a specular component and a diffuse component, as shown by the examples in Fig.(5.5).

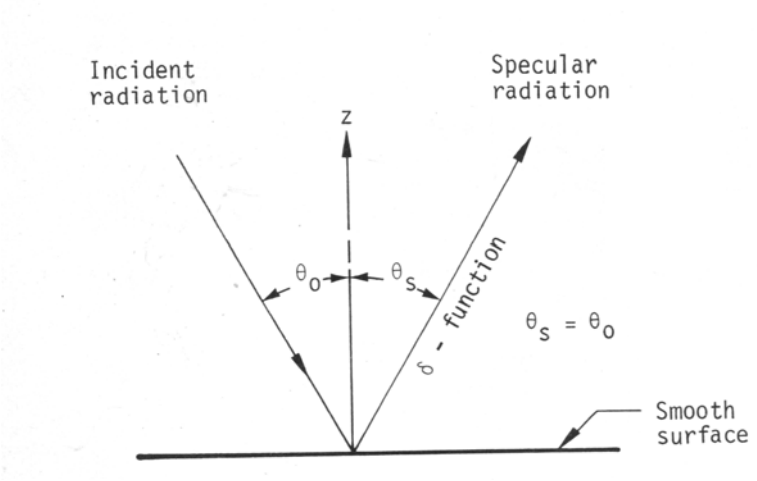

Fig.(5.5): Scattering Pattern for a perfectly flat surface-actually specular (delta function) [34]

In case of the perfectly flat surface, only the specular component exists, while for the rough surface (the scale of roughness is usually defined in terms of spatial variation relative to the wavelength of the incident energy) the incident power scatters in all directions in the upper hemisphere. The actual shape and magnitude of the scattering pattern is determine by the surface geometry, the subsurface geometry if penetration is possible, and the dielectric properties.

By applying Kirchhff's radiation law and incorporating the polarization properties of the surface, [31] developed generalized expressions for the surface polarized emissivity $\varepsilon_i(o)$ and the scattered temperature term $T_{sci}(o)$ in terms of the surface differential scattering coefficients $\gamma_{ii}(o,s)$ and $\gamma_{ij}(o,s)$:

$$\varepsilon_i(o) = 1 - \frac{1}{4\pi}\int\left[\gamma_{ii}(o,s) + \gamma_{ij}(o,s)\right]d\Omega_s \qquad \ldots(5.27)$$

5. 3.3 Scattering Models of Perfectly Smooth Surface Model

A surface can be defined as smooth if its height variations are much smaller than the radiation wavelength, usually by an order of magnitude or better.

Under this condition, the differential scattering coefficient will only have a specular component which mathematically can be described by a Dirac delta function δ as follows [32].

$$\gamma_{ij}(\theta_o,\phi_o;\theta_s,\phi_s) = \frac{4\pi\left|\rho_i\right|^2 E_s}{\sin\theta_o}\delta(\theta_s-\theta_o)/\,\delta(\theta_s-\theta_o) \qquad \ldots(5.28)$$

Where

$\left|\rho_i\right|^2$: i-polarized power reflectance coefficient

θ_o and ϕ_o: the specular direction

δ: Dirac delta function.

Furthermore, for $i \neq \mathrm{j}$, $\gamma_{ij=0}$; that is the absence of roughness , no depolarization by the surface takes place.

Inserting Eq.(5.28) in to Eq.(5.27), and using the definition of $d\Omega_s = \sin\theta_s d\theta_s d\phi_s$ we get

$$\varepsilon_i(\theta_o,\phi_o) = 1 - \frac{1}{4\pi}\iint \frac{4\pi|\rho_i|^2}{\sin\theta_o}\delta(\theta_s-\theta_o)\delta(\theta_s-\theta_o)\sin\theta_s d\theta_s d\phi_s \qquad \ldots(5.29)$$

Which reduces to the simple form:

$$\varepsilon_i(\theta_o,\phi_o) = 1 - |\rho_i(\theta_o)|^2 \qquad \ldots(5.30)$$

Chapter Six

Measurement and Results

6.1 Results of Measurement in Visible and I.R

In this work, the measurements of the design radiometer were done for pollution for the wavelength between 430 and 110 mm, the reason why we are restricted to this wavelength interval because that the intensify of solar radiation bellow 400 mm is very low and organic matter in water strongly absorbs violet light. The longer limit is also to some extent set up by the intensity of solar radiation , but the main reason in this case is that the water itself is strongly absorber of red and near infrared light.

This means that light can penetrate water outside the wavelength band of 400 to 110 nm, and consequently, we have no direct need for making optical measurement outside this range. A radiometer sensor has a field-of-view such that at any moment in time it is viewing a part of the water and recording how much radiation is being reflected from the water. The reflected radiation is first divided into different spectral components in the sensor (blue, green and red light etc) and the amount of radiation for each component is then recorded by a detector, or a row of detectors, as a digital number.

The design radiometer is a two channel instrument sensitive to energy in the visible spectrum (0.4 to 0. 75 μm) by using silicon photo detector diode and in the infrared region (0.8-1.1 μm) by using InGaAs PIN photodiode, with the specification data shown in appendix C.

The results of the measurement, for pure water, and different samples of polluted water are shown in tables (6.1),(6.2) and (5.3).

Table (6.1): Measured voltage for pure water of 6.25 liters , at $T = 300^o K$

Band (μm)	V_{in} **(mV)**	V_r **(mV)**
Blue (0.43-0.49)	440	36
Green (0.51-0.59)	435	31
Red (0.61-0.69)	425	13
I.R (0.8-1.1)	400	9

Table (6.2): Measured voltage for polluted water with salt (6.25 liters +1 Kg of salt) at $T = 300^o K$

Band (μm)	V_{in} **(mV)**	V_r **(mV)**
Blue (0.43-0.49)	440	44
Green (0.51-0.59)	435	42
Red (0.61-0.69)	425	26
I.R (0.8-1.1)	400	19

Table (6.3): Measured voltage for polluted water with one liter oil in 6.25 liter of pure water at $T = 300^o K$

Band (μm)	V_{in} **(mV)**	V_r **(mV)**
Blue (0.43-0.49)	440	36
Green (0.51-0.59)	435	26
Red (0.61-0.69)	425	10
I.R (0.8-1.1)	400	5

The result of calculation are shown in tables (6.4) (6.5) and (6.6), by using the following relation.

$$\rho_{(\lambda)} = \frac{V_r}{V_{in}} \quad \text{and} \quad \varepsilon(\lambda) = 1 - \rho(\lambda) \qquad \ldots(6.5)$$

The results of these calculations is shown in figure (6.1)

Table (6.4): Calculated spectral reflectance and emissivity for pure water of 6.25 liters at $T = 300^o K$

Band (μm)	$\rho(\lambda)$	$\varepsilon(\lambda)$
Blue (0.43-0.49)	0.084	0.916
Green (0.51-0.59)	0.072	0.928
Red (0.61-0.69)	0.036	0.964
I.R (0.8-1.1)	0.024	0.976

Table (6.5): Calculated spectral reflectance and emissivity for polluted water with salt (6.25 Liters +1 Kg of salt) at $T = 300^o K$

Band (μm)	$\rho(\lambda)$	$\varepsilon(\lambda)$
Blue (0.43-0.49)	0.100	0.900
Green (0.51-0.59)	0.098	0.902
Red (0.61-0.69)	0.062	0.938
I.R (0.8-1.1)	0.048	0.952

Table (6.6): Calculated spectral reflectance and emissivity for polluted water with one Liter oil in 6.25 liters of pure water at $T = 300^{o} K$

Band (μm)	$\rho(\lambda)$	$\varepsilon(\lambda)$
Blue (0.43-0.49)	0.083	0.917
Green (0.51-0.59)	0.060	0.940
Red (0.61-0.69)	0.024	0.976
I.R (0.8-1.1)	0.012	0.988

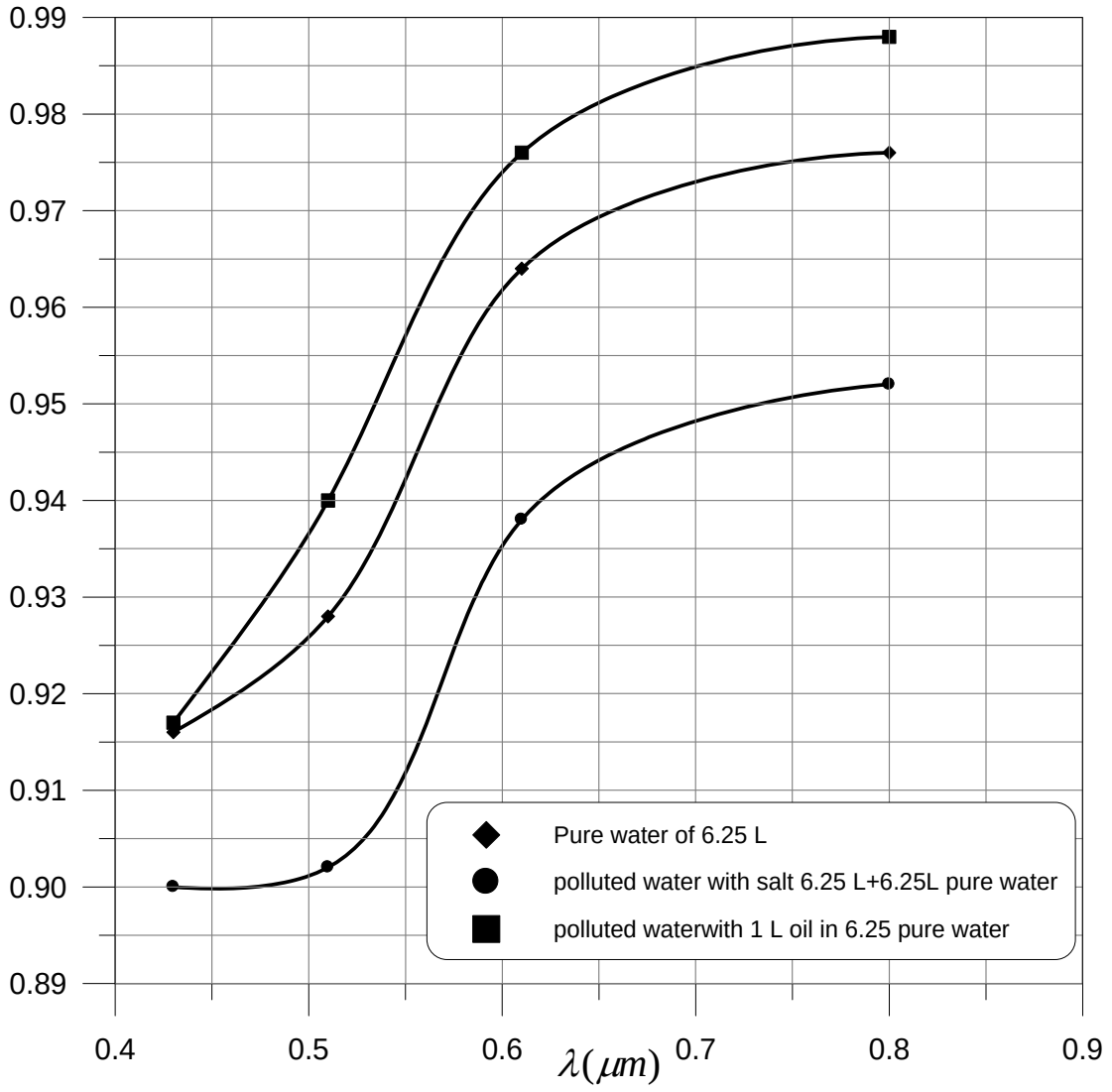

Fig. (6.1): Spectral emissivity of water as a function of wavelength of visible and I.R channel

To compare the results of the designed radiometer with the result calculated by theoretical model [35].

Because radiance reflectance is relatively independent of the illumination and has often been approximated as an empirical function of (Inherent Optical Properties) IOP_s of water [35]

$$R_r(\lambda) = 0.083\left(\left(b_b(\lambda)/a(\lambda)\right) + b_b(\lambda)\right) \quad \ldots(6.6)$$

Where:

$b_b(\lambda)$: is the backscattering coefficient

$a(\lambda)$: is the absorption coefficient.

The logic consequence of Eq.(6.6) are that, greater backscattering will increase the radiance reflectance and greater absorption will lower the radiance reflectance.

Pure water absorbs strongly beginning at about 550 nm and absorption increases with wavelength scattering is greatest for shorter wavelengths, which is the reason why pure water looks blue [36].

The results of measured and calculated emissivity for pure water are shown in table (6.7) and figure (6.2).

Table (6.7): Measured and Calculated emissivity of pure water at ($T=300\ ^oK$)

Band (μm)	**Measured spectral emissivity**	**Calculated spectral emissivity**
Blue (0.43-0.49)	0.916	0.895604
Green (0.51-0.59)	0.928	0.899216
Red (0.61-0.69)	0.964	0.923104
I.R (0.8-1.1)	0.976	0.93547

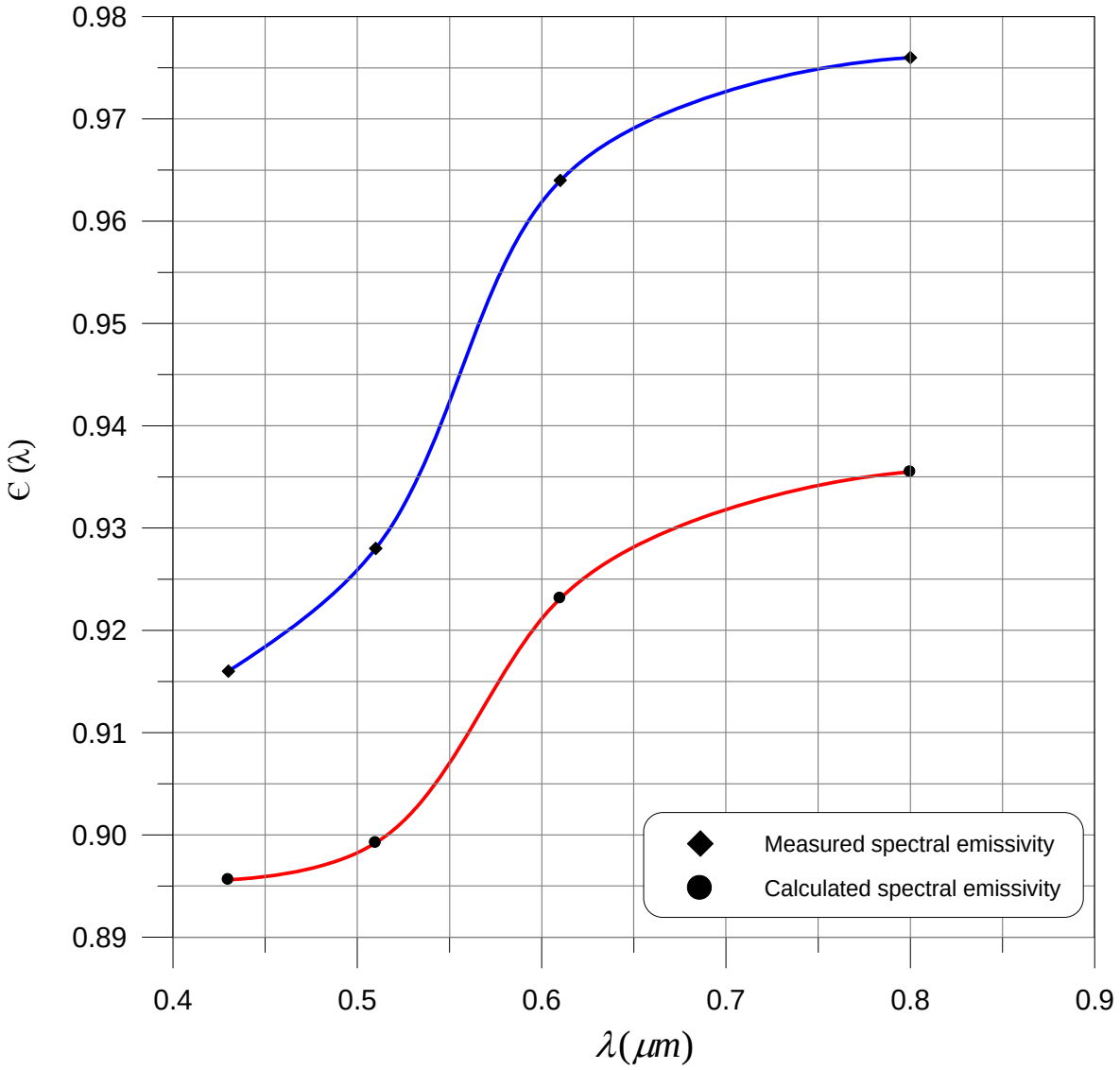

Fig. (6.2): Spectral emissivity of pure water as a function of wavelength of visible and I.R channel

6.2 Results of Measurement in Microwave ($\lambda = 2.8\,cm$)

The measurement was carried by using transmitter-receiver radar system working at wavelength of $2.8\,\mu m$. There are two reasons for using this technical of measurement, firstly the received signals from the reflection of water when using passive radiometer is very weak, secondly the interference due to mobile base-station at this wavelength is very strong. The measurement was done in two stages.

1. The transmitter and receiver antenna were pointed in the line-side of axis.
2. Then the measurement for polluted water were taking for different incident angles of receiving antenna.

Two different types of water pollutions were used; salt pollutants, and oil pollutants.

The result of these types of pollution were shown in tables (6.7),(6.8) and (6.9).

Table (6.8): Measured voltage for pure water ($T = 300\ ^{o}K$) of 6.25 liter.

Angle (degree)	Vertical polarization voltage (*mv*)	Horizontal polarization voltage (*mv*)
$T_x \rightarrow R_x$	200	200
10^{o}	60.6	49.2
20^{o}	47.2	48.9
30^{o}	40.4	47.5
40^{o}	27.6	45.5
50^{o}	26.8	44.1
60^{o}	0.8	41.4

Table (6.9): Measured voltage for polluted water with salt (6.25 Liter +1 Kg of salt).

Angle (degree)	Vertical polarization voltage (*mv*)	Horizontal polarization voltage (*mv*)
$T_x \rightarrow R_x$	200	200
10^o	49.5	49.4
20^o	49.1	48.9
30^o	47.9	47.6
40^o	46.3	45.7
50^o	44.2	44.1
60^o	39.1	41.4

Table (6.10): Measured voltage for polluted water with one Liter oil in 6.25 liter of pure water.

Angle (degree)	Vertical polarization voltage (*mv*)	Horizontal polarization voltage (*mv*)
$T_x \rightarrow R_x$	200	200
10^o	47.5	46.8
20^o	48.2	45.9
30^o	48.8	48.3
40^o	49.3	48.9
50^o	49.7	49.4
60^o	49.8	49.8

For the radiometer we can use the following equation to calculate the reflectance and emissivity from the result table (6.7),(6.8) and (6.9) by using the following Eqs.

$$\rho_{wi}(\theta) = \frac{V_{ri}(\theta)}{V_{Tx}} \quad \ldots(6.7)$$

$$\varepsilon_{wi}(\theta) = 1 - \rho_{wi} \quad \ldots(6.8)$$

Where

V_{Tx} : measured voltage of transmitter.

$V_{ri}(\theta)$: measured reflected voltage for different incident angle and polarization.

The result of calculation reflectance and emissivity as function of incidence angle are shown in table (6.10),(6.11) and (61.12)

Table (6.11): Calculated spectral reflectance emissivity for pure water of 6.25 liter at 11 AM.

Angle (degree)	$\rho_v(\theta)$	$\varepsilon_v(\theta)$	$\rho_h(\theta)$	$\varepsilon_h(\theta)$
10^o	0.303	0.697	0.440	0.560
20^o	0.236	0.764	0.569	0.431
30^o	0.202	0.798	0.602	0.398
40^o	0.138	0.832	0.639	0.364
50^o	0.134	0.866	0.669	0.331
60^o	0.004	0.998	0.702	0.298

Table (6.12): Calculated spectral reflectance emissivity for polluted water with salt (6.25 liter +1 Kg of salt) .

Angle (degree)	$\rho_v(\theta)$	$\varepsilon_v(\theta)$	$\rho_h(\theta)$	$\varepsilon_h(\theta)$
10^o	0.501	0.499	0.537	0.463
20^o	0.435	0.565	0.569	0.431
30^o	0.403	0.597	0.603	0.397
40^o	0.368	0.632	0.636	0.364
50^o	0.333	0.667	0.669	0.331
60^o	0.268	0.732	0.702	0.298

Table (6.13): Calculated spectral reflectance emissivity for polluted water with one Liter oil in 6.25 liter of pure water.

Angle (degree)	$\rho_v(\theta)$	$\varepsilon_v(\theta)$	$\rho_h(\theta)$	$\varepsilon_h(\theta)$
10^o	0.602	0.398	0.616	0.384
20^o	0.581	0.419	0.590	0.410
30^o	0.568	0.432	0.576	0.424
40^o	0.548	0.452	0.563	0.437
50^o	0.535	0.465	0.543	0.457
60^o	0.519	0.481	0.470	0.470

Figs.(6.4) and (6.5) show the measured emissivity as a function on incidence angle.

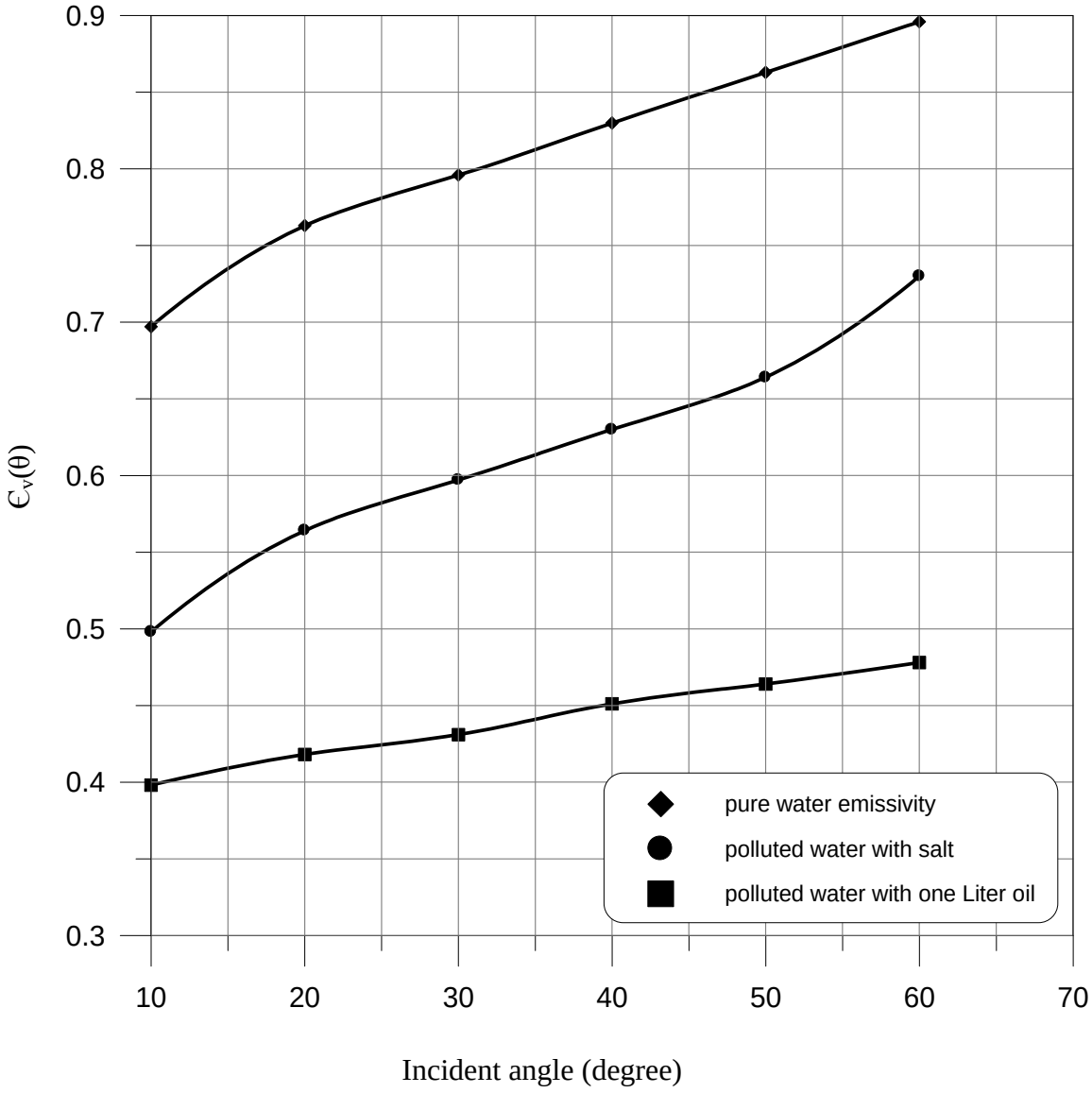

Fig.(6.3) Emissivity of water at wavelength (2.8 μ) as a function of incident angle, of vertical polarization for different types of polluted water

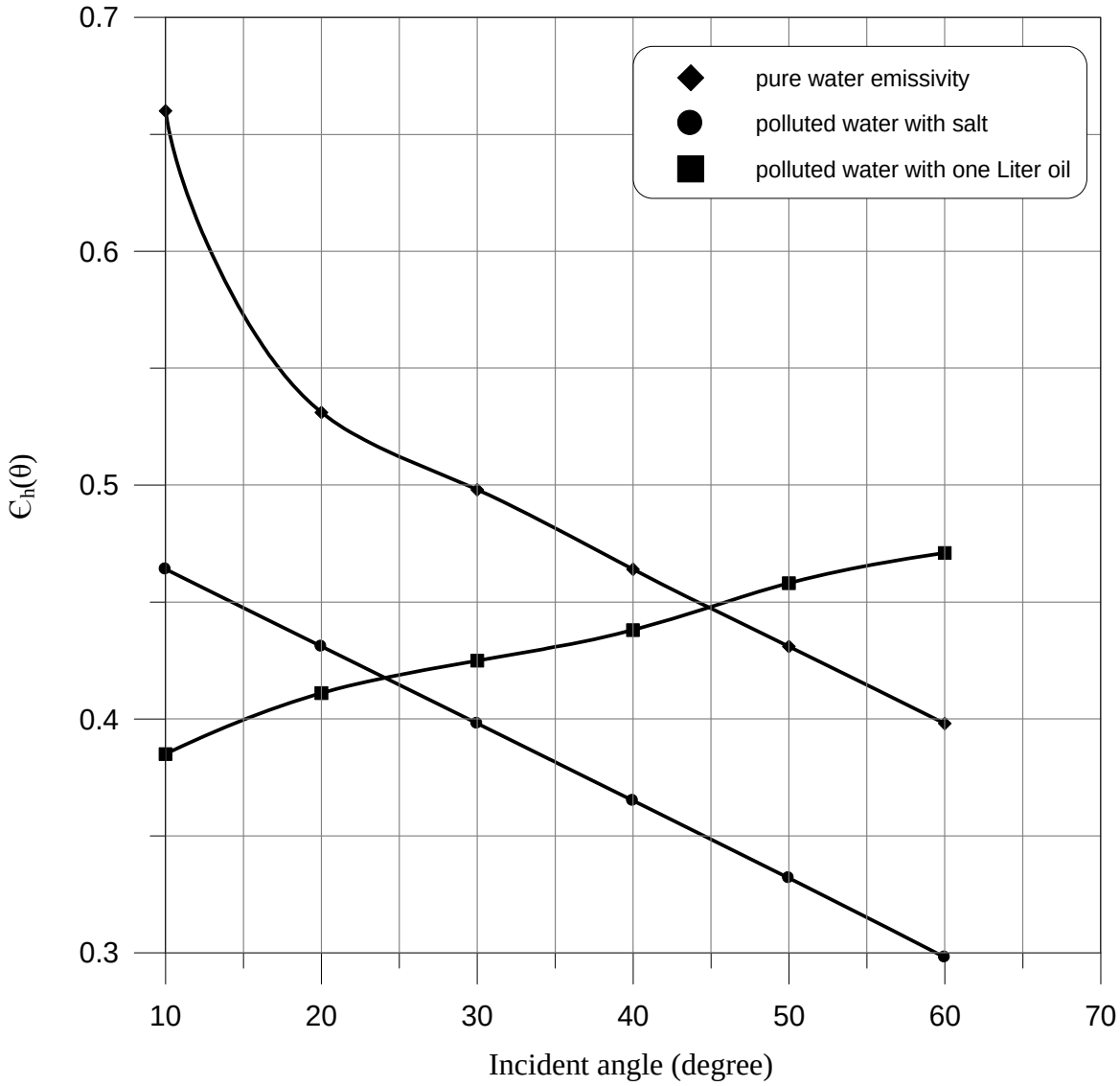

Fig.(6.4) Emissivity of water at microwave length (2.8 μ) as a function of incident angle, of horizontal polarization for different types of polluted water

To compare the results of the designed radiometer with the result calculated by theoretical model [34]. We considered the result of pure water at T= 300 ^{o}K , ($\lambda = 2.8$ *cm*) and by using the following relationships:

From [34] the dielectric constant of pure water:

$$k_r = 60 - j40 \qquad \ldots(6.16)$$

From equation (4.17)

$$R_h = \frac{\cos\theta - \sqrt{k_r - \sin^2\theta}}{\cos\theta + \sqrt{k_r - \sin^2\theta}} \qquad \ldots(6.17)$$

$$R_v = \frac{k_r \cos\theta - \sqrt{k_r - \sin^2\theta}}{k_r \cos\theta + \sqrt{k_r - \sin^2\theta}} \qquad \ldots(6.18)$$

And

$$\rho_i(\theta) = |R_i(\theta)|^2 \qquad \ldots(6.19)$$

$$\varepsilon_i(\theta) = 1 - \rho_i(\theta)$$

The table bellow shows, the experimental and calculated emissivity of pure water for different incidence angles polarizations

Table (6.14): Measured and theoretical spectral emissivity for pure water for different polarization .

Angle (degree)	Practical Results of emissivity at $T = 300\ ^{o}K$		Calculated emissivity at $T = 300\ ^{o}K$	
	$\varepsilon_h(\theta)$	$\varepsilon_v(\theta)$	$\varepsilon'_h(\theta)$	$\varepsilon'_v(\theta)$
10^{o}	0.560	0.697	0.367723	0.392353
20^{o}	0.431	0.764	0.343485	0.458993
30^{o}	0.398	0.798	0.299746	0.501218
40^{o}	0.364	0.832	0.242052	0.561923
50^{o}	0.331	0.866	0.182649	0.534016
60^{o}	0.298	0.998	0.116128	0.6518254

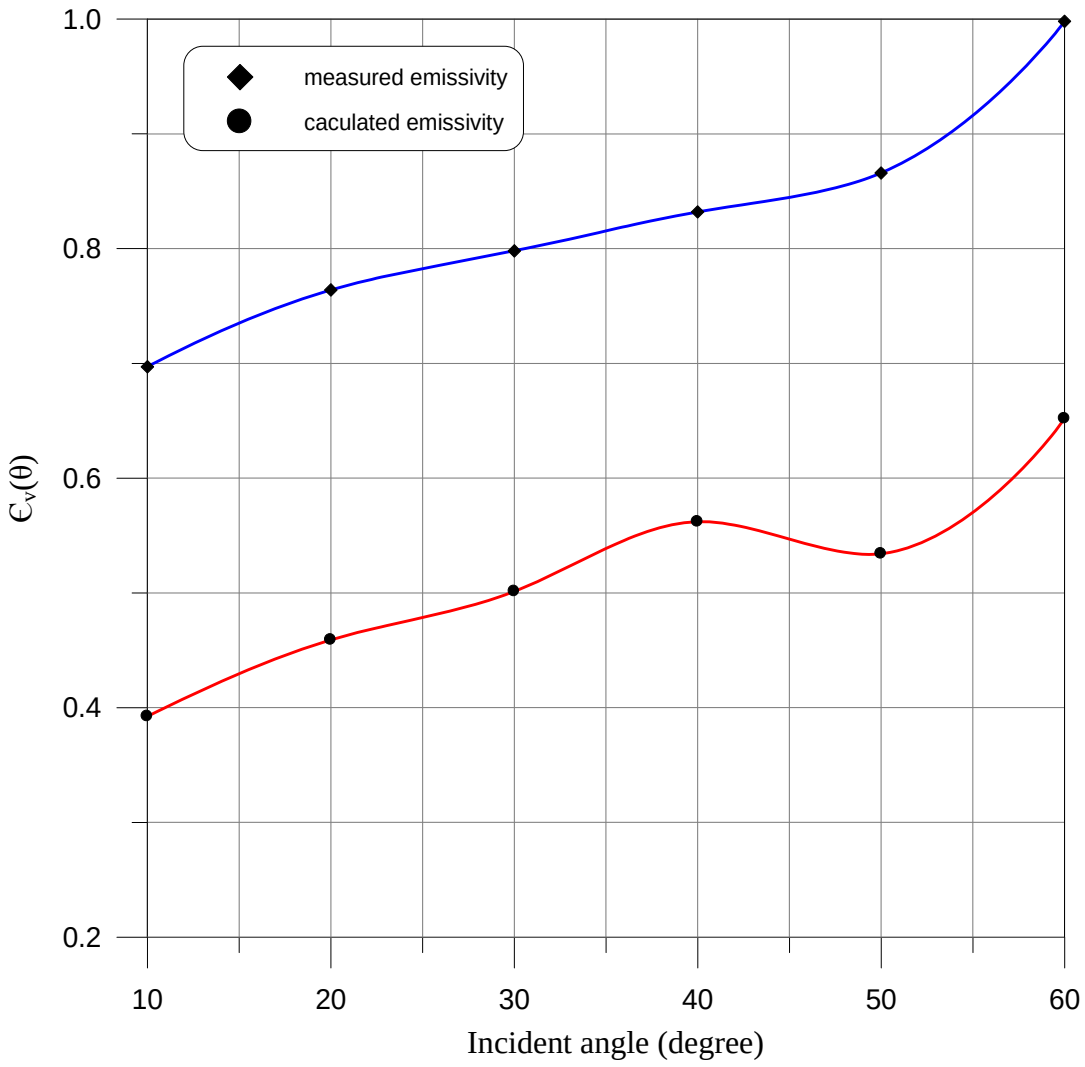

Fig.(6.5) Shows the deviation between measured and calculated emissivity of pure water for vertical polarization .

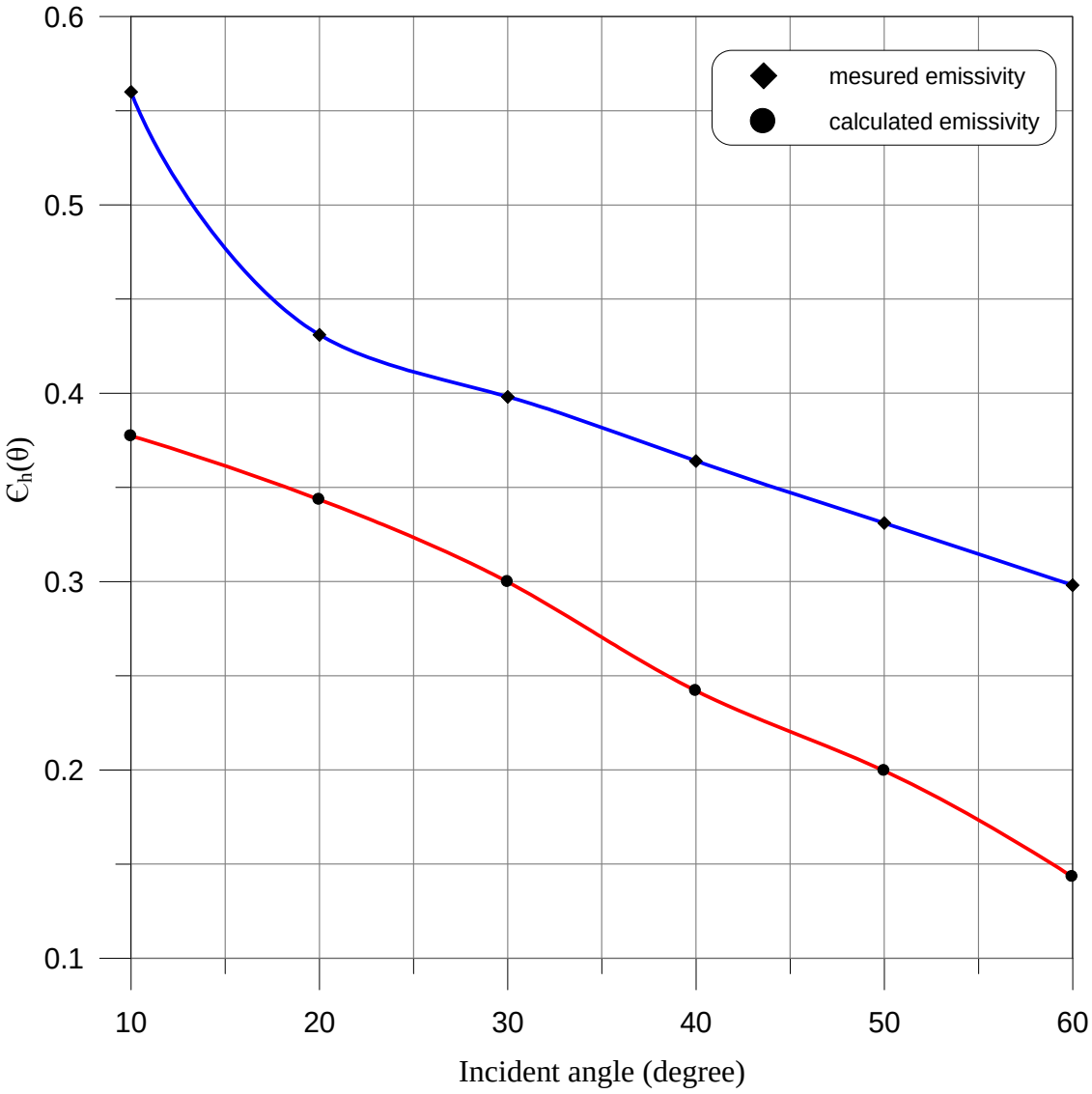

Fig.(6.6) Shows the deviation between measured and calculated emissivity of pure water for horizontal polarization .

6.3 Discussion

A. From the results of measured spectral emissivity in I.R and visible regions, the emissivity increases with increasing the wavelength and these in a good agreement with either results in references [21]. The reason for these, is the intensity of the light that penetrates the water surface will decrease exponentially with increasing depth. This process is known as attenuation and is composed by scattering and absorption of the light by water itself and substances in the water. Red light is attenuated faster than blue light and usually penetrates less than one meter. Blue light on the other hand can penetrate the water down to approximately 30 meters on the very clear water. At a certain depth, all light has been absorbed and targets located below this depth will be invisible to any remote sensing sensor.

B. From the results of measured emissivity for two polarization microwave radiometer, there is some difference in the values of emissivity compare with reference [31,34], the reasons for these are;

1. Although the plane surface scattering model is a poor representive of real water surface, it is commonly used as first-step approximation, practically for the water because of its simplicity and easy of calculation.
2. The error of measurements in the electronic radiometer is due to the offset of electronic components and the accuracy of calibration method.
3. However, as radiance inherently nonlinear as a function of temperature, sensor output is also nonlinear as a function of temperature.

4. The difference between temperature that its assume for the mathematical model and the experimental temperature, this give different in the value of emissivity.

Conclusions and Future Work

7.1 Conclusions

The main conclusions that can be drawn from this research are summarized as follows.

1. The result from the measuring parameter of design radiometers are relatively well to ground truth measurement.
2. The main conclusion after these studies is that the designed radiometer could be used for other than water pollution measurement, for example, rocks, soils etc.
3. It was concluded that the influence of absorption and backscattering need to be further investigated, by field measurements and laboratory analysis of process water in order to specify the concentration levels and substances detectable using radiometer technique.
4. It was also concluded that the results from sensor with at least three visible bands, should be useful for mapping of geomorphologic zones.
5. EM radiometer from oil slicks on the water surface provides unique and measurable signatures up to 70^0 k.
6. Both theory and measurements demonstrates that horizontally polarized microwave radiometer are more responsive to the oil films than those vertically polarized.
7. Microwave radiometer temperature of water surfaces with oil slicks increase, but the basic relationship is associated with the mass of oil per unit area.
8. Surface thermometric temperatures are difficult to measure accurately in the laboratory because direct contact measurement invariably disturb the surface temperatures equilibrium.

9. The field sample analyzed in laboratory supported the results from the investigation of the airborne data and like these types of sensors should be useful for detection of industrial plumes and within plume spectral variably.

7.2 Future Work

1. It is recommended that the water pollution radiometer in laboratory should be modified to use it in the field for testing the river and lake.
2. For I.R and visible radiometers the system can be modified by using automatic self calibration of the system by using two detectors at the same electronic circuit, one looking to reference sample and the other one looking at the water sample.
3. By using computer to control the operation of radiometers and take results from the sensor to calculate the different parameters for water quality.
4. By using remote sensing data with the measurement data of radiometers to get sufficiently close to the truth parameter for water quality.
5. It is quite likely that the future water monitory system will be producing information as output rather than data. The imaging system should then be adapted to the application and including in a system with a number of sensors on ground level which support the system with ground truth data.

Contents

List of Figures

List of Symbols

Symbol	Definition
Q_λ	spectral radiant energy
ϕ_λ	spectral radiant flux
E_λ	spectral irradiance
M_λ	spectral exitance
I_λ	spectral radiant intensity
L_λ	spectral radiance.
c	velocity of light
S	value of the signal.
λ_1	the effective spectral limits of response
λ_2	the effective spectral limits of response
λ	wavelength
T	absolute temperature in degrees Kelvin.
W_r	received power
W_t	transmitted power
G_t	gain of the transmitting antenna in the direction of the target
R	distance between radar and target
σ	radar cross section effective backscatter area of the target
A_r	effective receiving area of the receiving antenna aperture.
σ_o	scattering coefficient
$\sigma(\theta)$	backscattering coefficient of incident wave
k	wave number ($2\pi / \lambda$)
k_r	relative dielectric constant
$\sigma_\ell(\theta)$	backscattering cross section

Symbol	Definition
ω	radian frequency of the radiation
h	height variations above a plane in wavelengths
$\sigma_t(\theta)$	backscattering cross section for TE.
k	Permittivity.
μ	permeability.
dW	infinitesimal power,
B	brightness of container at position
$d\Omega$	infinitesimal solid angle,
ϕ	spherical coordinate angles
dA	infinitesimal area of plate surface,
df	infinitesimal element of bandwidth
k	Boltzmann's constant
E_i	incident electric field with *v* or *h* polarization.
E_r	reflected electric field with v or h polarization.
θ_i	angle of incidence of plane wave source.
k_{r1}	dielectric constant
k_{r2}	dielectric constant of water
σ_2	conductivity of water
k_o	permittivity of free space

List of Symbols

Symbol	Definition
θ	incident angle.
Rs	solar radiation
ε_s	emissivity of the radiation surface
σ	Stefan-Boltzmann's constant
D	the antenna gain and directivity
T_o	temperature of the medium surrounding the antenna.
T_g	T_g :ground temperature
$\rho_j(\theta)$	polarized reflection coefficient
$T_{air}(z)$	atmospheric thermometric temperature in °K,
α (z)	absortpion coefficient in nepers per unit length at height z above the surface
m	proportionality constant representing sensitivity and gain of the associated amplifier system (volts/amp);
A	area of water surface viewed by the detector (m^2);
a	surface area of detector
$\delta\lambda$	wavelength interval of single multispectral channel,
k'_{rw}	real part of k_r for water
k''_{rw}	imaginary part of k_r for water
k_∞	relative permittivity at frequencies much higher than the relaxation frequency f_o
k_s	static relative permittivity,
σ_i	ionic conductivity of the salt solution in mhos per meter.
A_s	area of the extended source with in sensor field of view.
A_c	effective area and collector optics.
$L_e\lambda$	spectral radiance of source.

Symbol	Definition
$\tau(\lambda)$	transmissivity intervening atmosphere over the wavelength
$\tau_o(\lambda)$	transmissivity of optics over.
NEP_λ	spectral noise equivalent power of the detector.
A_d	area of detector.
$\Delta\lambda$	electronic bandwidth (inversely proportional to observation time).
D^*_λ	spectral detectivity.
f	focal length of collector
G	Gain of the circuit
P_λ	receiving power.
$P_{n\lambda}$	noise power.
$R(\lambda)$	responsivety
τ_s	sampling time.
L	loss factor (reciprocal of gain) accounting for ohmic losses by antenna and transmission line.
η_a	antenna radiation efficiency
$L_{r\ell}$	transmission line loss factor
F_{rf}	noise figure of radio frequency (RF) amplifier
F_m	noise figure of mixer
F_{if}	noise figure of intermediate frequency (IF) amplifier
G_{rf}	power gain of RF amplifier
G_m	power gain of mixer
G_i	the gain of the ith stages
T_i	effective (not physical) noise temperature of the i^{th} stage.
C_d	square-law detector power sensitivity constant

Symbol	Definition
f_o	center frequency
$b_b(\lambda)$	is the backscattering coefficient.
$a(\lambda)$	is the absorption coefficient
ε_{wi}	emissivity of water surface
ρ_{wi}	reflectivity of water surface.
T_w	water surface temperature.
T_{sky}	sky temperature
V_{Tx}	measured voltage of transmitter.
V_{wi}	measured voltage for different incident angle and polarization.

List of Tables

REFERENCES

[1] Rober G, Reeves, ABraham Anson, and David lands, (1975)" Mannual of Remote sensing ", First edition, published by American Socity of Photogrammetry.

[2] Lillesand T. and Kiefer, R, 1999, " Remote Sensing and Image Interpretation" 4th Edition, John Wiley & Sons Inc.

[3] Mumby. P. and Edwards, A. 2002. " Mapping marine environment, 82(2-3), 248-257.

[4] Kannedy J.M, and E.G Wermund, 1971 " Oil Spils, IR and Microwave : Photogram. Eng Vol 37, P 1235-1242.

[5] Gordon, H.R, et al, (1975) " Computed relationship between inherent and apparent optical properties of a flat homogenous ocean". Applied optics 14; 417-427.

[6] Gordon, H.R, et al ,(1988), " A semianalytical radiance model of ocean color." Journal of Geophysical Research 93: 10909-10924.

[7] Morel, A. and L. Prieur (1977). " Analysis of variations in ocean color." Limnology and Oceanography 22:709-722.

[8] Sathy endranath, et al, (1987). " Variations in the spectral values of specific absorption of phytoplankton." Limology and Oceanography 32:403-415.

[9] Dekker, A.G(1993). " Dection of optical water resolution parameters for entrophic water, Free university.

[10] Bukata, R.P, et al .,(1979). " Dtermination of inherent optical properties of Lack Ontario coastal waters." Applied Optics 18:3926-3933.

[11] Dekker , A.G et al ., (1991). " Quantitative modeling of inland water quality for high-resolution MSS systems." IEEE Transactions on Geoscience and Remote Sensing 29:89-95.

[12] Daives-Colley, R.J. and W.N Vant (1987). " Absorption of light by yellow substance in freshwater lackes" Limnology and Oceanography. 32:416-425.

[13] Tassan, S and G.M. Ferrari (1995). " An alternative approach to absorption measurements of aquatic particals retained on Fillers." Limology and Oceanography 40: 1358-1368.

[14] Strombeck , N,(2001), " Correction methods for backscattering measurements in highly absorbing water." The Science of the Total Environment 268: 123-127.

[15] Tiuri, MarHiE., (1966). " Radio-telescope receivers; Chapter 7, Radio Astronomy (J.D, editor) Mc Graw-Hill.

[16] Kraus. S.P, et al (1977)," Radar Detection of Surface Oil Slicks" , photo, Eng. And Bem. Sens, 43 pp 1523-1531.

[17] Droppleman , J. (1970) " Apparent Microwave emissivity of sea Foam : Jour. Geophys. Res, V. 75. Pp 696-698.

[18] Allen. W.A and A.J. Richardson, (1968), " Interaction of light with a plant canopy" : J. Opt.Soc. Am. Vol 158, P1023-1028.

[19] Skolink, M.I (1980). "Introduction of Radar Systems", 2nd edition , MeGraw-Hill Book Company.

[20] Stogrn, A. 1967, " The Apparent Temperature of the Sea at Microwave Frequencies "; Trans, IEEE. Ant. And Prop. VOL AP-15.

[21] Maffione, R.A. and Dana, D.R. 1997. "Instruments and methods for measuring the backward-scattering coefficient of Ocean waters", Applied Optics, 36(24), 6057-6067.

[22] Moncrief F.J. (1980), "Side Looking Radar will Spot Oil Sliks", Microwave, 19, March, pp25-26.

[23] G.Matis, P. et al, RAD-9000 (2005). " Performance spectral radiometer for EO calibration applications" , Infrared Imaging

Systems: Design, Analysis , Modeling and Testing XVI, SPIE Proceding Volume 5784, Orlando, FL.

[24] Clarke, R.L. (1980). "Spectra of backscattered light from the sea obtained from aircraft as a measure of chlorophyll concentration ": Science Vol. 167, P. 1119-1121.

[25] Hale, G.M. et al., (1972), " Influence of temperature on the spectrum of water " : Optical Soc. Am. Jour, V. 62, P1103-1108.

[26] Derr, M, et al ,(1970), " A comparison of Remote Sensing of the Clear Atmosphere by Optical, radio and aconstic radar techniques" : Appl. Optics. V.9. P. 1976-1992.

[27] Sloan, H.J., (1971). " The Technique of Raman Spectroscope " : A state-of-the-art comparison to infrared : App l. Spectroscopy V.26, P. 430-439.

[28] Querry, M.R. (1972). " Optical constant in the infrared and aqueous solutions of NaCl " ; Optical Soc. Am. Jour., V.26, P.849-855.

[29] Pope, M. and Fry, E.S. (1997). " Absorption spectrum (380-700 nm) of pure water. II Integration cavity measurements" Applied Optics , 36(33), 8710-8723.

[30] Crane, R.K. (1981), " Fundamental Limitation Caused by RF propagation " . Proc. IEEE, 69.PP.196-209.

[31] Hersman. M.S and G.A Poe (1981). " Sensitivity of the total power Radiometer with periodic Absolute calibration", IEEE. Trans. Micro and Tech, MTT-29 PP 32-40.

[32] Hach, Johann-Peter (1968), " A very Sensitivity Airborne Microwave Radiometer using Two references Temperature IEE E Trans " . Micro. Theory and Tech, MTT-16.9, PP 629-636.

[33] G. Matis, et al . (2004). " Development of a high-performance spectral radiometer for EO calibration applications. Infrared Imaging systems "

; Design , Analysis Modeling and Testing XV, SPIE Proceeding Volume 5407, Orlando , FL,.

[34] Paris, Jak F., (1969). " Microwave radiometry and its application to marine meteorology and oceanhography" Texas ": A & M University Dep. Of Oceanography.

[35] Kirk, J.T (1994). " Light and Photosynthesis in aquatic ecosystems" Cambridge University Press, New, York.

[36] Pope, M. and Fry, E.S. (1997). Absorption spectrum (380-700nm) of pure water . II Integrating cavity ,measurement ". Applied Optics, 36(33), 8710-8723.

Republic of Iraq
Ministry of Higher Education and Scientific Research
University of Technology
Laser & Optoelectronics Engineering Department

RADIOMETRIC EVALUATION OF VISIBLE AND INFRARED IMAGING SYSTEM FOR POLLUTION STUDIES

A Thesis

Submitted to The University of Technology Laser and Optoelectronic Engineering Department

in Partial Fulfillment of the Requirements for the Degree of Doctor of Philosophy

In

Optoelectronics Engineering

BY

Mohammed M. Salih

(M.Sc. Electrical Engineering)

Supervised By

Dr. Abdul Razzaq T. Ziboon
Asst. Prof

Dr. Hussian Jumaa
Asst. Prof

1429 هـ

2008 م

وزارة التعليم العالي والبحث العلمي
الجامعة التكنولوجية
قسم هندسة الليزر والبصريات الالكترونية

بناء منظومة راديو متري

رسالة مقدمة إلى قسم هندسة الليزر والبصريات الالكترونية
الجامعة التكنولوجية
كجزء من متطلبات نيل درجة الدكتوراه
في علوم هندسة الليزر والبصريات الالكترونية ـ هندسة البصريات

من قبل
محمد مجبل صـــالح
بكالوريوس (هندسة كهربائية) 1998
ماجستير (هندسة الكترونية) 2002

بإشراف

الدكتور عبدالرزاق طارش زبون
استاذ مساعد

الدكتور حسين جمعة عباس
استاذ مساعد

اذار 2008 م
ربيع الثانى 1429 هـ